University of Alberta

Use of a solvent in the oxidative desulfurization of bitumen via autoxidation; effects on viscosity and oxidation

by

Jose Luis Garcia

A thesis submitted to the Faculty of Graduate Studies and Research
in partial fulfillment of the requirements for the degree of

Master of Science – Chemical Engineering

Chemical and Materials Engineering

© Jose Luis Garcia
Spring 2014
Edmonton, Alberta

To Natalia, for bringing joy to my life.

To my parents, for showing me the way to success.

ABSTRACT

This work describes the effect that including a solvent in the reaction media of the autoxidation of Cold Lake bitumen has on the viscosity and also on the oxidation degree reached. The comparison of viscosity was performed both in the basis of equal residence time and equal oxygen conversion showing that the solvent does not have a moderating effect on the viscosity increase of bitumen during autoxidation. Nevertheless, it is shown that the presence of a solvent greatly increases the oxidation rate.

All the efforts made to oxidize sulfur compounds in bitumen are worthless if there is not a viable route to remove the oxidized species and release the sulfur as SO_2. The release of SO_2 from oxidized bitumen by pyrolysis and the effect on the desulfurization level reached is explored.

Differential Scanning Calorimetry (DSC) was employed in the thermal analysis of reactions involving model compounds for autoxidation and pyrolysis.

ACKNOWLEDGEMENT

CONTENTS

LIST OF TABLES

LIST OF FIGURES

1. INTRODUCTION

1.1 Background

The upgrading of Oil Sands involves, besides the separation of the bitumen from the minerals present in the sand, a reduction in its heteroatom content, and a reduction on the molecular weight of the compounds present in it. Traditionally, the upgrading of bitumen is performed by mature refining technologies used also for vacuum residue. That is, material with a boiling point beyond 500˚C. The upgrading of Oil Sands derived bitumen tends to be costly due to its high viscosity and high heteroatom content. That is why new technologies that aim to upgrade this feedstock at a low cost, low capital and in an environmentally friendly manner are desired.

The main families of technologies available for the upgrading of bitumen are thermal conversion and catalytic conversion. In the thermal conversion side the most used process is coking, this process consists of treating the feedstock to high temperatures 485-540˚C in an oxygen starved atmosphere for an extended period of time. This generates three different products, light gases, liquids and coke; liquids are the preferred products. The obtained coke is rich in sulfur and other heteroatoms, hence its applicability and value is low. This process serves two purposes: First, to produce liquid products with increased H:C ratio to be fed to other units and also to mitigate the emission of CO_2 since the carbon waste can be considered as captured CO_2.

In the catalytic conversion side hydrogen is required for most processes; the main ones applied for bitumen upgrading are hydroprocessing and hydrotreating. All of these processes are performed at high pressure and temperature; 340-450 ˚C for temperature and 10 to 17 MPa. In the case of hydroprocessing the goal is to reduce the boiling range of the feedstock by cracking as well as to remove impurities such as metals, sulfur and nitrogen. Hydrotreating on the other hand is a process in which very little cracking occurs and the removal of contaminants is the priority [1] .

While the previously mentioned methods attempt to reduce sulfur by transforming it to H_2S, oxidative desulfurization (ODS) is a technology that promotes the reaction in the opposite direction, forming oxidized sulfur species like sulfones. These species differ from the parent sulfide molecules in that they exhibit big differences in their polarity and boiling point allowing them to be potentially separated by diverse means.

Oxidative desulfurization comes as a technology that potentially generates some benefits in the product such as a reduction in the sulfur content by decomposition of oxidized sulfur species and also a reduction in the total acid number (TAN)

during the decomposition step. This technology is attractive due to its inherent advantages as cheaper reactants (air), moderate process conditions and also, as mentioned by Ito and van Veen [2] *"The oxidative desulfurization seems to offer several advantages, compared to hydrodesulfurization ... the most attractive intrinsic aspect is the anticipated higher reactivity of more aromatic sulfur species, since the electrophilic attack on the sulfur atom is promoted with the increase of electron density at the sulfur atom by attached electron rich aromatic rings"*.

The proposed conversion process on a conceptual base is presented in Figure 1-1 and consists of the following steps:

In the first stage the oxidation takes place, bitumen is contacted with air as the oxidant in a reactor with or without a diluent. After reaction is completed, if solvent is used it needs to be separated and recycled; most likely a distillation or stripping column can be used for that purpose. After the solvent has been removed the actual desulfurization step in which the oxidized compounds sulfones are decomposed to release the sulfone group as SO_2; this step is projected as a pyrolysis step in which the C-S bonds of the sulfone are cleaved.
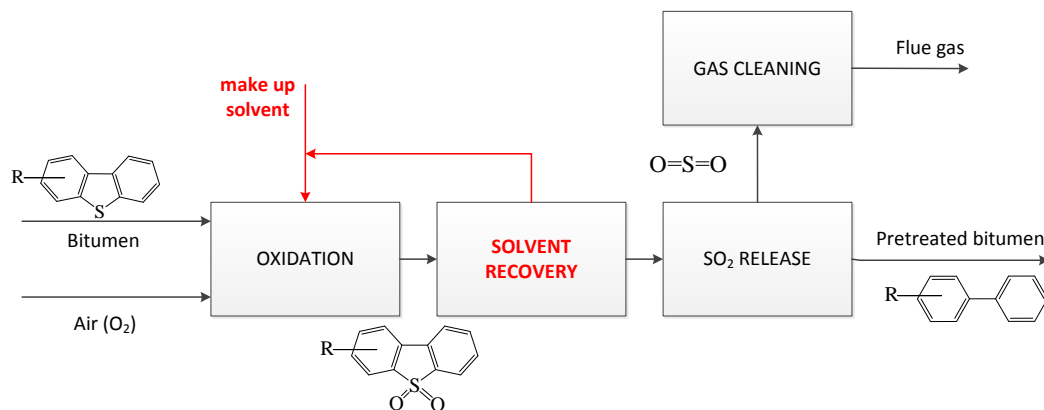
Figure 1-1. Simplified process flow diagram for the ODS of bitumen.

The generated gas stream can be treated by means of well-known methods. One of these is Flue Gas Desulfurization (FGD); this technology involves the reaction of SO_2 with a lime/limestone slurry producing calcium sulfite which can further be oxidized for the production of gypsum salt $CaSO_4 \cdot 2(H_2O)$, this product is used in the production of wallboard and as additive in cement and concrete as well [3, 4] . The main reactions are shown next.

$$CaCO_3 + SO_2 \longrightarrow CaSO_3 + CO_2$$

$$Ca(OH)_2 + SO_2 \longrightarrow CaSO_3 + H_2O$$
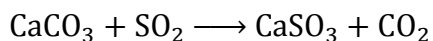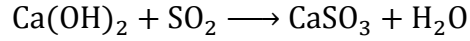
Although not obvious, SO_2 can potentially be removed from the gas phase by the modified Claus process. This process is usually performed to recover sulfur from H_2S streams. The first phase of it involves the oxidation of a fraction of the H_2S to produce SO_2 and water as shown next:

$$H_2S + {}^3/_2\,O_2 \longrightarrow SO_2 + H_2O$$
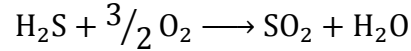
After this oxidation occurs the gases are cooled in a waste heat boiler and then introduced to a catalytic reactor where the production of liquid sulfur occurs [5] :

$$2\,H_2S + SO_2 \longrightarrow {}^3/_x\,S_x + 2\,H_2O$$
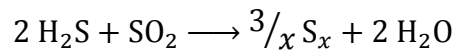
One of the main purposes of this work is to decide whether or not the presence of a solvent is required for the reaction to proceed efficiently. It is evident that the addition of a solvent carries consequences from a process engineering point of view such as larger equipment, need for separation equipment, and higher energy consumption in addition to the cost of the solvent itself.

In previous work developed in our research group it was observed that the autoxidation of bitumen and of bitumen-water mixtures results in an increase in viscosity. However that was not the case when *n*-heptane was employed as a solvent [6] . These results are presented in Table 1-1. The reason for the observed differences in the viscosity behavior were not determined as part of the work.

Table 1-1. Viscosity of Cold Lake bitumen before and after autoxidation at 145 and 175 °C, at near atmospheric pressure, for 6 hours in a batch reactor with continuous air flow of 1.5 $cm^3 \cdot min^{-1}$ per cm^3 bitumen.

Material	Bitumen viscosity (Pa·s)	
	at 45 °C	at 60 °C
Bitumen feed	53	10
Autoxidation of neat bitumen		
after autoxidation at 145 °C	66	17
after autoxidation at 175 °C	389	88
Autoxidation of bitumen:water = 1:1 vol/vol		
after autoxidation at 145 °C	296	63
after autoxidation at 175 °C	477	123
	(mPa·s)	(mPa·s)
Diluted bitumen:heptane feed = 1:0.8 vol/vol	1.31	1.02
Autoxidation of bitumen:heptane = 1:0.8 vol/vol		
after autoxidation at 145 °C	1.14	1.06

1.2   Objectives and scope of work

a) Objectives

- Determine whether or not the hypothesis that the low viscosity observed after autoxidation of bitumen in the presence of a solvent is caused not only by a dilution effect, but also due to solvent moderation of free radical addition or polymerization reactions.

- Determine the actual viscosity of oxidized bitumen after the solvent is recovered to quantify the actual increase in the viscosity.

- Assess the degree of oxidation reached in the bitumen under autoxidation conditions.

- Get an insight of the kind of conditions required for the release of sulfur from oxidized bitumen.

- Provide evidence that the employed conditions for autoxidation are beneficial for the quality of the product.

b) Scope of work.

The analysis of the desulfurization degree achieved by autoxidation of bitumen was studied earlier in our research group [7] and this work is a continuation of the research. The following topics were investigated in this work:

Chapter 3:   Autoxidation of thiophenic model compounds by means of HPDSC.

Chapter 4:   Comparison of the viscosity of bitumen under fixed autoxidation times in the presence and absence of a solvent in the reaction media.

Chapter 5:   Determination of the effect of the oxidation extent on the viscosity, comparisons in viscosity between neat and diluted oxidized bitumen are made on the basis of equal oxygen conversion.

Chapter 6:   A confirmation of the evolution of SO_2 from oxidized bitumen by pyrolysis is made; followed by an evaluation of the behavior of sulfones under pyrolytic conditions in the presence of a hydrogen donor solvent.

Chapter 7:   Development of a method to evaluate and quantify SARA fractions of bitumen by HPLC.

2. LITERATURE REVIEW

Abstract

This review intends to give a broad description of the composition and relevant sulfur compound classes found in bitumen, the state of the art of heavy oil oxidative desulfurization will be discussed, as well as a review on the analysis of hydrocarbons by means of HPLC.

Keywords: ODS, bitumen composition, desulfurization, SO_2 release, HPLC analysis of hydrocarbons

2.1   Introduction

This chapter will explain the basics of the issue of sulfur removal in bitumen. It will first describe the results achieved so far in the determination of the composition of Athabasca bitumen with focus in getting an insight of what type of molecules bear the sulfur in this complex mixture and their approximate relative abundance. Next, it will expose how oxidative desulfurization as a prerefining step is an alternative to improve the current technologies, going through a description of the chemistry and the research attempts to perform oxidative desulfurization on heavy hydrocarbon feedstocks.

In a previous work performed in our research group [7] a proof of concept was achieved: Air can be used as a bitumen oxidant without adding additional agents and a removal of up to 46% of sulfur can be achieved after autoxidation and liquid-liquid extraction with hot water. This literature review intends to achieve a better understanding of the chemistry and the nature of the sulfur containing molecules in bitumen.

2.2   Bitumen composition and sulfur components

This section is essentially entirely based the book from Strausz and Lown [8] which is an extensive updated review of the chemistry of Alberta Oil Sands.

The elemental composition of most Alberta bitumens varies between narrow limits; the compositions are shown in Table 2–1 as summarized by Strausz et al. [8].

Table 2–1 Average elemental composition of Alberta bitumen

Element	Content
carbon	$83.1 \pm 0.5\%$
hydrogen	$10.3 \pm 0.3\%$
nitrogen	$0.4 \pm 0.1\%$
oxygen	$1.1 \pm 0.3\%$
sulfur	$4.6 \pm 0.5\%$

Bitumen, as petroleum in general can be divided in four compound classes that can be physically separated: saturates, aromatics, resins and asphaltenes.

The first step for this class separation is the separation of asphaltenes which is performed by solvent precipitation using a low molecular weight alkane as solvent, usually *n*-heptane. In this way Asphaltenes are the fraction of bitumen that is not soluble in the above mentioned solvent; this makes it a solubility class. Asphaltenes are the highest molecular weight fraction of petroleum, being rich in heteroatoms, polyaromatics, and polar functional groups. It also has a marked propensity for aggregation. The deasphalted fraction of bitumen is called maltene, or also deasphalted oil. The average content of heptane insoluble asphaltenes in Athabasca bitumen is 17% containing 7.5%wt sulfur as shown in Table 2–2 and Table 2–3, from [8].

Table 2–2 Class composition of Alberta oil sand bitumens using the USBM-API-60 procedure.

Component	Weight %			
	Peace River	Wabasca	Athabasca	Cold Lake
Hydrocarbons	34	33	36	40
Saturated	15	15	18	21
Aromatic	19	18	18	19
Asphaltene	20	19	17	16
Resins	44	48	46	44
Acids+ amphoterics	12	10	14	15
Bases	7	6	7	7
Neutral N compounds	1	3	1	1
Neutral(others)	24	29	24	21
Total	98	100	99	100

Table 2–3 Elemental composition of various asphaltenes

Source	Wt%				
	C	H	N	O	S
Athabasca	80.6	7.9	1.1	2.8	7.5
	81.3	7.9	1.1	2.8	7.5
	79.9	8.3	1.2	3.2	7.6
Cold Lake	82.7	7.6	1.2	1.8	6.7
	81.5	8.0	1.1	1.7	7.9
	82.0	7.9	1.2	1.7	7.7

The resin fraction of petroleum can be defined in term of adsorption properties; specifically resins constitute the portion of the maltene that is adsorbed on a clay (attapulgus clay, Fuller's earth) or, alternatively, as the portion of maltene that is eluted from silica gel by polar eluants (e.g., methanol in benzene). In the latter case it has become common practice to denote the fraction as polars, rather than resins. The two definitions given before are not equivalent.

The polars content and elemental analysis of the polars fraction in bitumen is available in the work by Strausz et al. [8] these constitute 31.3% of bitumen and contain an average of 5.8% sulfur, Table 2–4.

Table 2–4 Elemental composition of Athabasca polar subfractions.

Subfraction	Solvent	Wt% of bitumen	C	H	N	O	S
					Wt%		
Polar I	benzene	8.8	82.4	9.5	0.7	1.51	5.9
Polar II	40% CH$_3$OH/ CH$_2$Cl$_2$	22.5	79.6	10.0	0.64	4.12	5.7

a Separated on silica gel from n-C5- deasphalted bitumen.

The saturates and aromatics are eluted from the adsorbent (attapulgus clay or silica gel) with *n*-pentane or benzene prior to elution of resins and constitute the oily fraction of the bitumen. The saturates are then separated from the aromatics on an alumina column: the saturates are eluted with *n*-pentane and the aromatics with benzene. A summary of the SARA class separation is shown in Figure 2–1.
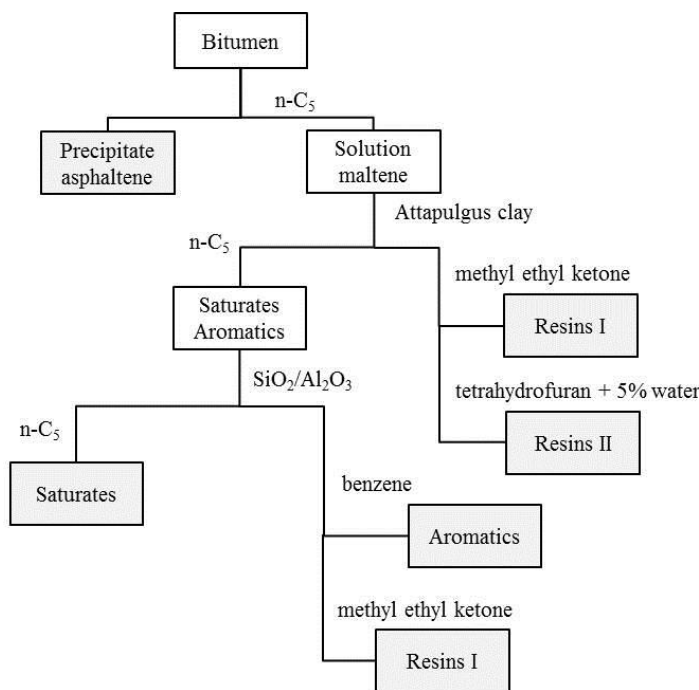
Figure 2–1 Flow diagram for the SARA class separation process

Strauzs et al. reported the chemical composition of the maltene fraction of bitumen that was analyzed by Field Ionization Mass Spectroscopy (FIMS), which is a technique that can ionize cyclic hydrocarbon without significant fragmentation. This causes that in the FIMS spectrum essentially only the parent molecular ions appear. The results of this is that the evaluation and the identification of molecules based on its elemental formula C$_n$H$_{2n+Z}$ easier. It is

important to mention that the technique does not provide information about the molecular structure and thus, all isomeric molecules contribute to their common molecular ion signal.

Prior to FIMS analysis the maltene was subjected to a series of chromatographic separations on a silica gel column resulting in 15 subfractions which were distilled at 240ºC and 0.13 Pa(a). The combined yield of the distillates was 66% of the maltene. A summary of the fractionation performed is shown in Figure 2–2.

Subfraction 1, accounting for 35.8% of the maltene was rechromatographed on a silver ion silica gel thin layer plate into four subfractions (Table 2–5).
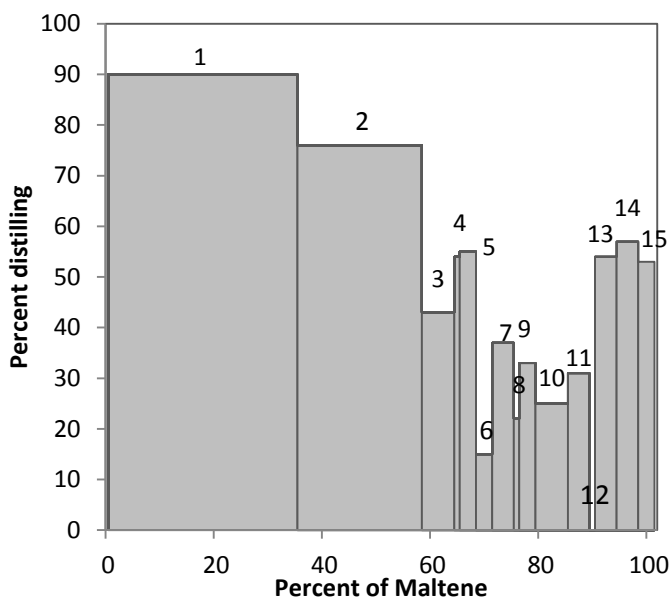
Figure 2–2 Fractionation of Athabasca maltene and distillation data (240ºC, 10^{-3} torr) for the 15 subfractions eluted from silica gel. From Strauzs et al. [8].

Table 2–5 Refractionation of the saturate subfraction 1 using Ag+-TLC Chromatography

Subfraction	% of			Functionality
	Subfraction 1	maltene	bitumen	
1a	56.4	18.2	15.1	Saturated hydrocarbons
1b	1.6	0.5	0.4	Not analyzed
1c	25	8.1	6.7	Monoaromatic Hydrocarbons
1d	17	5.5	4.5	

2.3 Chemical Composition of the Saturate Fraction [8]

Crude oil is mainly comprised by acyclic and cyclic saturated hydrocarbons and aromatic hydrocarbons. Unsaturated hydrocarbons as olefins are present only in trace quantities. For the case of Alberta bitumens the concentration of alkenes does not exceed 100 ppm. As mentioned before, saturates can be separated by column chromatography on silica gel and alumina followed by silver ion chromatography to remove the small amount of contaminant components. This saturate fraction only contains small quantities of heteroatoms and is mainly a pure hydrocarbon mixture. Bitumen in general does not contain a high concentration of saturates since bitumens are the result of microbial degradation of crude oils and these microorganisms prefer alkanoic hydrocarbons, therefore reducing the saturate content of bitumen over time.

The total saturate contents of Alberta bitumens vary between 14 and 22% as determined by the Syncrude SARA or the USBM-API-60 procedure. Due to its high H/C ratio, low heteroatom content and high volatility, this fraction is considered the most valuable fraction of bitumen. The elemental composition of this fraction is shown in Table 2–6. No further discussion will be considered regarding this fraction as its sulfur content is very low, making its detailed review irrelevant for this work.

Table 2–6 Elemental composition of the saturate fraction of Athabasca and Cold Lake bitumens

	Wt%						MW	H/C
	of maltene	C	H	N	O	S	$(g \cdot mol^{-1})$	atomic
Athabasca	24.8	85.0	12.9	0	0	0.15	365	1.82
Cold Lake	29.4	86.6	12.8	0.06	0.0	0.18	n/d	1.77

2.4 Chemical Composition of the Aromatic Fraction [8]

Aromatic compounds ranging from alkylbenzenes to large condensed polyaromatics and heteroatomic molecules are abundant in bitumens and heavy oils. These are usually alkyl- and naphtenic- substituted. By a combination of various column chromatographic methods it is possible to isolate an aromatic fraction and separate it into monoaromatic, diaromatic, triaromatic and polyaromatics subfractions.

The monoaromatic subfraction has the lowest heteroatom content, the highest (H/C) ratio and the lowest molecular weight of the subfractions. With increasing number of aromatic rings in the subfractions their (H/C) atomic ratios decrease and heteroatoms content increase. The monoaromatic fraction contains only a small amount of sulfur, but the rest of the fractions contain benzo-, dibenzo- and higher condensed thiophenes along with other sulfur compounds.

The analysis performed by Strausz et al. to determine the composition of the aromatic fraction involved a combination of chromatographic fractions followed by FMIS and high resolution electronic ionization mass spectroscopy (EIMS).

As shown in Table 2–5 the subfractions 1c and 1d are constituted by monoaromatic hydrocarbons. The subfraction 1c showed no presence of sulfur up to C_{40}, making it of low relevance to this study. This fraction is composed mainly of a series of alkyl aromatics with one and two naphthenic rings.

The subfraction 1d in turn, is found to have some sulfur as benzothiophenes and benzothiophenes with one naphtenic ring, as determined by EIMS. A summary of the composition of this fraction is presented in Table 2–7; it is divided by the parameter Z in the elemental formula. In this case: C_nH_{2n+Z}. However, as mentioned before, there might be some isomers that cannot be differentiated (see rows 1 and 2). For example, considering the first row of Table 2–7, the compounds with elemental formula C_nH_{2n-6} with n = 50 (MW = 12×50 + 1×(2×50 − 6) = 694 $^g/_{mol}$) and $C_nH_{2n-10}S$ with n = 48 (MW: 12×48 + 1*(2×48 − 10) + 32 = 694 $^g/_{mol}$) have the same molecular weight and cannot be differentiated only from the EIMS data. Nevertheless, a rough ratio between the isomers is provided in the table.

Table 2–7 Composition of the subfraction 1d

Z in C_nH_{2n+Z}	Relative abundance (%) in subfraction 1d	%	
		Maltene	Bitumen
-6 and $C_nH_{2n-10}S$	22.4	1.23	1.03, 0.69 as S compound
-8 and $C_nH_{2n-12}S$	24.7	1.35	1.13, 0.75 as S compound
-10	18.5	1.01	0.84
-12	14.3	0.78	0.65
-14	9.8	0.54	0.45
-16	6.2	0.34	0.28
-18	4.0	0.22	0.18
	99.9	5.47	4.55

[a]About two thirds of the Z=-6 and -8 series comprise sulfur compounds and the rest hydrocarbons. For n≤20 the hydrocarbon series are more abundant and for n ≥ 20 the sulfur-containing series is dominant [b] 5.06% after correction for non-distillable residue

So far we have reviewed that around 1.44% of bitumen is composed by monoaromatic thiophenes as the ones shown next, the predominant carbon number for these compounds was found to be n > 22.

$C_nH_{2n-10}S$ $C_nH_{2n-12}S$
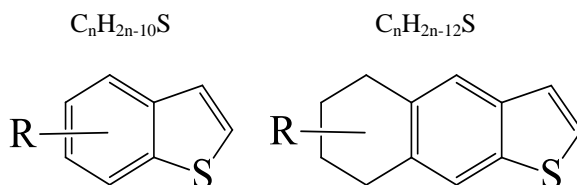
In order to analyze the diaromatic fraction of bitumen, it is necessary to go back to the subfraction 2 (Figure 2–2). This fraction accounted for 23.1% of maltene or 19.2% of bitumen and 76% of the fraction was distillable. This distillate was then fractionated on an alumina column into seven fractions (fractions 2a − 2f) adding to 14.5% of bitumen. Fractions 2f and 2g were not further analyzed (Table 2–8).

Table 2–8 Chromatographic separation of subfraction 2 on alumina

Subfraction	% of bitumen	
	Distillate	Distillable corrected for nondistillable residue
2a	6.27	8.25
2b	2.89	3.8
2c	2.79	3.7
2d	1.90	2.5
2e	0.52	0.7
2f	0.10	0.13
2g	0.07	0.09
Total	14.5	19.2

The FIMS analysis on each of the fractions belonging to the subfraction 2 is summarized on Table 2–9. At this point, not enough information is given to accurately calculate the relative abundance of the isotopes in a given Z series. It is clear though that the sulfur is present in molecules having the elemental formulas $C_nH_{2n-10}S$, $C_nH_{2n-12}S$, $C_nH_{2n-16}S$, $C_nH_{2n-18}S$ and $C_nH_{2n-22}S$ which are mainly substituted benzothiophenic compounds, as shown next.
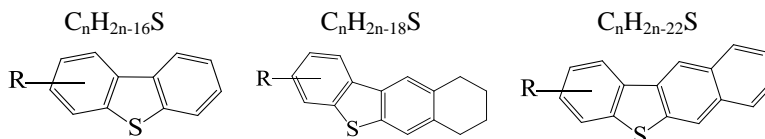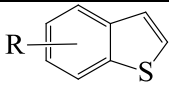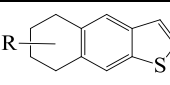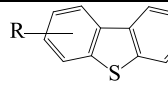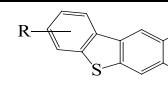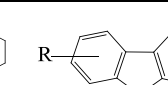
To sum up, in the maltene fraction of bitumen one can identify the dominant type of structures for sulfur compounds from the data in Table 2–10. Due to the presence of isomers in most of the structures it is not possible to quantify individual compounds in each of these compound classes with the techniques used by Strausz et al.

Table 2–9 Percentages of various Z series of compounds present in subfraction 2

Mass series "Z"	Possible elemental composition	% in subfraction				
		2a	2b	2c	2d	2e
-6	C_nH_{2n-6} C_nH_{2n-20} $C_nH_{2n-10}S$	14.1	14.8	14.7	18.0	15.1
-8	C_nH_{2n-8} C_nH_{2n-22} $C_nH_{2n-12}S$	12.6	9.0	6.0	8.2	14.3
-10	C_nH_{2n-10} C_nH_{2n-24}	8.7	3.4	3.5	4.4	8.5
-12	C_nH_{2n-12} $C_nH_{2n-16}S$	11.1	14.5	36.0	23.4	17.0
-14	C_nH_{2n-14} $C_nH_{2n-18}S$	20.9	31.8	19.5	13.1	5.8
-16	C_nH_{2n-16}	19.7	18.1	10.7	12.2	6.6
-18	C_nH_{2n-18} $C_nH_{2n-22}S$	12.8	8.4	9.6	20.6	32.7

It can be estimated however that these types of compounds can represent around 32±7%wt of the organic sulfur in Athabasca bitumen. This is based on an asphaltene content of 17% with 7.5wt% S (~28% of total sulfur) and polars content of 31.3% with 5.8wt% S (~39% of total sulfur) and bitumen containing 4.6±0.5 wt% S. The sulfur not present in the maltene fraction is probably present in the form of very large condensed molecules as the ones present in asphaltenes as well as large molecules that are part of the polar fraction of bitumen. Also, as shown in Table 2–6 the amount of sulfur in the saturate fraction is low, just around 0.04% of bitumen. The nature of the molecules in the asphaltenes and polar fractions is expected to be similar to what was found for the maltene in the sense that the sulfur will most likely be in the form of thiophenic structures.

Table 2–10 Dominant compound classes in the maltene fraction of bitumen.

2.5 Oxidation

2.5.1 Oxidative desulfurization

Oxidative desulfurization involves the reaction of an oxidant with the organic sulfur present in bitumen in order to produce oxidized species that are in principle readily removed. Oxidative desulfurization involves two separate processes [9]. The first one, namely sulfur oxidation, alters the functionality of the sulfur containing species by introducing S=O bonds in the structure. The second takes advantage of the chemical changes caused in the chemical functionality of the sulfur compounds by the oxidation to perform sulfur removal. A detailed review of this topic was published by our research group [9].

As described in the previous section, the sulfur containing molecules in bitumen are mainly substituted thiophenes and benzothiophenes, hence, the logical chemical conversion route involves the oxidation of these compounds to sulfoxides and sulfones as shown in equation (2.1) It is feasible though, that under certain conditions the sulfones reach higher oxidation states as sulfonic acids and sulfates [10].

$$RSR' \xrightarrow{ox} R\overset{O}{\underset{}{S}}R' \xrightarrow{ox} R\overset{O}{\underset{O}{S}}R' \xrightarrow{ox} RSO_3H \xrightarrow{ox} SO_4^{2-} \tag{2.1}$$
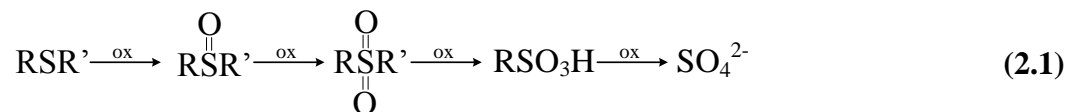
The motivation behind converting thiophenes into oxidized species, e.g. sulfones and sulfoxides arise from two distinctive properties that these compounds have. First, their polarity and therefore their solubility in polar solvents increase by the oxygen inclusion [11], opening an opportunity for selective solvent extraction or adsorption to remove the sulfur species. Second, the C-S bond strength is decreased when the sulfur is oxidized [9], allowing in principle to perform cleavage of the C-S bonds by catalytic [12] or thermal decomposition [13].

Another topic worth mentioning is that during hydroprocessing, most of the relatively simple organosulfur compounds as sulfides, disulfides and thiols are readily converted to H_2S. On the other hand, hydroprocessing is less effective in converting more complex compounds such as substituted and unsubstituted thiophenes because these compounds are sterically hindered for the catalytic reaction [14]. The advantage for ODS is that these refractive molecules are readily oxidized because of their increased electron density on the sulfur atom [15, 16]. It explained later in this Chapter that the mechanism for oxidation involves a nucleophilic attack from the sulfur atom to the hydroperoxide species; a higher electron density in the sulfur atom makes it a better nucleophile. As can be seen on Figure 2–3, the reactivity for the oxidation of sulfur compounds increases in the order dibenzothiophene (DBT) < 4-methyldibenzothiophene (4-MDBT) < 4,6-dimethyldibenzothiophene (4,6-DMDBT). From this result one can anticipate that the nature of the sulfur compounds in bitumen being heavily substituted might become an advantage for the oxidation step.
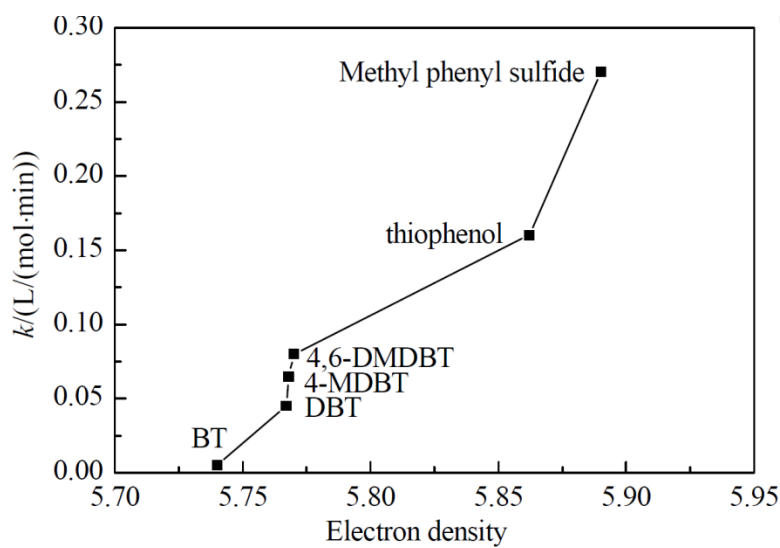
Figure 2–3 Relationship between the oxidation rate constants, k of model compounds and their electron densities, from [16].

2.5.2 Sulfur oxidation chemistries

The oxidation of sulfur containing compounds has been widely studied. Block [17] distinguished 19 different methods for the oxidation of sulfides. Applied to the field of desulfurization a narrower list can be suggested. Javadli, et al. [9] classified the oxidative desulfurization (ODS) processes in 5 types, namely, autoxidation, chemical oxidation, catalytic oxidation, photochemical oxidation and ultrasound oxidation.

One of the most efficient chemistries for the oxidation of organic compounds involves organic peroxides. Organic peroxide radicals can be defined as derivatives of hydrogen peroxide, in which one or both hydrogen atoms are replaced by organic radicals [18], the reactivity of these compounds is remarkably higher when only one hydrogen atom is substituted. The conditions required for oxidation with monosubstitutes derivatives as peroxy acids, alkyl hydroperoxides and hydrogen peroxide are usually mild [18]. It is suggested that the order of reactivity of these compound is as follows $RCO_3H > HOOH > ROOH$. The reactivity of the substrate will depend on the electron availability on the reaction center. As was shown before, the substituted dibenzothiophenes and other bulky organosulfur compounds tend to have high electron densities on the sulfur atom [16]. In general terms it is suggested that the oxidation mechanism through monosubtituted peroxy compound is as shown in equation (2.2) [18]. In this case the nucleophile, denoted as Nu:, corresponds to the sulfur end of the organosulfur compound.

$$Nu: \quad \rightarrow \quad \left[Nu-----O----O \right] \quad \rightarrow \quad NuO \quad + \quad ROH \qquad \textbf{(2.2)}$$
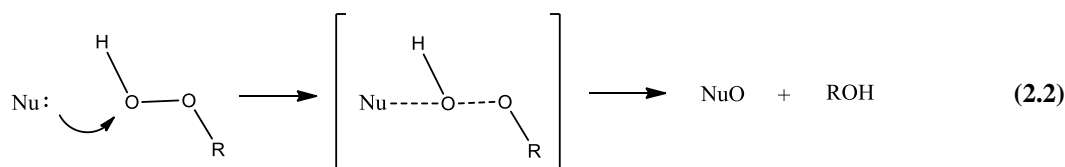
Peracids, formed by the combination of hydrogen peroxide with a short chain carboxylic acid has been used in several works as the oxidizing agent for desulfurization of liquid fuels. These compounds are proven to be effective oxidizers, but the whole idea of involving an additional component and possibly additional liquid phases does not make it sound attractive for the engineering context of this work. On the other hand, hydroperoxides are also commonly used in the oxidative desulfurization of hydrocarbons [19] for example: t-butyl hydroperoxide (TBHP) is widely used in the oxidation of cumene to phenol. This particular hydroperoxide offers some advantages compared to hydrogen peroxide or peracids as it has higher chemical stability, is less sensitive to contamination by metals, is more selective than hydrogen peroxide or peracids, is highly soluble in organic solvents, the oxidation conditions can be carried out in neutral conditions and finally, the co-product t-butanol (bp=83ºC) can be readily removed by distillation.

In this work however, additional chemicals will only be considered if proven to be indispensable. That is why the approach addressed was to generate hydroperoxides by the partial autooxidation of bitumen. It is known that the most common industrial hydroperoxides (TBHP, ethylbutyl hydroperoxyde and cumene hydroperoxide) are produced by liquid-phase autoxidation of hydrocarbons [20] fact that opens a window for the *in situ* production of hydroperoxides.

Regarding the oxidation step involving the hemolytic or heterolytic dissociation of hydroperoxides, it has been reported that thermal homolysis of hydroperoxides can be achieved at reasonable rates at temperatures above 100ºC [20, 21] which are in the range of the operational conditions previously used for the autoxidation of bitumen [6, 7]; hence the need for a catalyst for the hydroperoxide dissociation is initially deemed unnecessary.

2.5.3   Sulfur removal

Several references have suggested solvent extraction [2, 16, 22, 23] or adsorption [19] of oxygenated sulfur species as the method of choice for their removal in oxidative desulfurization, This is an attractive method when dealing with feedstock with a very low sulfur content because just a very small fraction of hydrocarbons will be transferred to the solvent. On the other hand, heavy feedstock as bitumen containing around 5 wt% of sulfur would lose too much of its mass if the sulfur is oxidized and then solvent extracted or adsorbed. As an example, picture that all 5% sulfur in bitumen is present as dibenzothiophene, a relatively small molecule (MW=184.26). If all dibenzothiophene is converted to the sulfone or sulfoxide and then extracted, about 29% of the initial mass will be

transferred to the solvent at the expense of removing the sulfur. Of course, the bigger the sulfur containing molecule, the higher the mass loss.

A more interesting approach for the removal of sulfur in feedstocks with high S content is to break the sulfur-carbon bonds in the oxidized compounds allowing the sulfur to be released as SO_2 and leaving the valuable hydrocarbon part in the liquid phase. Theoretically, in this way no carbon or hydrogen is lost in the process of removing sulfur.

Some work has been reported in the catalytic decomposition of sulfones to SO_2. Kim et al used Mg/Al layered double hydroxide [24] as a decomposition catalyst, a conversion of 82% was achieved using ODS diesel as a feedstock at 475ºC, 790 kPa and a weight hourly space velocity (WHSV) of 1 h^{-1}. You et al. [12] used mixed Mg/Al oxides deposited in mesoporous silica obtaining a dibenzothiophene sulfone conversion of 59% at 475ºC, 689 kPa and a WHSV of $5h^{-1}$ with a time on stream of 6 h. Park et al. [25] studied the SO_2 release from dibenzothiophene sulfone by using Mg based oxide catalyst reaching a conversion of 76.2% at 475ºC, 790 kPa and WHSV of $5h^{-1}$.

In a 2002 patent [14] it was claimed that amorphous aluminosilicates (with a SiO_2/Al_2O_3 ratio of about 3), amorphous magnesium oxide, and hydrotalcite which is a double layered hydroxide are effective in decomposing oxidized organic sulfur compounds from hydrotreated and oxidized diesel (567 $mg \cdot kg^{-1}$ S) and from diluted oxidized vacuum gas oil (VGO) (6347 $mg \cdot kg^{-1}$ S).

There are not many references regarding to the thermal decomposition of oxidized sulfur compounds. It is noted in Kocal et al. [14] that the reduction in sulfur content of oxidized hydrotreated diesel at 475ºC, 690kPa and a WHSV of 5 h^{-1} using glass beads as the reactor filling is only 4%. On the other hand, a patent from 1964 [26] claims that the thermal treatment at 400ºC for 1.5h of an oxidized Kuwait heavy oil is able to reduce its original sulfur content, 4.05%, to as low as 1.67%. This discrepancy in results may be explained by the fact that the liberation of the sulfone group from an aliphatic compound is likely much easier than from a thiophenic compound and the nature of sulfur molecules in different hydrocarbons varies significantly.

2.6 High Performance Liquid Chromatography (HPLC) Analysis of petroleum fractions

It is important to develop analysis methods that allow tracking of the compositional changes in bitumen after oxidation and thermal treatment. Traditional GC is not suited for the analysis of heavy fractions because of the high boiling range of bitumen, making it very difficult to vaporize.

HPLC is thought to be a helpful tool in the analysis of petroleum fractions since it does not involve the phase change of the sample. References dealing with the analysis of heavy hydrocarbon fractions date from the 1970's. These types of

applications are usually intended to separate the sample into their Saturates, Aromatics, Resins and Asphaltenes fractions (SARA fractions). The HPLC applications for hydrocarbons are usually gradient normal phase chromatography, where the mobile phase is non-polar and the column is polar, though there are some references on reversed phase chromatography.

In 1978 a study attempting to separate Athabasca Bitumen into its SARA fractions was published [27]. In this study two mobile phase systems were used. The first one was a mixture of 99% methanol 1% isopropanol (IPA) in gradient with tetrahydrofuran (THF). The second system used a mixture of 90% acetonitrile and 10% water in gradient with methylene chloride. The runs were 25 minutes long and made use of a 25cm Aerograph Micropak CH-10 column in series with a 25cm Aerograph Micropak CN-10 column. The injection volume was 2-5 µl and the sample concentration range was 10-20 mg/ml. An UV detector was employed and the mobile phase flow was 1 ml/min. In 1982 a paper dealing with the separation of aromatic hydrocarbon model compounds was issued [28]. The mobile phase used was a gradient of hexane and methylene chloride and the sample concentration ranged from 0.1 mg/ml for 4 ring components to 10 mg/ml for monoaromatic compounds. Then in 1983 a work was published using HPLC coupled with FIMS attempting to determine hydrocarbon composition of non-distillable coal liquids [29]. The chromatographic column used was a µBondapak NH_2 (3.9 mm id., 30 cm). On 1986 a method for the determination of SARA hydrocarbon types in crude oil residues was released [30]. This system besides using two different columns, cyano (Supelco 5µm LCCN 25cm × 4.6 mm) and aminocyano (Whatman 10µm PAC 25cm × 4.6mm), used a backflush valve to ease the elution of more polar components and a FID detector. In 1989 a research article aimed to quantify the resin content and study the asphaltene fraction from heavy crude oil [31]. Precipitated asphaltenes were dissolved in THF and passed through a series of gel permeation chromatography (GPC) columns (ultrastyragel 3.9mm × 30 cm) to obtain the molecular size distribution. For the isolation of resins the method by Dark (1982) was used as a starting point. Their method used an Energy analysis NH_2 column (3.9 mm × 30 cm) with 2 ml/min hexane as the mobile phase.

During the 1990's the published works on HPLC analysis of hydrocarbons kept on the same line that is the SARA analysis. Of course some technologic improvements occurred. In 1991 Lamey et al. [32] used semipreparative HPLC for the analysis of liquid fuels achieving a separation between saturates and aromatics by ring size. The fractions collected were then analyzed by GC-MS to collect further compositional information. The mobile phase used consisted on a mixture of 97.5% 1,1,2-trichlorofluoroethane and 2.5% chloroform, the column used was a Whatman partisil 10 PAC (aminocyano). Other hyphenated techniques included Liquid Chromatography (LC) coupled with Thermospray-(TSP) Mass Spectrometry, this attempted to determine molecular weight distributions and compound classes on high boiling aromatic hydrocarbons [33]. In 1993 Akhlaq [34] established a simple HPLC method for the separation of hydrocarbon in SARA fractions using a gradient of hexane and chloroform across three

µBondapak NH_2 (300 × 3.9 mm) columns connected in series that also made use of a backflush valve to facilitate the elution of polar compounds and colloids. In 1994 the same author Akhlaq [35] released the first reference for reversed phase HPLC for the analysis of crude oils. First obtaining five cuts with the same procedure previously published and then performing injections on a system containing a Nucleosil C18 (125mm × 4mm) with a 30 mm precolumn with a 5 µm particle size (System I) and a Nucleosil C_{18} (150mm × 4mm) with a 11mm precolumn with a 5 µm particle size (System II) under a gradient system of water and acetonitrile in order to achieve an enhanced resolution for each of the cuts obtained. A study conducted in India in 1997 [36] achieved the separation of heavy distillates in saturates, mono-, di-, poly- aromatics, and polars by normal phase chromatography on two µBondapack (300 × 3.9mm) columns connected in series. The flow of hexane as the mobile phase was 1 ml/min and the injected sample volume 20 µl. In 1997 also another study on hyphenated HPLC techniques was released [37], in this case a sulfur chemiluminescence detector was interfaced to a hyphenated HPLC-High resolution gas chromatography (HRGC) system to detect different organosulfur compound classes. The column used was a (250 × 2 mm) glass lined stainless steel tubing packed with aminosilane-bonded silica (SGE Scientific Ltd) with *n*-heptane as the mobile phase.

In 2003, Ali [38] performed the quantification of ring type aromatics by HPLC using *n*-hexane elution. The instrument was equipped with a 3.9×300mm Energy Analysis (NH_2) column with a mobile phase flow of 2 ml/min and an injection volume of 20µl. In 2004 Woods et al. [39] implemented preparative SARA separation of coker gas oil from Athabasca bitumen by HPLC in order to perform further characterization analyses on the cuts obtained. Among them: GPC, vapor pressure osmometry (VPO) and GC-MS to calculate average molecular weight, elemental analysis NMR and FTIR to determine structural characteristics. One of the most recent studies, from 2008 [40], is a comparative study of the SARA fractions of several Canadian crude oils separated by using HPLC and performing further analyses as NMR, GPC, XPS and N and S analysis.

3. ANALYSIS OF DECOMPOSITION OF SULFUR COMPONENTS FOUND IN BITUMEN BY MEANS OF HP-DSC AND FTIR

Abstract

For the application of a chemical reaction to a complex mixture such as bitumen, it is important to get some level of understanding of how model sulfur compounds present in it behave under autoxidation conditions. Differential Scanning Calorimetry (DSC) is a versatile tool for this purpose, since it essentially can work as a reactor that can be operated over a wide range of temperatures and pressures and it provides information on the energetic changes associated with chemical reactions. It was found that 4-methyldibenzothiophene (4-MDBT) only undergoes oxidation at temperatures close to 300°C in the absence of solvent.

Note: Parts of the experimental work presented in this chapter was carried out for the term project for the course *CHE694* Winter 2012*, Thermal analysis* taught by Dr. Yadollah Maham.

Keywords: ODS, bitumen composition, desulfurization, SO_2 release, HPLC analysis of hydrocarbons

3.1 Introduction

The purpose of this study is to investigate the conditions at which model sulfur compounds with a structure similar to the compounds found in bitumen oxidize to sulfones, as shown below:
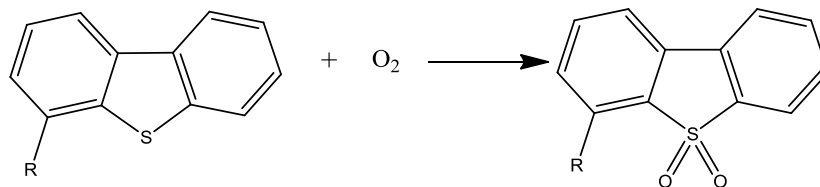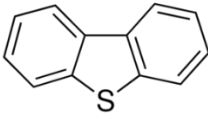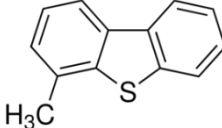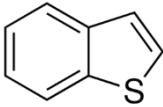
Having an understanding of the thermodynamic conditions at which decomposition of the sulfur compounds occurs at a proper extent, will provide essential guidelines to perform oxidation reactions in actual samples of bitumen.

It has been found that most of the sulfur present on bitumen is found as thiophenes, mainly homologous series of benzothiophene and dibenzothiophene with or without naphthenic rings attached [8]. It is of special interest to study the conditions at which these compounds oxidize under air atmosphere. As might be expected, these high molecular weight compounds are not commercially available. Nevertheless, it was possible to get the following compounds from Sigma-Aldrich: dibenzothiophene, thianaphthene and 4-methyldibenzothiophene, a brief summary of their physical properties is shown in Table 3–1. These compounds have the structural characteristics of typical sulfur compounds present in bitumen [8]; i.e. one aromatic ring attached to a thiophenic ring for the case of benzothiophene, two aromatic rings connected by a thiophene as dibenzothiophene and an alkyl substituted dibenzothiophene. Of course these compounds have a smaller molecular weight than the sulfur compounds in bitumen.

Thermogravimetric analyses were performed on each compound under oxidative atmosphere; air is preferred over oxygen as oxidizing agent, in order to avoid very fast oxidation reactions that may hide some important changes in the samples during TGA and DSC analysis [41]. According to the literature it is possible that the samples may evaporate or sublimate prior to the detection of any oxidizing reaction [41], this was taken into account during the experiments.

The low temperature oxidation of bitumen was previously studied [6, 7] and it was found that for the oxidative desulfurization of bitumen temperatures below 150°C are preferred due to improved sulfur removal, compared to samples treated at 170°C.

Table 3–1. Properties of selected compounds

	COMPOUNDS		
Characteristic	Dibenzothiophene DBT	4-Methyldibenzothiophene 4-MDBT	Thianaphthene BT
Structure			
Purity*	98%	96%	98%
Appearance	White to gray powder with chunk	White to Light Yellow	N/A
Melting point	97-100 °C	64-68 °C	30-33 °C
Boiling Point	332-333 °C	298 °C	221-222 °C
Enthalphy of fusion	114.0 – 117.2 J/g	N/A	88.2 J/g
Enthalpy of vaporization	302.3 J/g	N/A	N/A

* As reported by the supplier Sigma-Aldrich on the specification data sheet for each compound.

3.2   Experimental

3.2.1   Materials.

Dibenzothiophene, 4-methyldibenzothiophene and thianaphtene were purchased from Sigma-Aldrich and were used with no further purification; the purity of these compounds is noted on Table 3–1, as reported by the supplier. Synthetic extra dry air was purchased from Praxair.

3.2.2   Experimental Procedures.

- Thermogravimetric Analysis (TGA): The instrument used was a TA Q500 with an air flow for the sample of 40 ml/min and 60 ml/min for the balance, using platinum open crucibles. The amount of sample loaded was 39 ±2 mg
- High pressure DSC: Analyses were conducted in a Mettler Toledo HP-DCS (Switzerland) equipped with a FRS5 detector, in a static air atmosphere of 950kPa as registered by the cylinder regulator gauge. The crucibles used were standard aluminum with a capacity of 40 μl; these were used without lid in order to allow contact area between the sample and air.
  The temperature program used was from 25°C to 400°C at a heating rate of 10°C/min, performed in 950 kPa of air.
  The instrument calibration was checked by melting Indium, a metal with a well-defined melting temperature and enthalpy of fusion. The values obtained from the check are compared with literature values and if the instrument data lies within the tolerance the check is passed.
- FTIR: An ABB MB3000 unit equipped with a MIRacle^{TM} ATR (USA) sampling accessory was used, the conditions were the following:

  Resolution: 2 cm^{-1}
  Scans: 120
  Acquisition mode: Transmittance
  Wavenumber range: 400 to 4000 cm-1
  Detector gain: 81

3.3   RESULTS.

3.3.1   Atmospheric TGA.

Experiments were performed in air flow. Under atmospheric pressure conditions the only change detected by TGA was the evaporation of these compounds (Figure 3-1), not any sign of chemical reactions. Based on these results, the need to perform experiments at a higher pressure, in order to increase their boiling point and to keep the samples in the liquid state was evident.
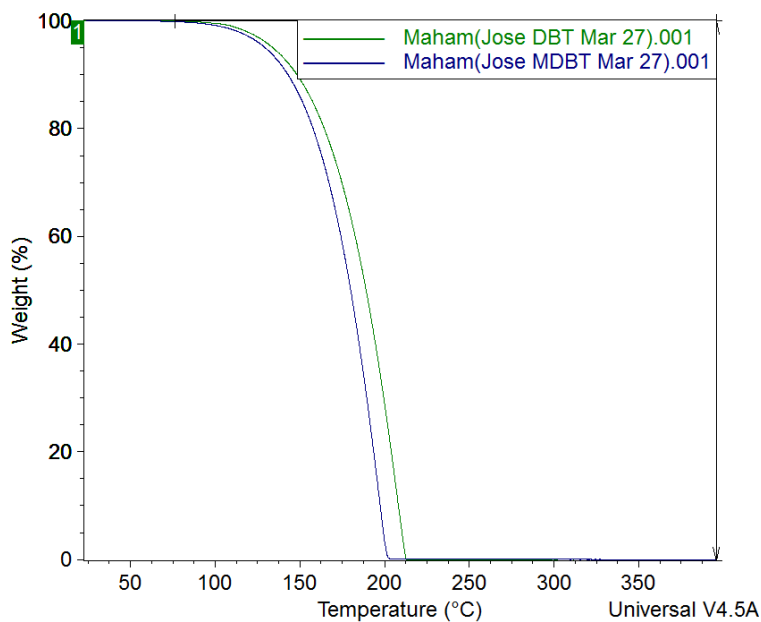
Figure 3-1 Atmospheric TGA Curves for DBT and 4-MDBT in an air flow of 50 ml/min and heating rate of 10°C/min

3.3.2 High pressure Differential Scanning Calorimetry (HPDSC)

In order to get an insight of the behavior of the samples under increased pressure, a set of HPDSC runs were conducted at 950 kPa it is expected that the increase in pressure helps to prevent the vaporization of the compounds by increasing their boiling temperature. Results are shown in Figure 3-2. In all cases the curves are characterized by a first endothermic peak, corresponding, by comparison with the literature values (Table 3–1), to the melting point of each compound. In the case of benzothiophene (BT) and dibenzothiophene (DBT) there is a smooth decline on the baseline after melting and a sharp jump in the heatflow at a certain point. This phenomenon is certainly caused by the evaporation of the sample, and it was confirmed by checking that there was no residue left in the crucibles after analysis. At that moment, with the available equipment it was not possible to operate at higher pressures. 4-methyldibenzothiophene (4-MDBT) on the other side, showed two exothermal peaks in the first set of analyses (238 and 302 °C respectively), which may indicate oxidation reactions. It is important to mention that after analysis of 4-MDBT a darkish, coke like residue was left on the crucible and the sample compartment of the instrument. A summary of the changes observed in Figure 3-2 is presented in Table 3–1.

Due to the negative results obtained with benzothiophene and dibenzothiophene it was decided to put these two compounds aside and continue working only with 4-MDBT, because it is clear that at the working pressure available (950kPa) the samples will evaporate before any oxidation reaction would proceed (Figure 3-2).
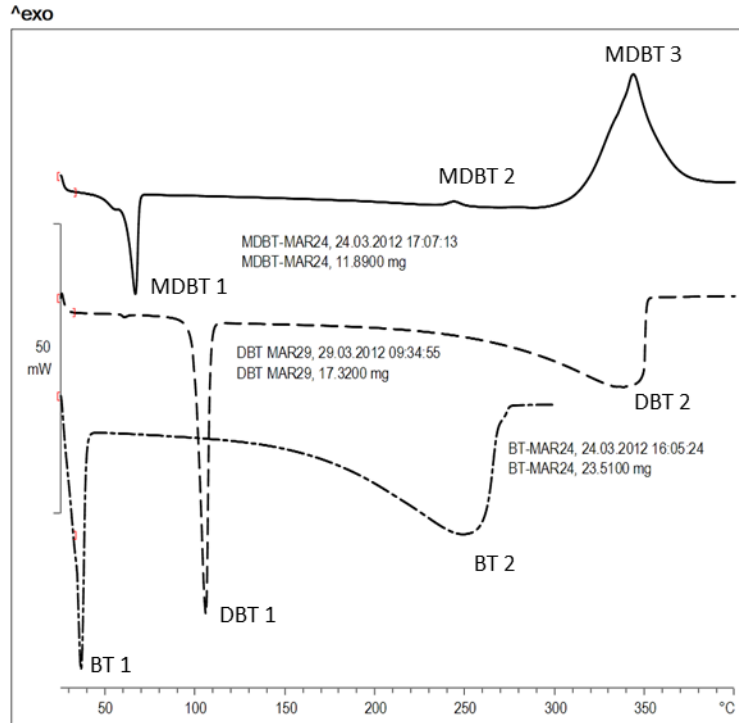
Figure 3-2. Comparison of calorigrams of BT (dot dashed), DBT (dashed), 4-MDBT (Continuous), in 950 kPa of air, performed with a temperature program from 25°C to 400°C β=10°C/min

Table 3–2. Thermal changes detected in the autoxidation of 4-MDBT, DBT and BT (Figure 3-2)

Peak Number	Onset Temperature [°C]	Exo or Endothermic	Heat [J/g]	Expected Cause
MDBT 1	61	Endothermic	-40.04	Melting
MDBT 2	238	Exothermic	5.26	Decomposition of impurities
MDBT 3	302	Exothermic	286.5	Oxidation
DBT 1	100	Endothermic	-112.71	Melting
DBT 2	265	Endothermic	-248.89	Evaporation
BT 1	25	Endothermic	-69.04	Melting
BT 2	174	Endothermic	-301.09	Evaporation

In order to check the detailed behavior of 4-MDBT in air atmosphere, a more complex run was performed as it is shown in Figure 3-3. The detected changes are summarized in Table 3–3, the temperature program applied was the following:

30 – 75°C	β = 2 °C/min
75 – 450 °C	β = 10°C/min
600 °C Isothermal	t = 10 min

The last section of the method was initially conceived merely as a burn off step since residue was accumulating in the sample chamber of the instrument. In Figure 3-3, besides the peaks previously showed in Figure 3-2, a considerably bigger exothermal peak appears when temperature is increased to 450 °C; this peak may correspond to the combustion of the sample residue. However, the reported literature value for the heat of combustion of 4-MDBT is much higher (36351.1±9.7 J/g [42]). The low heating rate program at the low temperature zone (2°C/min) was used up to resolve the hump detected on the melting point peak (Figure 3-2), this hump was resolved in two peaks, #1 and #2 in Figure 3-3 the first one may be associated with an impurity in the product since its purity was of 96%.
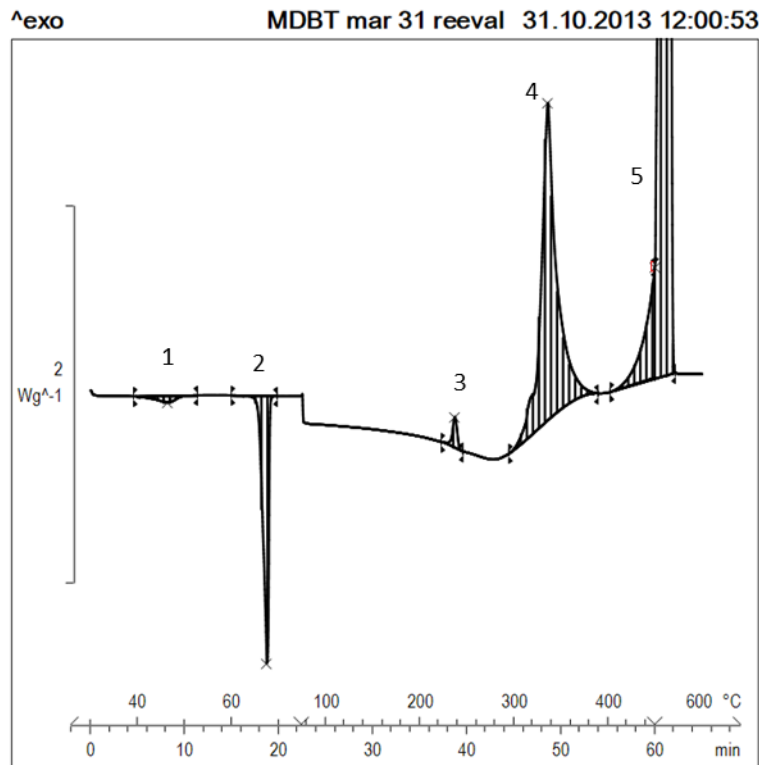
Figure 3-3. HPDSC calorigram of 4-MDBT in 950 kPa of air, the heat evolved in the peak #4 is 197 J/g, peak #5 corresponds to 1009 J/g.

Table 3–3. Detected peaks in the autoxidation of 4-MDBT

Peak Number	Onset Temperature [°C]	Exo or Endothermic	Heat [J/g]	Suspected Cause
1	41.76	Endothermic	-5.01	Solid phase transition or melting of impurity
2	65.97	Endothermic	-57.57	Melting
3	232.83	Exothermic	5.55	Decomposition of impurity
4	324.60	Exothermic	196.98	Low temperature oxidation
5	450 - 600	Exothermic	1009.45	Oxidation, residue combustion

It was speculated that the temperature at which peak #4 in Figure 3-3 occurs might be actually lower. The reason behind that is that oxidation reactions are frequently characterized by the presence of an induction period [43] in which hydroperoxides are formed. In order to verify whether or not the oxidation peak showed by 4-MBDT would appear at lower temperatures, a series of isothermal runs at 100°C, 200°C, 250°C and 300°C were performed for 1 h. The results are shown in Figure 3-4. In all cases, before reaching the isothermal temperature, a temperature ramp starting at 25°C, with a heating rate of 15°C/min was used. As can be observed, there is no presence of peaks after the isothermal temperature is reached below 250°C. In contrast, a broad exothermic peak occurs at 300°C. This result shows that there is a temperature threshold for the oxidation of 4-MDBT under the applied conditions at around 300 °C. However it is possible that the induction times at temperatures of 250˚C and lower are higher than 1h. It is noticeable also that the small exothermic peak that was labeled as #3 in Figure 3-3 is persistent in the calorigrams performed at 250 and 300 °C.

3.3.3   FTIR

FTIR analyses were performed on dibenzothiophene sulfone in order to determine characteristic peaks on the spectra due to the formation of S=O bonds generated by oxidation of the sulfur on the thiophenic compounds, all measurements were performed under the above mentioned conditions.

The absorption frequencies of sulfones have been published extensively. For example Silverstein et al. [44] state that sulfones show strong adsorption bands at $1350 - 1300$ and $1160 - 1120$ cm^{-1} arising from asymmetric and symmetric SO_2 stretching, respectively. And that hydrogen bonding results in adsorption near 1300 and 1125 cm^{-1}. Schreiber [45] defines the zone from 1120 to 1160 cm^{-1} and the zone from 1300 to 1350 cm^{-1} as characteristic of sulfones. Castillo et al. [46] shows the detection of sulfones in oxidized light gas oil (LGO) as 1165 and 1289 cm^{-1}
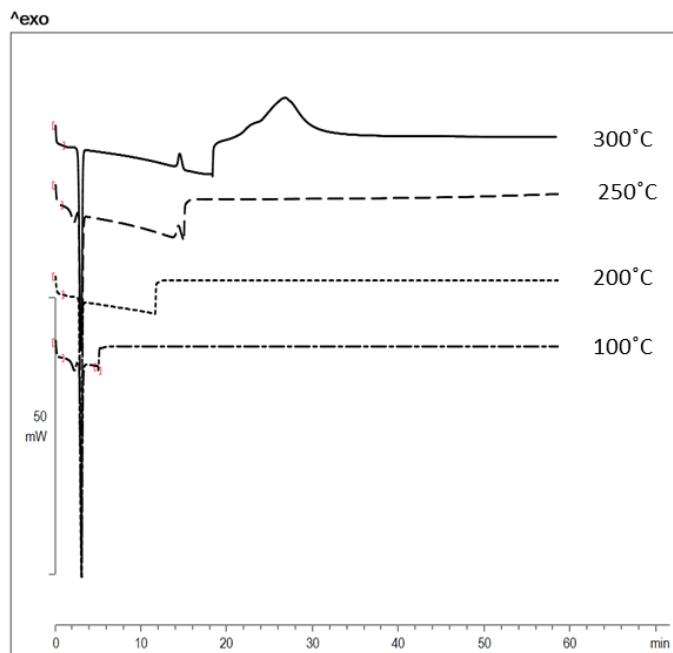
Figure 3-4. Isothermal HPDSC calorigram of 4-MDBT at: 100°C (dot dashed), 200°C (short dashed), 250°C (long dashed), 300°C (continuous), 950kPa of air.
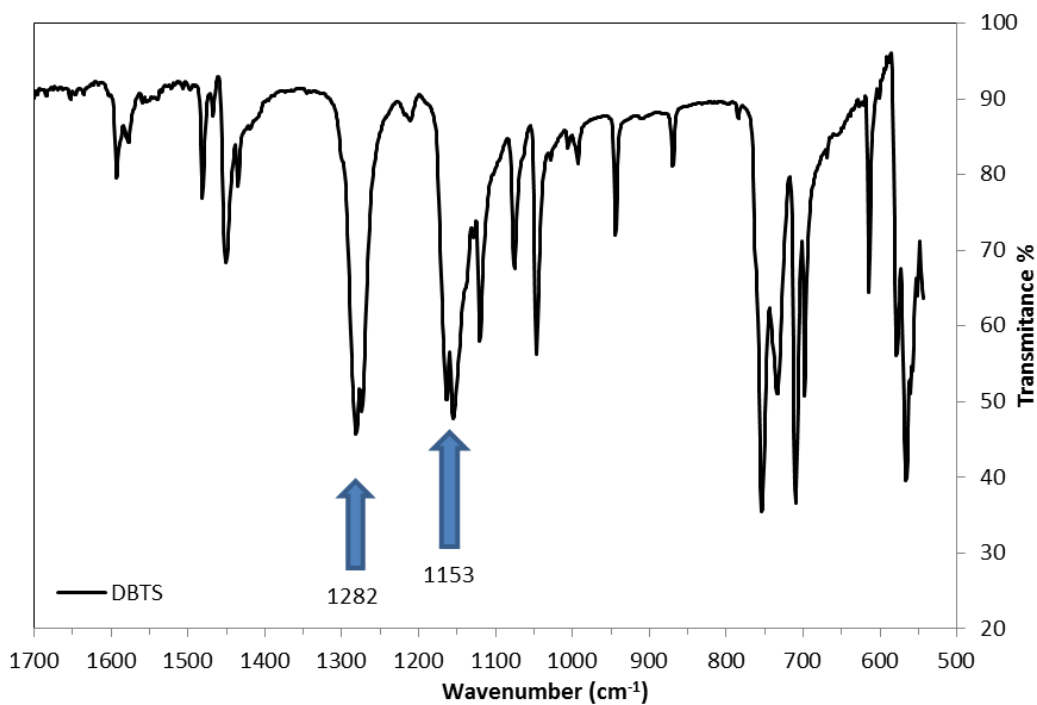
Figure 3-5. FTIR spectra of dibenzothiophene sulfone. The peaks signaled by arrows correspond to the characteristic absorptions of S=O bonds.

In order to get an insight of the behavior of the specific type of sulfones employed, the FTIR spectra of dibenzothiophene sulfone was measured. (Figure 3-5). In this case, the main absorptions associated with the sulfone group are

detected between 1130 and 1180 cm^{-1} and 1250 to 1300 cm^{-1} as well as the characteristic band for aromatic rings between 700 and 800 cm^{-1}.

FTIR analysis for pure 4-MDBT and for the residue left on the DSC crucibles after analysis of 4-MDBT samples was performed, the samples were collected at temperatures close to the ones that showed exothermic peaks in its DSC curve, namely 260°C and 300°C (see Figure 3-4).

The FTIR spectra of the samples after HPDSC analysis and blank (pure 4-MDBT) is shown in Figure 3-6, in this graph the regions enclosed correspond, as mentioned earlier, to the wavenumbers characteristic to sulfones. The first observation is that the sample of 4-MDBT treated at 260°C basically overlaps the spectra of the untreated sample, indicating that no substantial chemical reaction occurred on the sample. On the other hand, the one treated at 300°C is considerably different to the untreated sample. A summary of the changes that are thought to be relevant is presented in Table 3–4.
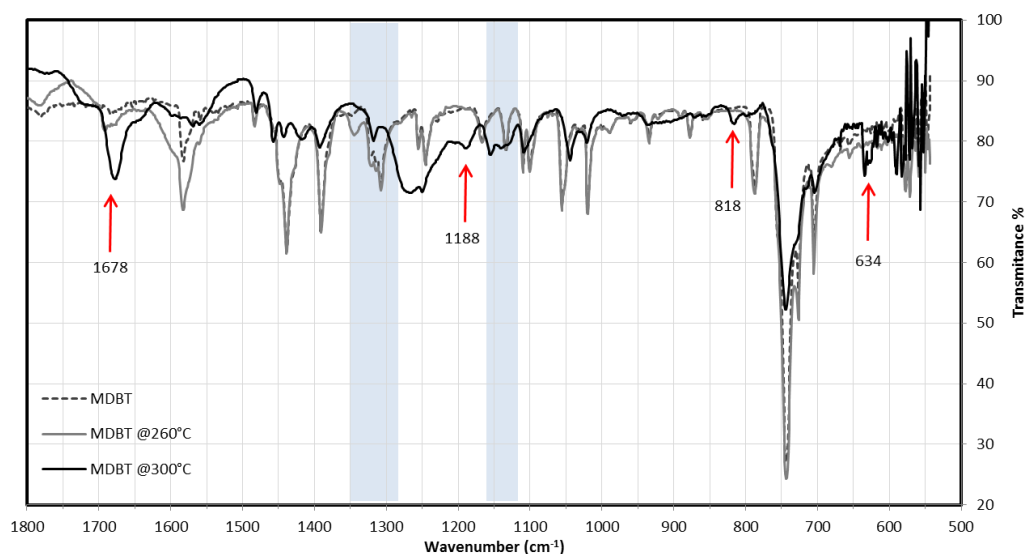
Figure 3-6. FTIR spectra of 4-MDBT thermally treated at 260 and 300 °C in 950 kPa of air on HPDSC and of pure 4-MDBT.

3.4   Discussion

The results of the HP-DSC experiments performed on BT and DBT, showed that in 950 kPa of air, there is no evidence that any oxidation reaction proceeded before the compound vaporizes, it would be then necessary to perform trials at higher pressure. By doing this, two improvements are foreseen. First, the partial pressure of oxygen in the gas phase increases, making more oxygen available; and second, a higher pressure will consequently suppress the vaporization of the compounds allowing to go higher in temperature.

Table 3–4. FTIR absorption changes after oxidation of 4-MDBT

Wavelength [cm-1]	Description	Possible cause
1678	Appearance of a peak	C=O stretch (oxidation)
1580	Reduction of an existing peak	Reduction in C – C stretching
1440	Reduction of an existing peak	Demethylation
1390	Reduction of an existing peak	Demethylation
1318	Appearance of a peak	Sulfone
1188	Appearance of a hump	–
1155	Appearance of a peak	Sulfone
818	Appearance of a peak	–
634	Appearance of a peak	–

4-MDBT showed that the temperature required for oxidation at 950 kPa of air is of approximately 300°C, the product after oxidation clearly shows signs of degradation but failed to become a sulfone which was the desired product. At this point it will be important to determine the influence of a solvent on the oxidation reaction because all experiments were performed on pure components. Some of the changes observed are: Peaks associated with the presence of methyl groups as the symmetrical bending vibration near $1375cm^{-1}$ and the asymmetrical bending vibration near $1450cm^{-1}$ are diminished, this could mean that the oxidation that was observed by HPDSC happens first at the methyl substituent and not at the sulfur atom. On the other hand, some other peaks are present in the sample treated at 350°C that are not in the original sample the appearance of a peak at $1678cm^{-1}$ is likely related to the C=O stretch, this would mean that the CH_3 substituent might have been converted into a ketone.

The reason why BT and DBT did not present any changes during the HP-DSC analysis might be related to their low electron density on the sulfur atom [19, 22], It is known that the reactivity of the sulfur atom is related to electron density (Figure 2–3) it was proven that the order of reactivity for these compounds was 4-MDBT > DBT > BT [16], this graph suggests that the electron density on the sulfur atom in this type of compounds increases with the number of aromatic rings and alkyl groups [2]. This result might explain why on previous works, the oxidative desulfurization of bitumen samples, having large sulfur containing molecules with multiple aromatic rings and alkyl substitutions [8] proceeded at remarkably lower temperatures under air, than the ones used in this work [6]. Also it is worth to mention that in this work, the reaction system was restricted to air and pure compound, this makes the generation of hydroperoxides in the sample difficult. It is known that hydroperoxide species are required in the mechanism that leads to the formation of sulfoxides and sulfones [2, 16, 19]. For future work similar experiments should be performed for the same compounds but in the presence of materials that can be more readily oxidized to generate hydroperoxides.

3.5   Conclusions

- For the three compounds studied there is no evidence that any oxidation reaction proceeds in air at atmospheric pressure, all the samples were vaporized during the DSC and TGA runs.

- For BT and DBT it was proven that no oxidation reaction proceeds on the liquid phase at 950 kPa with air. Under a temperature program these compounds vaporize before exhibiting any exothermal change.

- 4-MDBT exhibits two exothermal peaks during HPDSC analysis, the first one occurring at 237°C and the second one at 311°C. As determined by FTIR, the first peak does not generate changes in the sample's main functional groups hence the detected peak is likely to be associated with an impurity.

- At 300°C the decomposition of the 4-MDBT is evident, after examination of the FTIR spectrum it is suggested that the oxidation occurs in the methyl substituent of the molecule rather than in the sulfur atom, that was evidenced by the suppression of the peaks associated with the methyl group and the appearance of a C=O stretch peak probably generated by a ketone.

4. VISCOSITY BEHAVIOR OF BITUMEN IN AUTOXIDATION - SOLVENT EFFECTS

Abstract

This section deals with the effect that having a solvent in the reaction medium during the autoxidation of bitumen has on the viscosity. Mesitylene was selected as the solvent due to its high boiling point (165 °C) that allows the reaction to be carried out under atmospheric pressure and also, due to its non-hydrogen donor properties. The comparison of viscosities was performed on the basis of equal reaction times and as will be explained, on the basis of solvent saturation of the mixture. A statistical test of the means is also presented in order to confirm if the differences found in the viscosity are significant or not. No attempts were made to describe the oxidation extent achieved; these will be presented in the following chapter.

Keywords: Autoxidation, t-test, viscosity, bitumen, solvent.

4.1 Introduction

The sulfur content of Canadian oil sands derived bitumen is high, typically around 5 wt% [8]. Industrially the sulfur is removed either by coking with part of the sulfur being rejected as coke, or by hydrocracking, with the sulfur being removed as H_2S. One of the technologies that hold promise of reducing material loss and H_2 requirements is oxidative desulfurization (ODS) of the heavy oil [9]. One of the challenges in ODS of bitumen is oxidative bitumen hardening. It was observed that autoxidation of neat bitumen and of bitumen with water, resulted in a measurable increase in viscosity, but not when bitumen was diluted with *n*-heptane (Table 4-1) [6].

Table 4-1. Viscosity of Cold Lake Bitumen Before and After Autoxidation in a Bubble Column at 145 °C for 6 hours.

Material	Viscosity, 60 °C (Pa·s)[a]
Bitumen (neat feed)	10
Autoxidation of bitumen	17
Autoxidation of bitumen:water, 1:1	63
Bitumen:*n*-heptane, 1:0.8 (diluted feed)	0.001
Autoxidation of bitumen:*n*-heptane, 1:0.8	0.001

Viscosity was not meaningfully changed during autoxidation in the presence of *n*-heptane (Table 4-1), but the reason for this was not determined. Since the *n*-heptane was also oxidized [9], it matters from a process design point of view whether oxidation can be performed with neat bitumen and then be diluted to lower viscosity, or whether the diluent played a role during autoxidation, by moderating the free radical addition reactions that causes hardening. Furthermore, some deasphalting occurs when bitumen is diluted in n-heptane, which could also affect the observed viscosity behavior. This chapter will look into the role of the solvent in moderating oxidative hardening during ODS of bitumen. Mesitylene (1,3,5 trimethylbenzene) was selected as solvent due to its high boiling point (T_b=165 °C), its ability to effectively dissolve bitumen without causing asphaltene precipitation and its non-H-donor properties.

The goal of these experimental runs is to differentiate the effect that solvent has on the viscosity when used as a diluent in the oxidation media. Basically there were two possible outcomes expected: the first one is that the solvent is merely acting as an inert diluent, meaning that it will have no interaction with the free radicals that are being formed during autoxidation. The other expected outcome is that the solvent will moderate the viscosity increase by controlling the extent of chain propagation in bitumen but allowing the oxidation of the target species, namely, organic sulfur compounds.

4.2   Experimental

4.2.1   Materials

Canadian Cold Lake Bitumen provided by Imperial Oil was employed as the bitumen feed; some of its properties are provided in Table 4-2.

Table 4-2. Properties of Cold Lake Bitumen

Property	Value
Viscosity	11 Pa·s at 60˚C
API gravity	9.8

ELEMENTAL ANALYSIS

C	H	O	N	S
82.76%	10.03%	1.49%	0.55%	4.49%

SARA ANALYSIS[†]

Saturates	Aromatics	Resins	Asphaltenes
16.8 ± 2.4 %	46.1± 2.7 %	17.7 ± 1.2%	18.7 ± 0.55 %

Mesitylene 98%, Sigma Aldrich Canada, was employed as a solvent without any further purification.

[†] Analysis performed by Mohammad Sidiquee based on ASTM D-2007

Compressed extra dry air, O_2 19.5% - 23.5% from Praxair Canada was used as oxidizing agent.

4.2.2 Experimental apparatus

The apparatus employed for all oxidation reaction is shown in Figure 4-1. It consisted of a 250 ml three neck glass reactor connected to an air supply line on the first neck, to a reflux condenser set to 10°C to allow the exit of excess air and gaseous products, and to a sampling port on the third neck. The temperature level was supplied by an oil bath set on top of a *Heidolph MR Hei-Standard* hot plate; the temperature control was performed indirectly using a *Heidolph EKT Hei-Con* thermometer to control the oil bath temperature.

Flow control of air was performed with a certified Riteflow® rotameter connected on the inlet line.

Viscosity measurements were performed in a *Brookfield DVIII ultra rheometer* using a probe # 14 at 60°C. A rotation speed of 50 rpm was used with a shear rate of 20 s^{-1}

4.2.3 Experimental Conditions

The reaction temperature selected was 140°C. This temperature selection was based on a previous study that showed relatively good desulfurization degree with a moderate increase in viscosity [7]. The reaction time was set at 180 min and the air flow set at 100 ml/min corresponding to 1.3 ml/($g_{bitumen} \times$ min). The bitumen load was 80g and when solvent was used 80g were used as well. The reaction mixture was magnetically stirred using a 2.5cm stirrer at 500rpm.

Solvent was removed from the reaction mixture by vacuum rotary evaporation using a *Heidolph Hei-VAP Advantage ML/G3* rotary evaporator set at 150°C and 10 kPa for 1 hour time.

The mixture was preheated to the reaction temperature and only after the temperature was reached the supply of air started. In this way oxidation was limited during the preheating process.
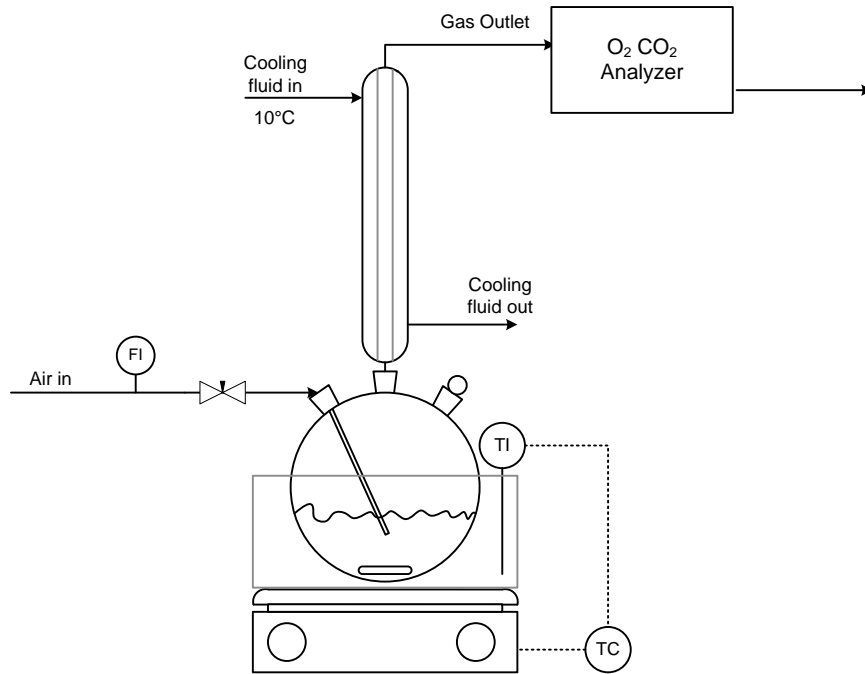
Figure 4-1 Experimental apparatus employed for the oxidation of bitumen.

4.3   RESULTS

4.3.1   Viscosity of oxidized bitumen, with vs. without solvent.

The first set of experiment aimed to compare the resulting viscosity of oxidized bitumen in the absence of solvent with oxidized diluted bitumen once the solvent was distilled off. This experimental methodology is graphically depicted on Figure 4-2 and the results are shown in Figure 4-3.
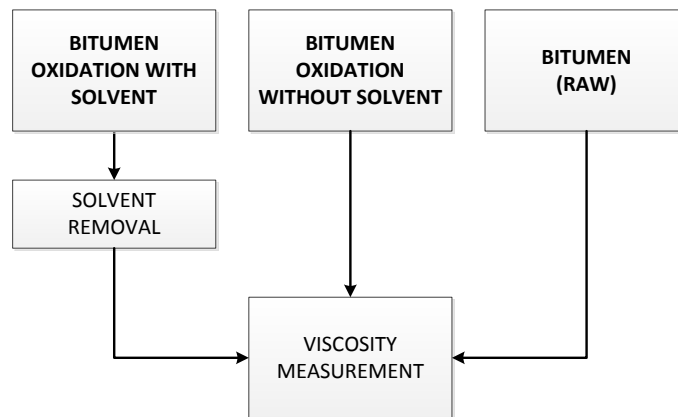
Figure 4-2. Initial experimental methodology for the comparison of viscosity.
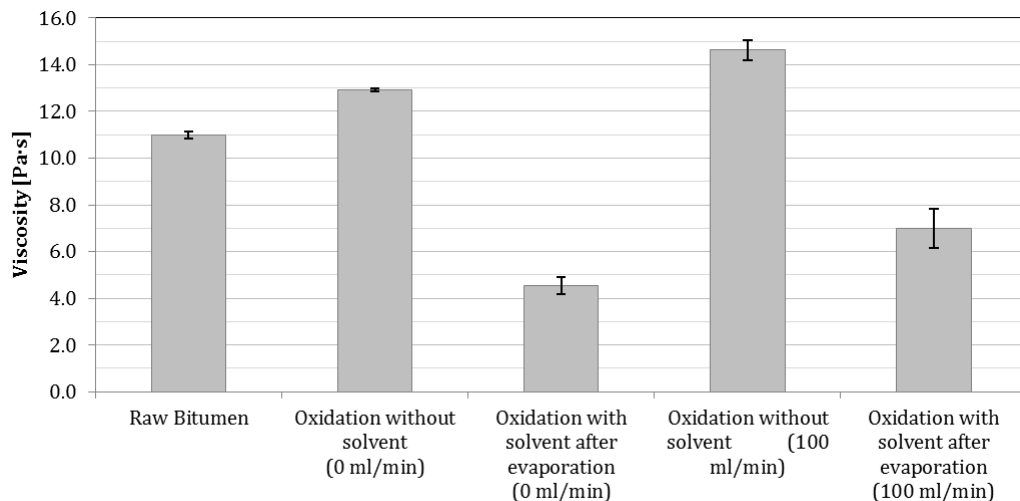
	Bitumen	Oxidized Bitumen - No Solvent - 0 ml/min*	Oxidized Bitumen- No Solvent- 100 ml/min	Oxidized Bitumen- Solvent- 0 ml/min	Oxidized Bitumen- Solvent- 100 ml/min
	Viscosity [Pa·s]				
	10.8	12.9	14.3	4.1	6.1
	11.0	12.9	14.5	4.6	7.0
	11.1	13.0	15.1	4.9	7.8
Mean	11.0	12.9	14.6	4.5	7.0
Standard deviation	0.15	0.04	0.42	0.38	0.85

*Air flowrate.

Figure 4-3. Viscosity results for oxidation of bitumen with and without solvent under two air flow regimes.

At first glance one can tell that the resulting viscosity for samples oxidized with solvent are very low in comparison to the others. This was explained by the fact that it is extremely difficult to completely remove the solvent after reaction by evaporation. Complete solvent removal was not possible even by keeping the temperature level more than 50°C above the equilibrium temperature of the pure solvent at the evaporation pressure, as shown in the vapor curve line of mesitylene (Figure 4-4). The vapor pressure of mesitylene was calculated based on the available Antoine equation parameters [47].
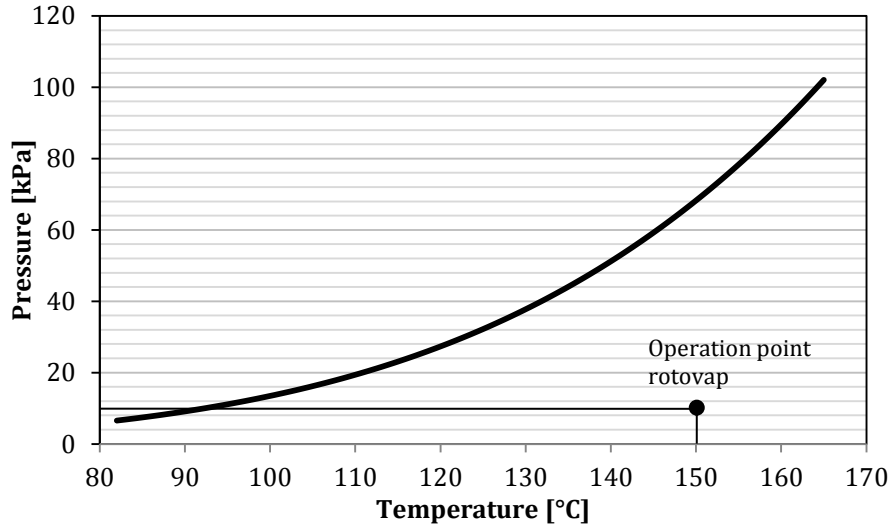
Figure 4-4. Vapor pressure curve for mesitylene showing the operation condition of the rotoevaporator

When performing a mass balance on the evaporation process, an increase of 3 to 8% of the bitumen mass was determined after evaporation, as described in Figure 4-5. This excess weight corresponds to the amount of solvent "trapped" in the bitumen matrix. Of course this outcome made it impossible to compare the viscosity results on the same basis since viscosity is very sensitive to solvent content.
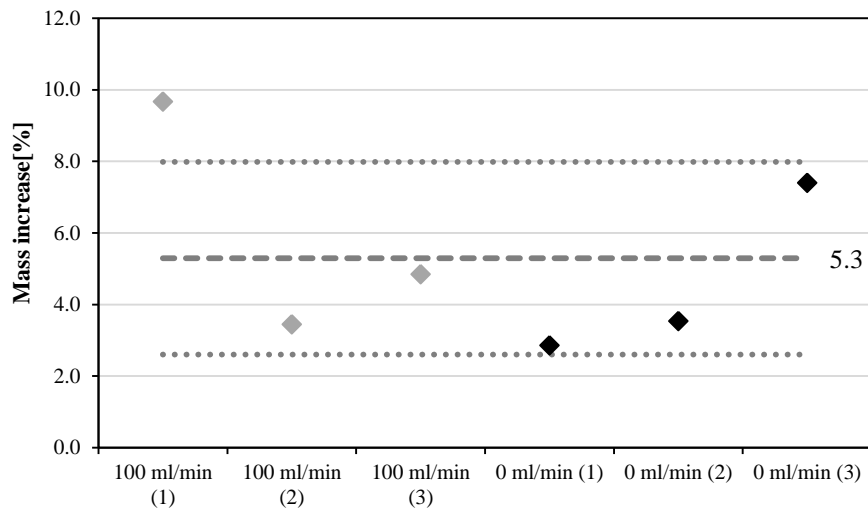
Figure 4-5. Mass increase of bitumen after oxidation due to solvent retention.

However, some learning was achieved from this round of experimental work and particularly this has to do with developing scientific criteria to tell whether or not the measured values for viscosity are statistically different among themselves. This is explained in the following section and will be used later in this work without much further description.

4.3.2 Statistic comparison of results

It is of interest to know if the obtained viscosity values are statistically different among different sets of experiments. For this matter, a statistical inference test for couples of samples was employed in order to determine whether or not the mean values for viscosity were statistically different or not. There are several specific statistical tests that allow one to evaluate hypotheses on the difference or equality of means of populations based on a limited sample number. All of the statistical tests have specific conditions that need to be met beforehand and have to do with the assumption that the studied population falls on a normal distribution, with the assumption that the variances are equal or not and with the knowledge of the population variances.

First of all, a few statistical terms need to be defined before continuing with further explanation of the statistical test employed:

H_0 : Statistic hypothesis
μ_i : Mean of the population
$\bar{X}_i$: Mean of the sample
Δ_0 : Difference in the means of the population
n_i : Number of samples
σ_i^2: Variance of the population
s_i : Standard deviation of the sample
α : Level of significance
j_i : observation number $(1,2,3,\ldots,n_i)$

The conditions assumed for all the statistical analyses were the following:

1. The variances of the population σ_1^2, σ_2^2 are unknown.
2. The variances are not assumed to be equal $\sigma_1^2 \neq \sigma_2^2$
3. The viscosity values follow a normal distribution.

Under these conditions it is possible to establish the following hypothesis $H_0: \mu_1 = \mu_2$; meaning that statistically the mean of the population of the two sets of experiments that are being compared is the same. The alternative hypothesis $H_1: \mu_1 \neq \mu_2$ of course means that the mean values are statistically different. Certainly, the parameters of interest are going to be the mean viscosity values determined for two different sets of samples μ_1 and μ_2 and it is of interest to determine whether $\mu_1 = \mu_2$ or not.

The statistic test under the specified conditions is the following [48]:

$$t_0^* = \frac{\overline{X_1} - \overline{X_2} - \Delta_0}{\sqrt{\dfrac{S_1^2}{n_1} + \dfrac{S_2^2}{n_2}}}$$

And it is distributed approximately as t with v degrees of freedom given by:

$$v = \frac{\left(\frac{s_1^2}{n_1} + \frac{s_2^2}{n_2}\right)^2}{\frac{(s_1^2/n_1)^2}{n_1 - 1} + \frac{(s_2^2/n_2)^2}{n_2 - 1}}$$

If v is not an integer, it should be rounded down to the next integer, this variation of the traditional definition of the degrees of freedom i.e. $v = n_1 + n_2 - 2$ is recommended for the conditions of the analysis. Specifically, that the variances are not assumed to be equal ($\sigma_1^2 \neq \sigma_2^2$).

Once values for t_0^* and v are calculated for every pair of data sets it is then necessary to define the level of significance α at which the test will be performed. A common used value for α is 0.025 meaning a 95% confidence interval. With this information it is possible to look up the percentage points $t_{\alpha,v}$ for the t distribution and compare them with the statistical test performed t_0^*.

In order to support the assumption that measured values for viscosity actually follow a normal distribution, normal probability plots were made for each set of experiments Figure 4-6. As explained by Montgomery [48]. *"If the hypothesized distribution adequately describes the data, the plotted points will fall approximately along a straight line; if the plotted points deviate significantly from a straight line, the hypothesized model is not appropriate. Usually, the determination of whether or not the data plot as a straight line is subjective"*

In assessing the "closeness" of the points to the straight line, Montgomery [48] suggests to imagine a "fat pencil" lying along the line. If all the points are covered by this imaginary pencil, a normal distribution adequately describes the data. Since the points in Figure 4-6 would pass the "fat pencil" test, we conclude that the normal distribution is an appropriate model. It is acknowledged however that the amount of data points is low and the result might not by completely accurate yet it is the best approach available.

In this plot the standardized normal scores (z_j) are plotted against the results for viscosity $x_{(j)}$. The way to calculate z_j is based in the fact that the standardized normal scores satisfy the following:

$$\frac{j - 0.5}{n} = \Phi(z_j)$$

After calculating $\Phi(z_j)$, the values for the z_i can be easily obtained by interpolation from a cumulative standard normal distribution table or using an inverse normal function in Excel (NORM.S.INV()).
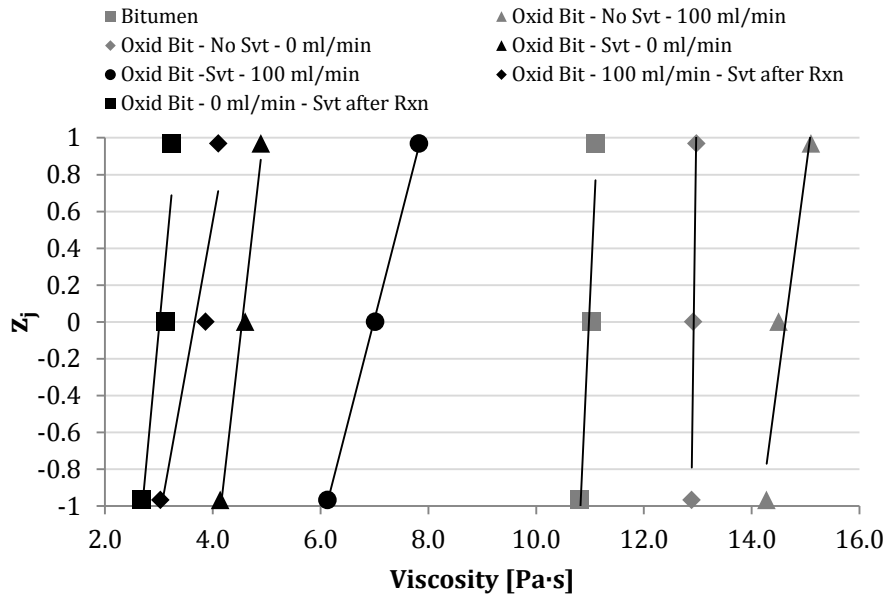
Figure 4-6. Normal probability plots for the viscosity measurements performed on bitumen samples. **Key:** Oxid Bit: Oxidized bitumen, Svt: Solvent, the flow rate (ml/min) is the air flow rate supplied to the reactor.

The summary of the results for the statistical test are reported in Table 4-3. As expected, this statistical test led to the confirmation of the differences among the resulting viscosities under different oxidation conditions.

Table 4-3. Statistical test results for different couples of experiments

Set A	Oxidized Bitumen - Solvent –100 ml/min	Oxidized Bitumen - No Solvent - 100 ml/min	Oxidized Bitumen - No Solvent - 100 ml/min	Oxidized Bitumen - No Solvent - 0 ml/min
Set B	Oxidized Bitumen - Solvent - 0 ml/min	Oxidized Bitumen - No Solvent - 0 ml/min	Bitumen	Bitumen
t_0^*	4.55	6.86	13.96	21.85
ν	2	2	2	2
$t_{\alpha=0.025,1}$	4.303	4.303	4.303	4.303
Test result	$\mu_A \neq \mu_B$	$\mu_A \neq \mu_B$	$\mu_A \neq \mu_B$	$\mu_A \neq \mu_B$

4.3.3 Viscosity of oxidized bitumen, with solvent vs. solvent added after reaction

As mentioned before, it was not possible to compare the obtained results in the first set of experiments due to the solvent retained in the bitumen matrix after oxidation and rotary evaporation. To overcome this matter a "normalizing" step was included in the experimental methodology, this step essentially involved adding solvent in excess to the bitumen samples that were oxidized without any and then remove it with the same rotoevaporation conditions employed for the other samples.
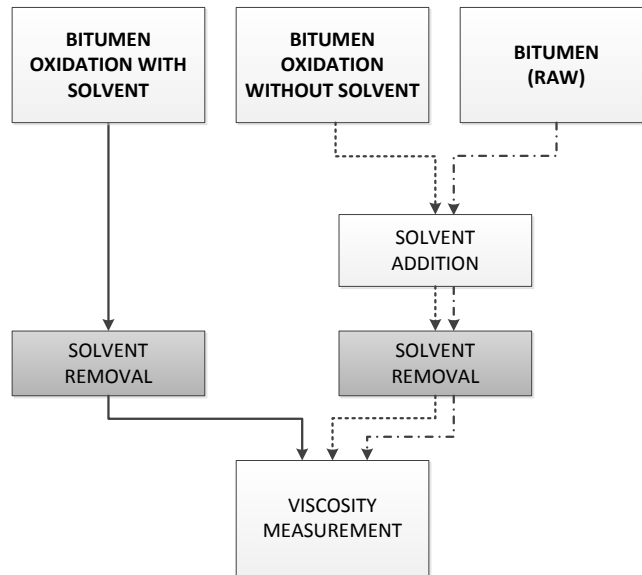
Figure 4-7. Experimental methodology for viscosity determination after a common solvent removal step

It was expected that this step would generate samples that can actually be compared on the same basis. The result for this set of experiment is shown in Figure 4-8. It is evident when comparing the resulting viscosities with the ones shown in Figure 4-3 that these are now closer in magnitude. The results of the statistical analysis for this set of samples are shown in Table 4-4.

The outcome of the statistical analysis including the new set of experiments is that there is not meaningful difference between the viscosities of oxidized bitumen and raw bitumen after the samples are saturated with solvent. Also, in both air flow regimes (0 and 100 ml/min) the resulting viscosity was statistically higher when solvent was used during reaction than when solvent was added afterwards.
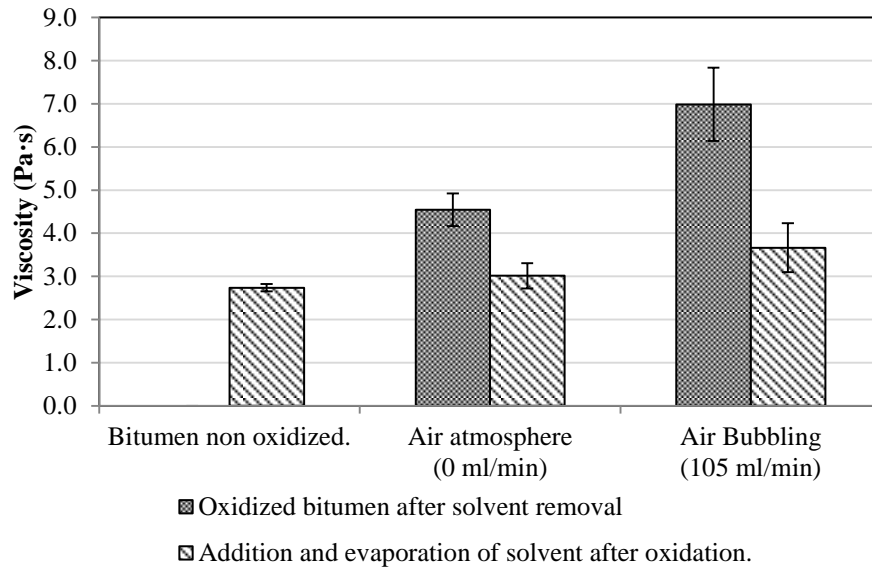
Sample Origin	Oxidized Bitumen - 0 ml/min*	Oxidized Bitumen - 100 ml/min air	Neat bitumen
Viscosity (Pa·s)	3.1	4.1	2.8
	3.2	3.0	2.7
	2.7	3.9	
Mean	3.01	3.67	2.74
Standard deviation	0.29	0.57	0.09

* Air flowrate.

Figure 4-8. Viscosity results for oxidized of diluted bitumen after solvent evaporation (180min at 140°C) and for oxidized neat bitumen (180 min at 140°C) with solvent added after reaction.

Table 4-4. Statistical test results for different couples of experiments.

Set A	Oxidized Bitumen - 100 ml/min* - Solvent after reaction	Oxidized Bitumen - Solvent - 0 ml/min	Oxidized Bitumen - Solvent - 100 ml/min	Bitumen – Solvent
Set B	Oxidized Bitumen - 0 ml/min* – Solvent after reaction	Oxidized Bitumen - 0 ml/min - Solvent after reaction	Oxidized Bitumen - 100 ml/min* - Solvent after reaction	Oxidized Bitumen - 100 ml/min* - Solvent after reaction
t_0^*	1.97	5.55	5.64	2.79
ν	2	3	3	2
$t_{\alpha=0.025,\nu}$	4.303	3.182	3.182	4.303
Test Result	$\mu_A = \mu_B$	$\mu_A \neq \mu_B$	$\mu_A \neq \mu_B$	$\mu_A = \mu_B$

It is possible that the reason for the viscosity difference when bitumen is oxidized in the presence of a solvent has to do with the degree of oxidation reached. As has been reported [49, 50], there is a direct correlation between the degree of oxidation of bitumen and its viscosity. Since the bitumen-solvent mixture is orders of magnitude less viscous than bitumen, it will result in a reduction of the mass transfer limitations during oxidation which might increase the degree of oxidation of the diluted samples and hence the viscosity. This analysis will be subject of study in the next chapter.

4.4   Conclusions

- The employed solvent (mesitylene) does not have a moderating effect in the viscosity behavior of bitumen during autoxidation.
- It is speculated that the higher viscosity obtained for the samples oxidized with solvent is a result of a higher oxidation degree.

5. INFLUENCE OF THE OXIDATION EXTENT ON THE VISCOSITY

Abstract

So far the effect of the oxidation on the viscosity increase was studied only at fixed temperature and reaction times. This chapter aims to generate more information on how the presence of a solvent in the reaction medium affects the degree of oxidation reached. It is shown that in the presence of a solvent, the rate of oxidation is increased. However, the resulting viscosity at same level of oxidation is higher when solvent is used. Also some insight on the effect of temperature on the oxidation level and viscosity is presented.

5.1 Introduction

In the previous chapter it was suggested that mesitylene as a solvent does not have a moderating effect on the viscosity behavior of bitumen during oxidation. The first part of this chapter will address the viscosity behavior of oxidized bitumen diluted and undiluted versus its degree of oxidation. This attempts to question further the reason why the difference in viscosities is observed. This analysis resulted in the conclusion that the difference in oxidation extent among these products was major. As a result, it was possible that the observed difference in the viscosity was caused by the increased amount of oxidized species in the mixture.

To resolve this issue the next set of experiments attempts to compare the viscosity of the products under the same oxygen conversion level, not under the same reaction time. For this to be quantified, an oxygen analyzer was added at the gas outlet of the reactor. On the same direction, a comparison of viscosities resulting from the oxidation of bitumen at different temperatures and those of bitumen oxidized at 140°C for extended periods of time is presented in the final section of the chapter.

The results from these experiments will provide more useful information on the influence of the degree of oxidation on the viscosity of bitumen, as well as useful knowledge on the influence of temperature both on the oxidation degree and on the viscosity.

5.2   Experimental

5.2.1   Materials

The same materials used in Chapter 3 were used for these experimental runs.

5.2.2   Experimental apparatus

The apparatus employed for all oxidation is similar to that presented in Chapter 4. Nevertheless some improvements were made. Heating was no longer supplied by an oil bath but by a solid heating block set on top of a *Heidolph MR Hei-Standard* hot plate and the temperature control was performed directly on the reaction medium. Compare Figure 5-1 and Figure 4-1.

Outlet gas was analyzed online by an *ALPHA OMEGA INSTRUMENTS SERIES 9600 CO_2 and O_2 analyzer* in order to quantify the Oxygen conversion.

Viscosity measurements were performed in a *RheolabQC Anton-Paar viscometer* using a probe CC17 at 60°C. The shear rate employed was 10 s^{-1}.

Elemental analysis of the samples was performed trough an external laboratory, the equipment used was a *Carlo Erba EA1108 elemental analyzer for CHNS and Oxygen*

5.2.3   Experimental Conditions

In contrast to the experiments performed previously the only parameters that were kept constant for the experiments discussed in this Chapter is the air flow which is set at 100 ml/min corresponding to 3.39×10^{-4} $g_{(O_2)} \times$ml $_{(bitumen)}^{-1} \times$min^{-1}, the bitumen load which was 80g and when solvent was used 80g were used as well.

Solvent was removed from the reaction mixture by vacuum rotary evaporation using a *Heidolph Hei-VAP Advantage ML/G3* rotary evaporator set at 150°C and 10 kPa for 1 hour time.
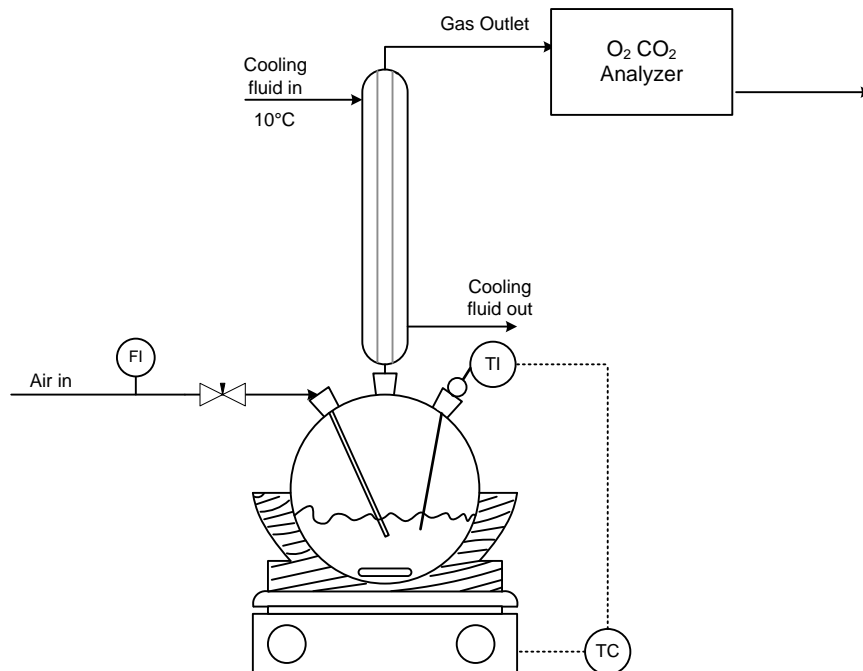
Figure 5-1 Experimental apparatus employed for the oxidation of bitumen.

5.3 RESULTS

5.3.1 Oxidation extent. Diluted vs. undiluted Bitumen.

The same samples used in Chapter 3 were analyzed for oxygen content by duplicate. The results are shown in

Figure **5-2**. As can be observed, the error bars associated with the measurements are very large and overlap each other. Hence, any analysis based on these results is merely speculative.

The amount of oxygen in the oxidized diluted bitumen appears to be higher than that of oxidized neat bitumen. If one compares, the average oxygen increase it shows that the diluted bitumen incorporates 124% more oxygen after reaction compared to the undiluted bitumen. Even though the results are not statistically different, these raise the question of whether or not the higher viscosity of diluted bitumen is associated with the higher oxygen uptake. This result also holds back the conclusion that the use of solvent is not beneficial since it seems to increase the oxidation degree for the same reaction time; probably due to a reduction of the mass transfer limitations in the reactor (lower viscosity). When comparing the oxygen incorporation for bars 2 and 3 in

Figure **5-2** it can be observed that the average oxygen incorporation achieved by the diluted bitumen in three hours is comparable with the neat bitumen oxidized for six hours, twice the time; this outcome is relevant from a process engineering

point of view, since higher oxidation levels achieved in lower times imply that the residence time and therefore the volume of the reactor can be potentially reduced.
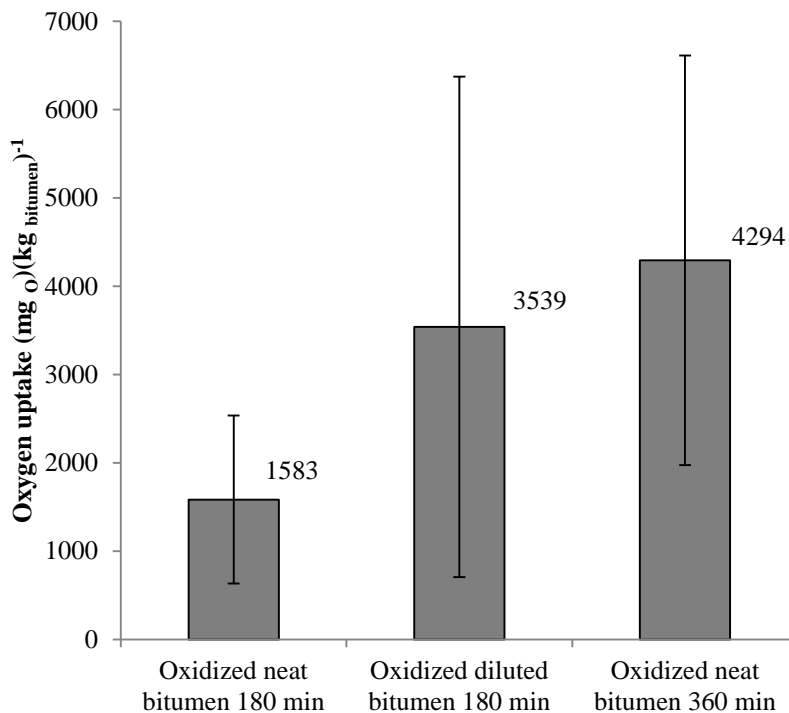
Figure 5-2. Effect of the reaction conditions on the oxygen uptake of bitumen during autoxidation.

5.3.2 Viscosity of oxidized bitumen, with vs. without solvent same oxidation level.

In order to compare the viscosity results of bitumen and diluted bitumen on a more appropriate basis than running the experiments for identical reaction times as described in Chapter 3, a different approach was undertaken. This consisted in comparing the viscosity of oxidized neat and diluted bitumen under approximately same levels of oxidation. For this purpose an O_2 and CO_2 analyzer was installed in the outlet of the gas stream of the reactor to measure the oxygen conversion and CO_2 evolution of the reaction mixture.

By comparing the viscosity at these same levels of oxygen conversion, information about the role of the solvent on the reaction is obtained. It is possible that the resulting higher viscosity associated with the oxidation of diluted bitumen is caused by a higher level of oxidation.

To perform this task it was necessary to establish a basis for comparison. That is, a level of oxygen conversion at which the mixtures of bitumen – solvent will be compared; at this point the reaction is stopped by cutting the air flow and allowing the reactor to cool down. The sum of the average oxygen intake of neat bitumen and that of pure solvent during 3 hours was used as the target value.

The oxygen conversion was calculated by a simple mass balance on the reactor performed at small time intervals. The duration of the time intervals is 8s, defined by the data acquisition interval of the oxygen analyzer which is and adding/integrating the oxygen conversion over the reaction time. The procedure employed is as follows:

$$m_{O_2 in}(dt) = m_{O_2 out}(dt) + m_{O_2 converted}(dt)$$

Under the following assumptions:

$$(T,P)_{air,in} \approx (T,P)_{air,out} \; ; \dot{V}_{air,in} \approx \dot{V}_{air,out} \rightarrow m_{in} = m_{out} \; ; \; \rho_{air,in} \approx \rho_{air,out}$$

The calculation for the O_2 mass from the data provided by the O_2 analyzer is:

$$m_{O_2 in}(dt) = \frac{\% \, O_2 \,(in)}{100} \left[\frac{ml_{O_2}(in)}{ml_{air}}\right] \times \dot{V} \left[\frac{ml_{air}}{min}\right] \times \rho_{O_2} \left[\frac{g_{O_2}(in)}{ml_{O_2}(in)}\right] \times dt[min]$$

$$m_{O_2 out}(dt) = \frac{\% \, \boldsymbol{O_2} \,(\boldsymbol{out})}{\boldsymbol{100}} \left[\frac{ml_{O_2}(out)}{ml_{air}}\right] \times \dot{V} \left[\frac{ml_{air}}{min}\right] \times \rho_{O_2} \left[\frac{g_{O_2}(out)}{ml_{O_2}(out)}\right] \times dt[min]$$

Replacing in the mass balance:

$$m_{O_2 consumed}(dt) = \frac{\% \, O_2 \,(in)}{100} \left[\frac{ml_{O_2}(in)}{ml_{air}}\right] \times \dot{V} \left[\frac{ml_{air}}{min}\right] \times \rho_{O_2} \left[\frac{g_{O_2}(in)}{ml_{O_2}(in)}\right] \times dt[min]$$
$$- \frac{\% \, \boldsymbol{O_2} \,(\boldsymbol{out})}{\boldsymbol{100}} \left[\frac{ml_{O_2}(out)}{ml_{air}}\right] \times \dot{V} \left[\frac{ml_{air}}{min}\right] \times \rho_{O_2} \left[\frac{g_{O_2}(out)}{ml_{O_2}(out)}\right] \times dt[min]$$

Finally the total O_2 conversion is calculated by:

$$m_{O_2 converted}\,(total) = \sum_{1}^{n} m_{O_2 converted}(dt)$$

Note:

As will be seen in the following graphs, the maximum drop in the concentration of O_2 in the air stream is of 1.8% O_2 (Figure 5-5). The assumption of equality in the mass of air in and out of the reactor is affected by the consumption of oxygen by the reaction and also by the generation of H_2O and CO_2; however, after performing a mass balance without taking into account the generation of some CO_2 and H_2O but considering the consumption of O_2 it can be shown that the maximum error on the outlet mass flow associated with this assumption is 2.32%.

A detailed sample of the calculations that lead to this conclusion is presented in Appendix A.

The profiles for oxygen concentration and for oxygen conversion for the previously described runs is presented in Figures 5–3 to 5–5. A summary of the results obtained is presented in Table 5-1. As shown, the average oxygen

conversion to which the diluted bitumen was taken to was approximately 861 g O_2 per kilogram of mixture this value was obtained from the weighted average of the oxidation of neat bitumen and neat solvent for 180 minutes.
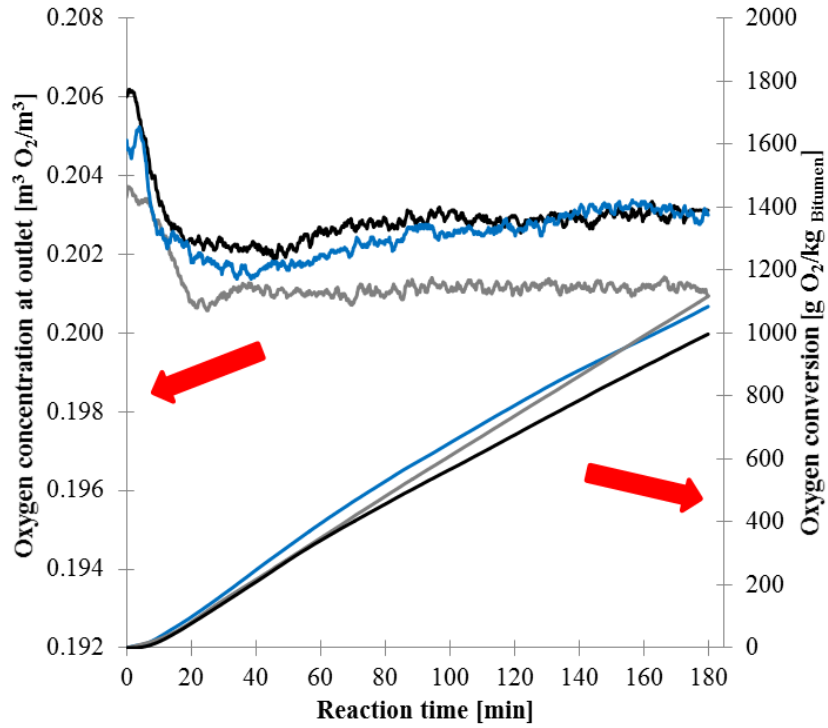
Figure 5-3. Oxygen concentration and oxygen conversion profile for neat bitumen
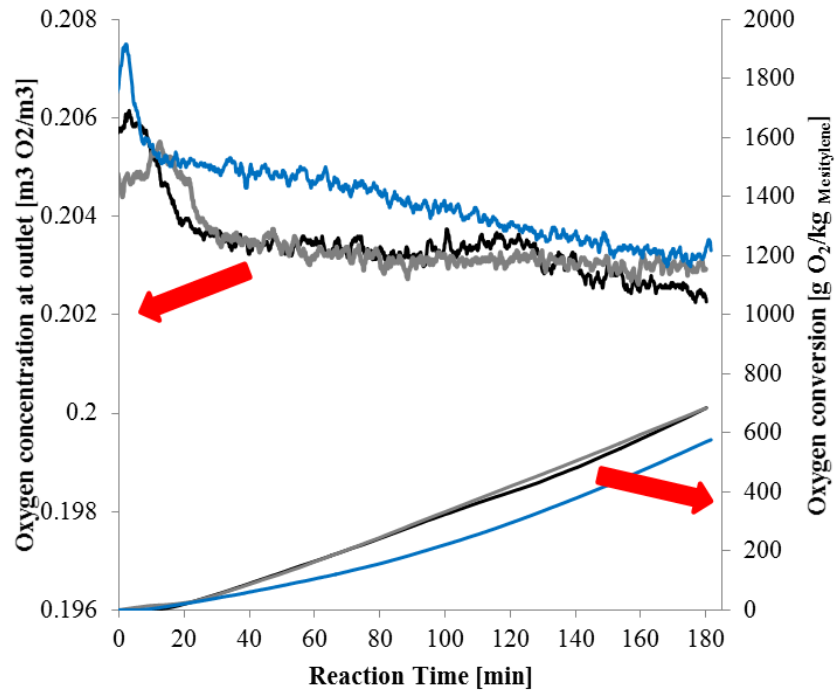
Figure 5-4. Oxygen concentration and oxygen conversion profile for mesitylene
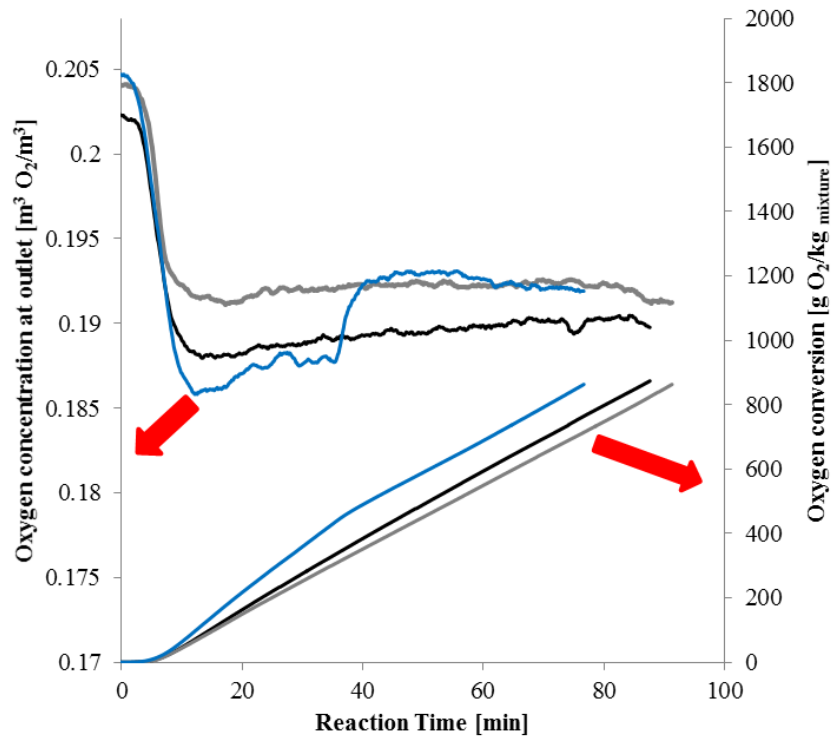
Figure 5-5. Oxygen concentration and oxygen conversion profile for diluted bitumen in mesitylene

Table 5-1. Oxygen conversion after oxidation

Reaction	Run 1	Run 2	Run 3	Average	Standard deviation
A. Mesitylene 3h oxidation [g O_2/kg $_{Mesitylene}$]	685	684	598	656	50
B. Bitumen 3h oxidation [g O_2/kg $_{Bitumen}$]	1117	997	1084	1066	62
Weighted average O_2 Conversion [g O_2/kg $_{mixture}$]				861	
Bitumen - Mesitylene oxidation [g O_2/kg $_{mixture}$]	874	863	863	867	6
Bitumen - Mesitylene oxidation reaction time [min]	87.6	76.7	91.3	85.2	7.6

It is shown in Table 5-1 that the oxygen conversion for neat bitumen is in average 1066 g O_2/kg $_{Bitumen}$. This result is lower compared to what was reported in Figure 5-2 (1580 g O_2/kg $_{Bitumen}$) however it falls within the same order of magnitude and error bars.

The viscosity results for this set of experiments is presented in Table 5-2. These show that the viscosity of oxidized diluted bitumen is apparently higher than the viscosity of oxidized neat bitumen after saturation with solvent. This consolidate the results shown previously in Chapter 3, that the presence of the solvent is not beneficial in moderating the viscosity increase of bitumen caused by oxidation. Additionally, the concentration of solvent in the samples is also reported in Table 5-2 to make clear that the observed differences in viscosity are not caused by solvent content.

Table 5-2. Viscosity results for oxidation of diluted and undiluted bitumen under the same level of oxidation

Category	Oxidized diluted Bitumen		Oxidized Bitumen – Solvent added after oxidation	
Property	Viscosity [Pa·s]	Solvent concentration [wt %]	Viscosity [Pa·s]	Solvent concentration [wt %]
Runs	4.7	4.37	3.5	4.39
	4.5	4.83	3.9	3.21
	4.4	3.91	3.3	4.60
Mean	4.5	4.37	3.6	4.07
Standard deviation	0.15	0.46	0.32	0.75

In order to confirm that the viscosity results are statistically different and that the solvent content in the samples was approximately the same, a statistical test for difference in the means was applied to the data under the same conditions used

previously in Chapter 3 [48]. The result of the statistical test is presented in Table 5-3. As can be seen there, under a 95% confidence interval it can be concluded that the viscosities are truly different; meaning that as suspected, the resulting viscosity of oxidized diluted bitumen is higher than the viscosity of oxidized neat bitumen under the same level of oxygen conversion. And on the other hand, that the concentration of solvent in the samples after evaporation was essentially the same.

Table 5-3. Statistical test result to determine the difference in means of the viscosity of diluted and undiluted oxidized bitumen

Set A	Oxidized diluted Bitumen	
Set B	Oxidized Bitumen – Solvent added after oxidation	
	Viscosity	Solvent Concentration
t_0^*	4.77	0.59
ν	2	3
$t_{\alpha=0.025,1}$	4.303	3.182
Test result	$\mu_A \neq \mu_B$	$\mu_A = \mu_B$

5.3.3   Temperature effect on the viscosity and oxidation level

Some experiments were carried out with the purpose of evaluating the viscosity and rate of oxygen uptake of bitumen under different reaction temperatures. These served two purposes. First, they show how much the rate of oxidation changes with the temperature, and second, detecting whether or not the increase in viscosity is affected, not only due to the oxidation extent, but also by the temperature at which oxidation is carried out. If the reaction temperature plays a major role it would imply that other non-oxidative reactions are taking place in parallel and that these non-oxidative reactions also influence the viscosity increase.

Figure 5-6 shows the oxygen conversion profile as a function of reaction time at different temperatures. It is evident that there is some increase in the degree of oxidation caused by the increase in temperature. The most interesting about this graph is that from 180 to 200°C a jump occurs in the oxygen conversion. This can be associated not only with a higher reaction rate as consequence of the Arrhenius law, but also with a change in the selectivity of the process.
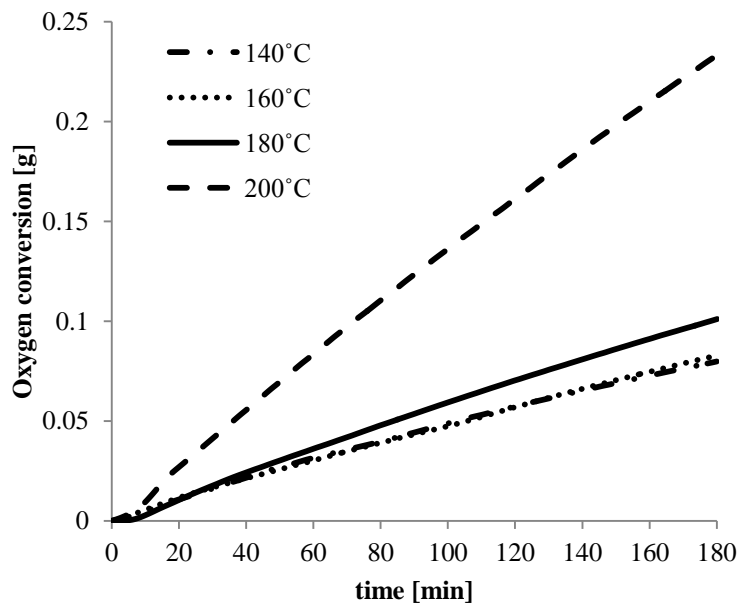
Figure 5-6. Oxygen conversion rate at different temperatures.

As can be observed in Figure 5-7 the temperature at which oxidation is performed affect the viscosity not only through the degree of oxidation attained. This may be caused by differences in the chemical path that the reaction follows. It is quite evident for example that when comparing reaction temperatures of 140, 160 and 180 °C the gain in the oxygen uptake is not measurably different, however the increase in viscosity is noticeable. On the other hand, the profile for the reaction performed at 140 °C over an extended period of time shows a sharp increase in viscosity after a degree of oxidation of 3000 mg O_2/kg bitumen is reached.

The sharp viscosity increase of oxidized bitumen at 140 ˚C can be caused by a change in selectivity happening after long reaction times. It is speculated that the sharp increase in viscosity is caused by bulkier molecules produced by polymerization or crosslinking that are deemed as a main undesired reaction product.
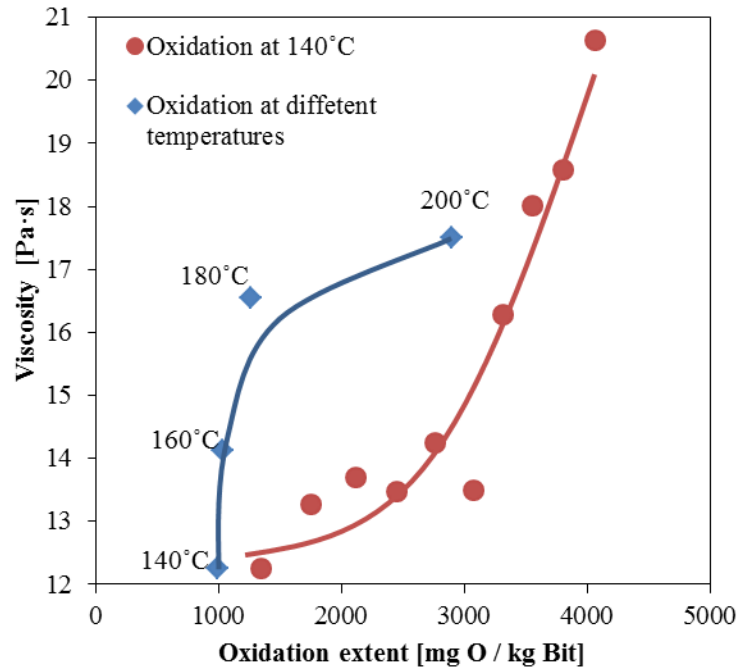
Figure 5-7. Viscosity dependence on the oxidation extent at a single (12 hour run at 140°C) vs. multiple reaction temperatures (3 hour runs) the exposed trends are shown for illustration purposes and are not confirmed statistically.

5.4 Conclusions

- The use of a solvent increases the rate of oxidation of bitumen under autoxidation conditions, this is most likely associated with the reduction of the medium viscosity and hence the reduction of mass transfer limitations.

- At equivalent oxidation extent, the product of oxidation of diluted bitumen shows a higher viscosity than oxidized neat bitumen.

- Besides increasing the rate of oxidation, the increase of temperature dramatically increases the viscosity at same oxidation levels. That might indicate a lack of selectivity at temperatures beyond 140°C

6. THERMOLYSIS AS AN ALTERNATIVE FOR THE REMOVAL OF SO$_2$ FROM OXIDIZED SULFUR COMPOUNDS

Abstract

All the efforts made to oxidize sulfur compounds in bitumen would be worthless if there is not a viable route to remove the produced oxidized species and release the sulfur as SO$_2$. The first section of this chapter explores the release of SO$_2$ from oxidized bitumen by pyrolysis and the effect on the desulfurization level reached. The second section has the purpose to illustrate how some oxidized model compounds, particularly sulfones, behave under pyrolytic conditions and the effect that a hydrogen donor solvent has on the reaction.

Keywords: Pyrolysis, thermolysis, desulfurization, SO$_2$ release, sulfones.

6.1   Introduction

It was mentioned in Chapter 2 that some studies have been carried out on the decomposition of oxidized sulfur compounds e.g. sulfones to SO$_2$. These studies were mainly focused on the catalytic decomposition of feedstocks containing low sulfur concentrations, i.e. ppm range [12, 14, 24, 25]. Very little is published on the thermal decomposition of these compounds. According to published literature [9, 13] the C-S bond is weakened when oxygen is bonded to the sulfur atom as shown Table 6–1; this characteristic leads to the hypothesis that pyrolysis of oxidized organosulfur compounds might be effective for the release of SO$_2$.

Table 6–1. Bond dissociation energy for selected organosulfur compounds.

Compound classes[a]	Bond dissociation energy (kJ mol^{-1})
Unoxidized sulfur	
CH$_3$S-CH$_3$	320
PhS-CH$_3$	290
Oxidized sulfur	
CH$_3$(SO)-CH$_3$	230
CH$_3$(SO$_2$)-CH$_3$	280
Ph(SO$_2$)-CH$_3$	240

[a]Ph = Phenyl group –C$_6$H$_5$

As a first step, samples of oxidized bitumen were subjected to common pyrolytic conditions. The goal of these experiments was to determine whether or not SO_2 was evolved from the reaction mixture and also to check what was the desulfurization level reached versus the product of the pyrolysis of untreated bitumen. These results will indicate if the oxidation of bitumen in some extent generated oxidized sulfur species that are desulfurized by pyrolysis, and on the other hand it will indicate if the desulfurization level after pyrolysis is improved or worsened with oxidation. As a second step, the stability of selected model compounds was studied by means of High Pressure Differential Scanning Calorimeter (HPDSC) aiming to get an insight into the reaction conditions required for the thermolysis and release of SO_2.

One of the most complete reviews on thermochemical properties of sulfones is that made by Herron [13]. Aromatic sulfones are of special interest since these are the derivatives of most organosulfur compounds found in bitumen once they are oxidized, as discussed in Chapter 2. The available data for aromatic sulfones from Herron is shown in Table 6–2. Unfortunately there is no thermochemical information available on benzothiophenic and dibenzothiophenic sulfones in the literature.

Table 6–2. Thermochemical data for selected aromatic sulfones

Name	Formula	$\Delta_f H^0 / kJ\ mol^{-1}$	
		Condensed	Gaseous
Methyl phenyl sulfone	$C_7H_8O_2S$	-345.4±0.9	-253.4±3.1
Diphenyl sulfone	$C_{12}H_{10}O_2S$	-225±1.6	-118.7±3.3
Di-*p*-tolyl sulfone	$C_{14}H_{14}O_2S$	-311.3±0.8	-201.7±3.1
Dibenzyl sulfone	$C_{14}H_{14}O_2S$	-282.6±1.2	-157.1±3.2

In regards to the decomposition behavior of sulfones some work was carried out by Gipstein [51] aiming to determine the effect of the amount of β hydrogen atoms and hydrocarbon structure on the thermal stability of sulfones. β hydrogen atoms refer to the hydrogen atoms attached to the β carbon (α carbons are bonded directly to the sulfur atom and β carbons are bonded to α carbons). Again, just a few aromatic sulfones were considered in this study and none of them were of the benzothiophenic or dibenzothiophenic type. The procedure was to measure the extent of decomposition of the sulfones at 275°C in the absence of a solvent. The main conclusion of this work is that neat aromatic sulfones as diphenyl or dibenzyl are more stable compared to their aliphatic counterparts as shown on Table 6–3 There is some data available regarding phase transition temperatures for sulfones; what is available is shown in Table 6–4 [8-11]. There is not much information on boiling point temperatures, probably because of the fact that these compounds might decompose before boiling.

Table 6–3. Effect of β-hydrogen atoms on the thermal stability of Sulfones at 275˚C for 1 hr

Sulfone	Number of β-hydrogen atoms	Decomposition, mole%
dimethyl	0	0.03
diphenyl	0	0.14
dibenzyl	0	0.73
Isobutyl phenyl	1	1.2
Benzyl butyl	2	1.5
diisobutyl	2	3.1
Dibutyl	4	0.7
Didodecyl	4	0.21
Cyclopropyl phenyl	4	0.84
Isopropyl phenyl	6	2.8
Diisopropyl	12	4.5
Di-*t*-butyl	18	85.8
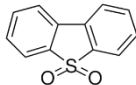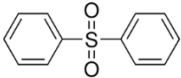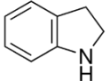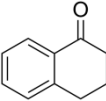
Table 6–4. Melting and boiling points of some sulfones.

Compound	Melting point (˚C)	Boiling point (˚C)
Di-*p*-tolyl sulfone	150 ±8	405
Dibenzyl sulfone	152	290 decomposes
Diphenyl sulfone	127 ±3	379
Methyl phenyl sulfone	88 ±3	
4,6-dimethyldibenzothiophene sulfone	152.8 - 154.2 from[52]	
4-methyldibenzothiophene sulfone	66 from[53]	
Dibenzothiophene sulfone	236.04 from[54]	

From [55] unless otherwise stated.

For the experimental runs performed in this work the compounds present in Table 6–5 were employed. Their properties and structure are shown as well. The use of indoline and α-tetralone will be explained later in the Chapter.

Table 6–5. Properties of model compounds used in this study.

Compound	Structure	Purity	Appea-rance	Density [kg/m^3]	MW [g/mol]	Melting Point [˚C]	Boiling Point [˚C]
Dibenzothiophene sulfone		97%	White needles	-	216.26	236	N/A
Diphenyl sulfone		97%	White powder	-	218.27	124-130	379
Indoline		99%	Yellow liquid	1063	119.16	–21	220-221
α-Tetralone		97%	Amber liquid	1099	146.19	2-7	113-116 [6 mmHg]

6.2   Experimental

6.2.1   Materials

- Raw bitumen was provided by Imperial Oil
- Oxidized bitumen is the product of oxidation of bitumen for a reaction time of 3 h. The method for the oxidation is previously described in Section 4.2.
- Dibenzothiophene sulfone, diphenyl sulfone, α-tetralone and indoline were purchases from Sigma Aldrich and used without further purification, their properties are listed in Table 6–5.

6.2.2   Experimental apparatus

Pyrolysis of neat and oxidized bitumen was performed in a batch 20ml stainless steel (Swagelok) micro autoclave in nitrogen atmosphere. The temperature control was provided by a fluidized bed sand bath.

Pyrolysis of sulfones was performed initially in a High Pressure Differential Scanning Calorimeter HPDCS (Mettler Toledo, Switzerland) equipped with a FRS5 detector. The crucibles used were standard aluminum with a capacity of 40 μl; these were used with a pinhole in the lid in nitrogen atmosphere. The specific temperature program is detailed for every case. Furthermore, some pyrolysis runs for the sulfone model compounds were performed under the same conditions used for bitumen aiming to obtain enough sample for complementary analyses.

Collected pyrolysis gas was analyzed by means of mass spectrometry in an OMNI Star[TM] GSD 320 O1 Quadrupole Mass Spectrometer (Pfeiffer Vacuum) at 500ms/amu using a Faraday detector.

An ABB MB3000 FTIR, equipped with a MIRacleTM ATR (USA) sampling accessory was employed for FTIR the analysis of the liquid samples. With this technique changes in the functional groups of the samples were to be detected.

6.3   RESULTS

6.3.1   Pyrolysis of oxidized bitumen

In order to determine that some of the sulfur compounds in bitumen would liberate sulfur as SO_2, the following approach was established: Some of the sulfur compounds in bitumen must be converted to sulfones or similar oxygenated compounds during reaction, these compounds when subjected to thermolysis should release the sulfur as SO_2 due to the susceptibility of S-C bonds to be thermally cleaved [26].

Samples of oxidized and raw (non oxidized) bitumen were pyrolyzed in 2100 kPa of Nitrogen at 400˚C for 1.5 hours in order to check if the resulting pyrolysis gas contained SO_2. The gas was collected and analyzed by mass spectrometry aiming to detect the peaks in the characteristic spectra of SO_2 (Figure 6-1). The resulting spectra are shown in Figure 6-2 and Figure 6-3. If SO_2 is detected only in the gas originated from oxidized bitumen, which may indicate the presence of oxidized sulfur compounds.
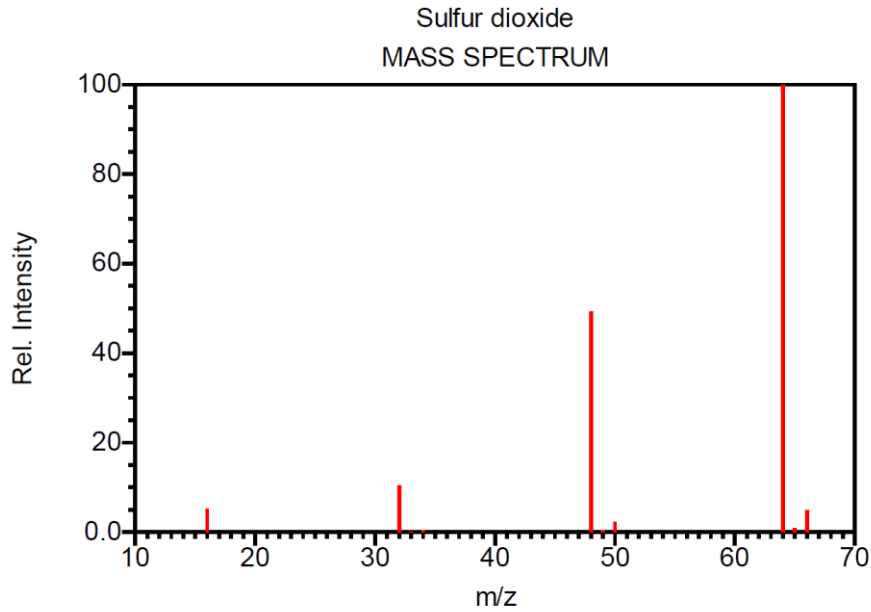
Figure 6-1. Electronic Ionization Mass Spectrometry (EIMS) spectra of SO_2 [56].
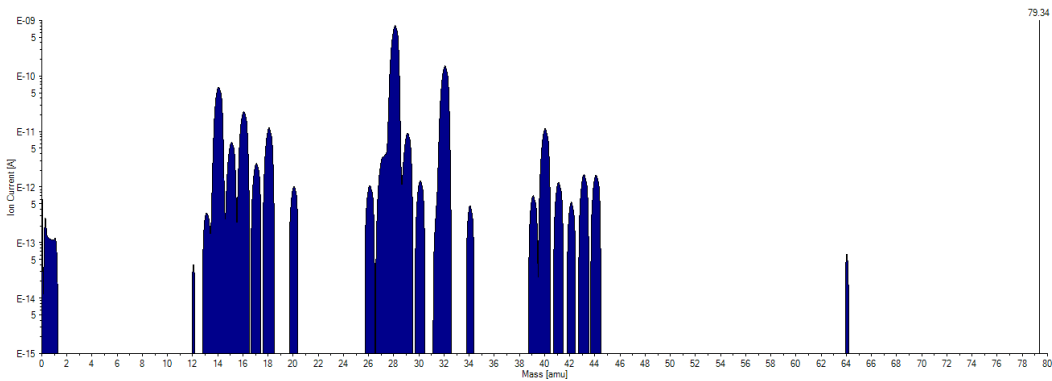
Figure 6-2. Spectrum of the pyrolysis gas from raw Cold Lake bitumen.
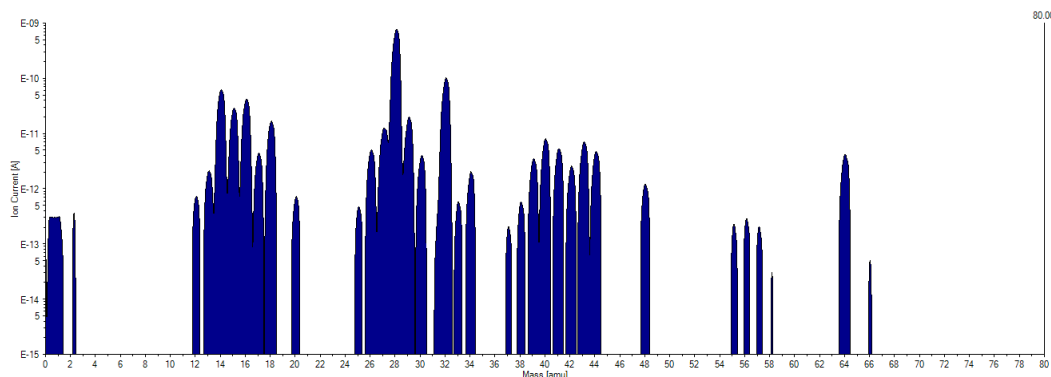
Figure 6-3. Spectrum of the pyrolysis gas from oxidized Cold Lake bitumen.

As can be seen in the spectra, there is a presence of peaks representative of SO_2 (64, 66 and 48 m/z) in the sample coming from oxidized bitumen (Figure 6-3). These peaks do not appear together in the spectra for the gas coming from raw bitumen where only a small peak at 64 m/z is encountered. This result indicates that at least some of the sulfur components originally present in bitumen were oxidized effectively and that they can liberate to SO_2 during pyrolysis.

In order to quantify what was actually the extent of sulfur release in the pyrolysis, the resulting oil was analyzed for sulfur obtaining the following results.

Table 6–6. Sulfur content of pyrolysis oil from oxidized and raw bitumen.

Description	Sulfur Content		Sulfur Release
	S wt	s %RSD	On pyrolysis (%)
Pyrolysis oil from raw bitumen	3.74	0.44	31.0
Pyrolysis oil from oxidized bitumen [3h 100ml/min]	3.71	1.81	35.9
Cold Lake Bitumen	4.58		-

For the pyrolysis of oxidized bitumen, the release of sulfur as gas product, namely SO_2 and H_2S, is only 4.9% higher than the pyrolysis of untreated bitumen. It is speculated that the reason for that increase is the ease of release of SO_2 versus H_2S during pyrolysis. However this decrease in sulfur content after pyrolysis is not quite significant. After performing a statistical test on the means (Table 6–7), with the same procedure employed in Chapter 4 it is shown that the values for sulfur content are statistically equivalent.

Table 6–7. Statistical test on the means of sulfur content of pyrolysis oil from neat and oxidized Bitumen.

Set A	Pyrolysis oil from Raw Bitumen
Set B	Pyrolysis oil from oxidized bitumen
t_0^*	0.432
ν	1
$t_{\alpha=0.025,1}$	12.706
Test result	$\mu_A = \mu_B$

On the other hand, it is key to mention that even if the release of sulfur is not dramatically higher in the case of oxidized bitumen the fact that some of the sulfur is rereleased as SO_2 vs. H_2S carries the implicit advantage that the sulfur atom is not leaving with hydrogen atoms as H_2S, but some of it as SO_2 preserving the hydrogen content in bitumen. This is explained next using idealized reactions paths.

When dibenzothiophene is desulfurized by pyrolysis it requires four equivalents of hydrogen free radicals to generate the desired product and stabilize the hydrocarbon, two of these radicals leave the liquid phase as H_2S.
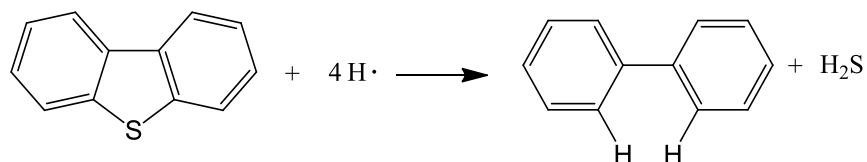
On the other hand, the pyrolysis of dibenzothiophene sulfone only requires 2 equivalents of hydrogen free radicals and the gaseous product do not carry any hydrogen. In this way, the amount of hydrogen in the liquid is better preserved. These reactions are idealized and do not include the potential generation of water as a byproduct.
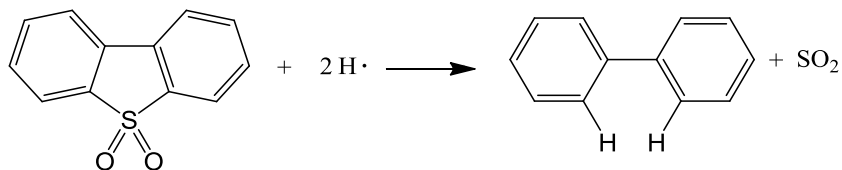
6.3.2 Thermolysis of Sulfones in the absence of solvent

The thermal stability of dibenzothiophene sulfone (DBTS) and diphenyl sulfone (DPS) was determined by differential scanning calorimetry. The experiments were performed in a Mettler Toledo HPDSC-1 in nitrogen at 6MPa without purge

gas. The temperature program used is 100˚C to 550˚C at a heating rate of 10˚C/min.

The DSC analysis of pure sulfones (Figure 6-4) shows that heating in a nitrogen atmosphere results in decomposition only at elevated temperatures, for the case of DBTS the decomposition starts around 505˚C, for DPS two changes are detected, there is a small change in the slope at 375˚C and what seems to be the actual decomposition starts around 537˚C.

What is clear from these results is that sulfones are thermally stable even at high temperatures; it is possible that the thermal stability of these compounds is caused by the absence of easily transferable hydrogen or hydrogen donating species in the medium. However, it is pertinent to recall that the conditions used for the catalytic SO_2 removal from sulfones has been carried out at temperatures around 475˚C [12, 24, 25]. Removing SO_2 from sulfones is not easy, that is why it is pertinent to determine how these compounds behave in pyrolytic conditions when diluted in a hydrogen donor solvent. Some experiments have shown that the solubility of sulfones in a typical hydrogen donor solvent, such as tetralin, is too low to be able to detect chemical changes on the sulfone by DSC [57]. This is attributed to the polar nature of the sulfones. In a way to work around this issue, some compounds were found that are able to behave as hydrogen donors while being polar in nature. Dutta et.al. [58] used tetrahydroquinoline and indoline as hydrogen donor solvents for the thermal upgrading of petroleum residues. On the other hand a molecule like α-tetralone (Table 6–5) with a structure similar to tetralin should also have a hydrogen donor capability, tetralone was then included as a potential polar hydrogen donor solvent.
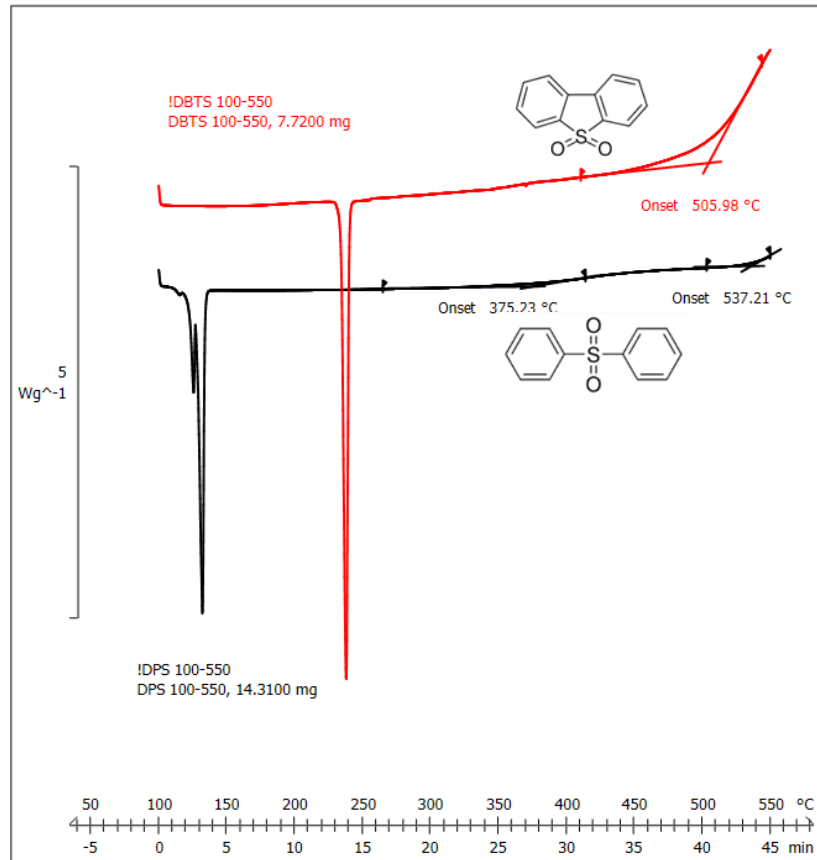
Figure 6-4. HPDSC curves for dibenzothiophene sulfone (up) and diphenyl sulfone (down) carried out in 6 MPa of N$_2$.

6.3.3 Thermolysis of Sulfones with solvent.

Saturated solutions of DBTS and DPS were prepared both in α-tetralone and indoline with the purpose of reaching the highest concentration possible. The runs were performed in a HDSC-1 (Mettler Toledo) in nitrogen atmosphere at 4 MPa. Purge gas flow was set at 50 ml/min (standard conditions) by means of a Brooks mass flow controller and the pressure was kept constant by a Swagelok back pressure regulator. The temperature program used is 100˚C to 450˚C at a heating rate of 15 ˚C/min.

When evaluating the thermal behavior of pure α-tetralone, it was seen that it only undergoes evaporation (Figure 6-5). When mixtures of diphenyl sulfone (DPS) and tetralone were analyzed, besides a considerable reduction in the evaporation of the solvent likely due to the reduction of its vapor pressure in solution, a recurrent small yet noticeable exothermic peak was detected at 330 ˚C, this peak may indicate the reaction between the solvent and the sulfone, possibly a hydrogen transfer. This is followed by a change in the curve slope at around 430 °C a positive increase in the slope make evident the occurrence of decomposition or an exothermic transformation. A very similar behavior is detected for samples of α-tetralone with dibenzothiophene sulfone (DBTS) with the only difference

that the onset temperature is slightly lower 303˚C (Figure 6-6). Once again a positive change in the slope around 420°C evidences the decomposition of at least one component of the mixture.
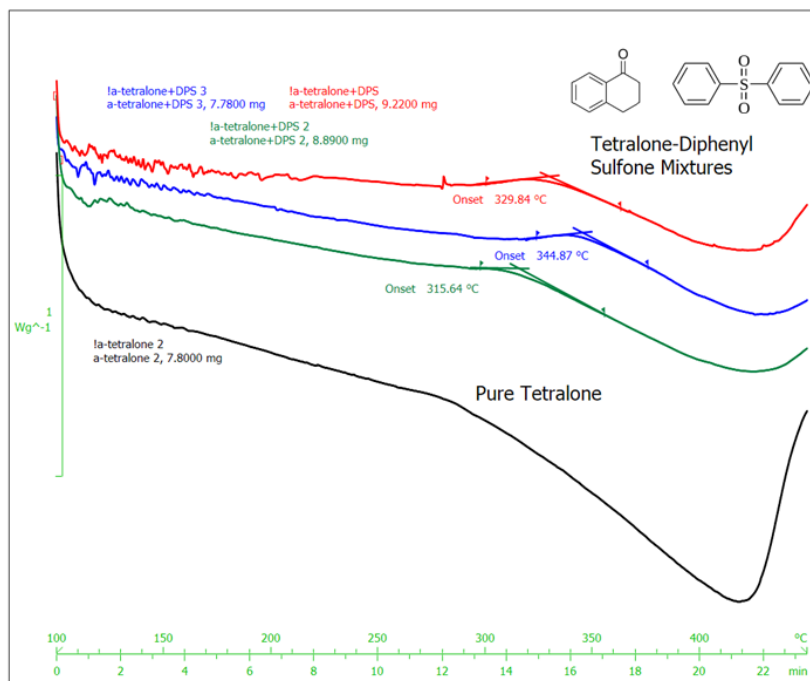
Figure 6-5. HPDSC curves for neat α-tetralone (bottom) and for saturated solutions of DPS in α-tetralone.
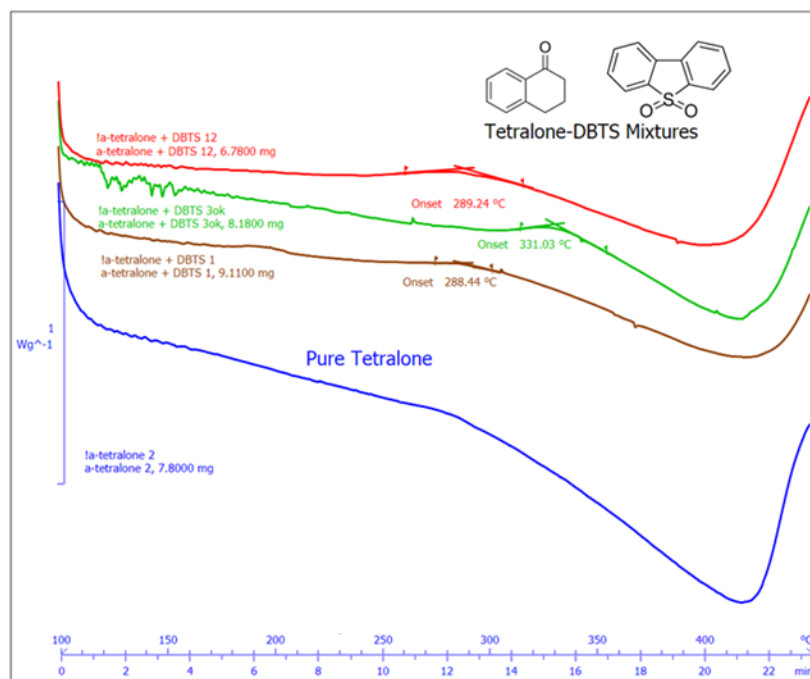
Figure 6-6. HPDSC curves for neat α-tetralone (bottom) and for saturated solutions of DBTS in α-tetralone.

In the case of indoline pyrolysis, a sharp decomposition peak was detected at 290˚C (Figure 6-7); the residue of this analysis was a coke like solid. Surprisingly, when mixtures of indoline with the sulfones DPS and DBTS were analyzed, these resulted in the suppression of the decomposition peak. It is possible that this effect is caused by a stabilization of the solvent in the presence of the sulfones.

Similar to the case of α-tetralone as a solvent, a very small exothermic peak is detected when a mixture of DPS and indoline is analyzed (Figure 6-7). This is followed by a change in the curve slope which is associated with evaporation. The onset for this exothermic peak is 258˚C the decomposition at 420°C still undergoes with this solvent. Indoline – DBTS mixtures show a change in the slope of the DSC curve but do not show a defined exothermic peak (Figure 6-8), however the decomposition detected for DBTS in tetralone at 420°C is now drifted at slightly lower temperatures in indoline 410°C roughly.
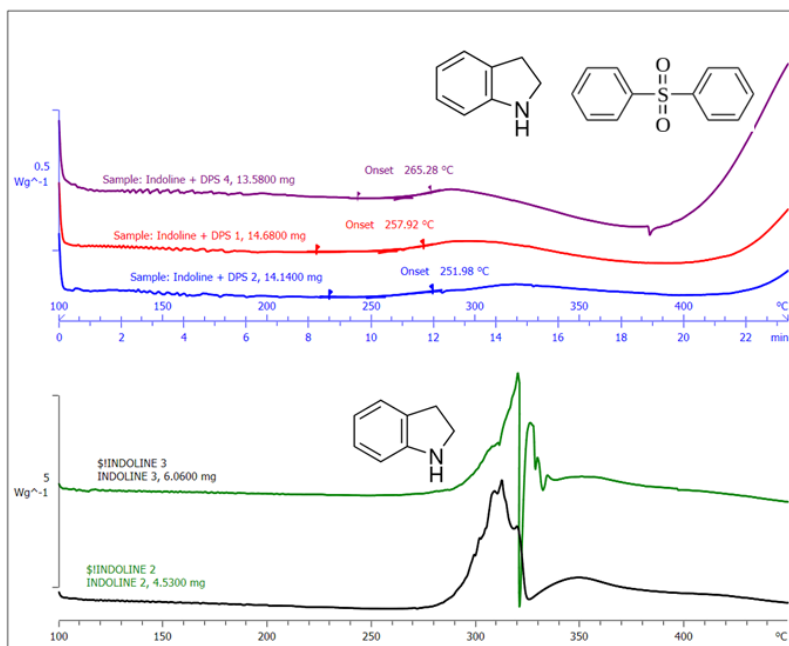
Figure 6-7. HPDSC curves for neat indoline (bottom) and for saturated solutions of DPS in indoline.

6.3.4 ANALYSIS OF PRODUCTS

Since the amount of sample used in the previous DSC analyses is very small, it is very difficult to analyze the same sample by other analytic techniques, it is important however to have an indication of the nature of the reaction products. In order to achieve this, samples of the sulfone-solvent mixtures were subjected to pyrolysis with the purpose of recovering enough sample mass to perform additional analyses; specifically MS and FTIR were of interest.
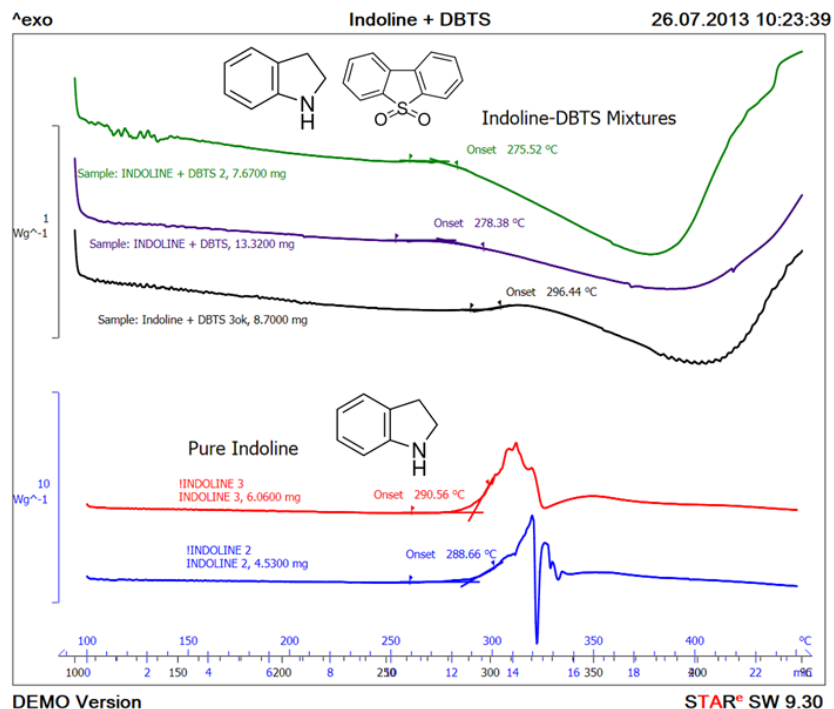
Figure 6-8. HPDSC curves for neat indoline (bottom) and for saturated solutions of DPS in indoline.

Reactions were performed in stainless steel microautoclaves immersed in a sand fluidized bed, under the following conditions.

Sample amount	1 g
Time	30 min
Sand bath temperature	290 ˚C
Atmosphere	N_2 - 4 MPa

The temperature was selected based on the small peaks that appeared to be recurrent in Figure 6-5 to Figure 6-8. If these peaks are associated with the release of sulfur dioxide from the sulfone, then the analysis of the liquid and gas product should be able to evidence it. FTIR is used to detect changes in functionality in the liquid and Mass Spectrometry aims to directly detect sulfur dioxide in the gaseous product, similar to Section 6.3.1.

a) FTIR

Figures 6-9 and 6-10 show the FTIR spectra of the liquid product of the pyrolysis of solutions of diphenylsulfone and the chosen solvents. At first sight not many differences are observed. It is clear however that a band appearing around 2360 cm^{-1} is common in the pyrolyzed product both for tetralone and indoline as solvent. Unfortunately this band does not seem to be characteristic for the expected product that is benzene. It is possible that this 2360 cm^{-1} absorption is caused by CO_2 absorbed in the liquid.
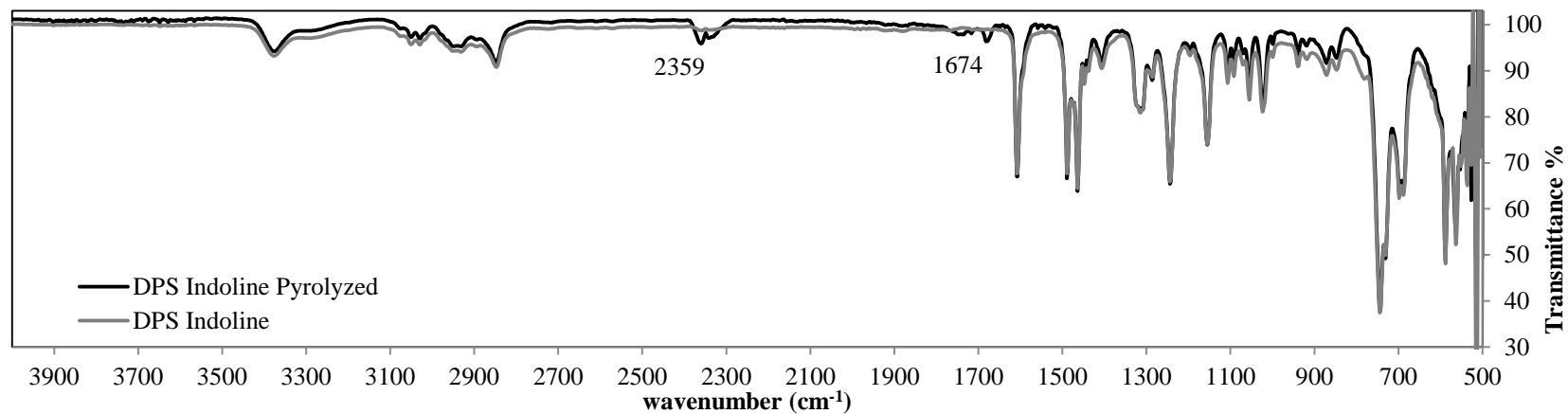
Figure 6-9. FTIR spectra of a DPS-indoline solution and its pyrolyzed counterpart.
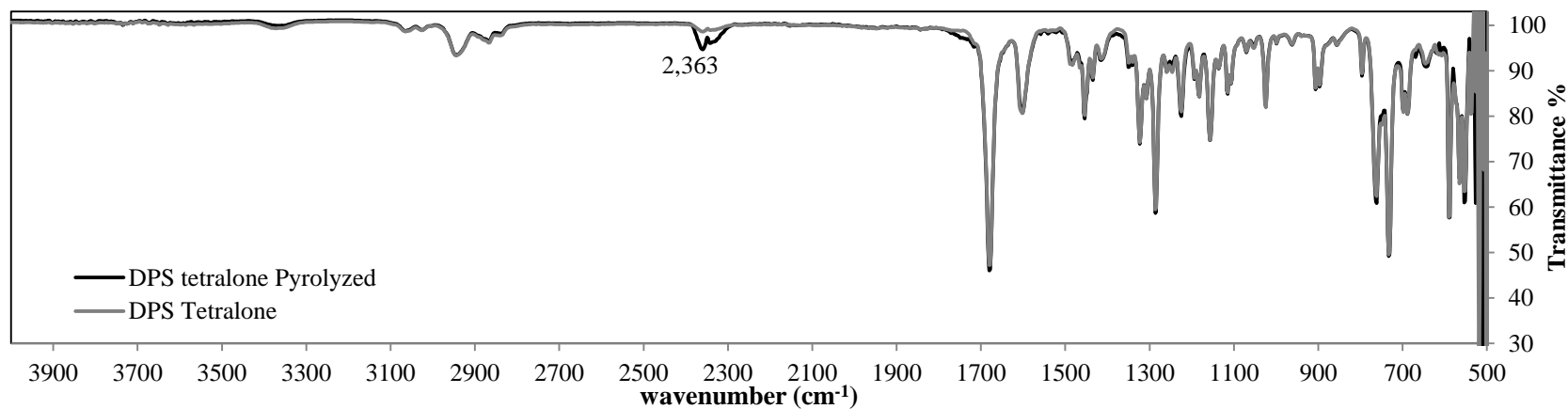
Figure 6-10. FTIR spectra of a DPS-α-tetralone solution and its pyrolyzed counterpart.
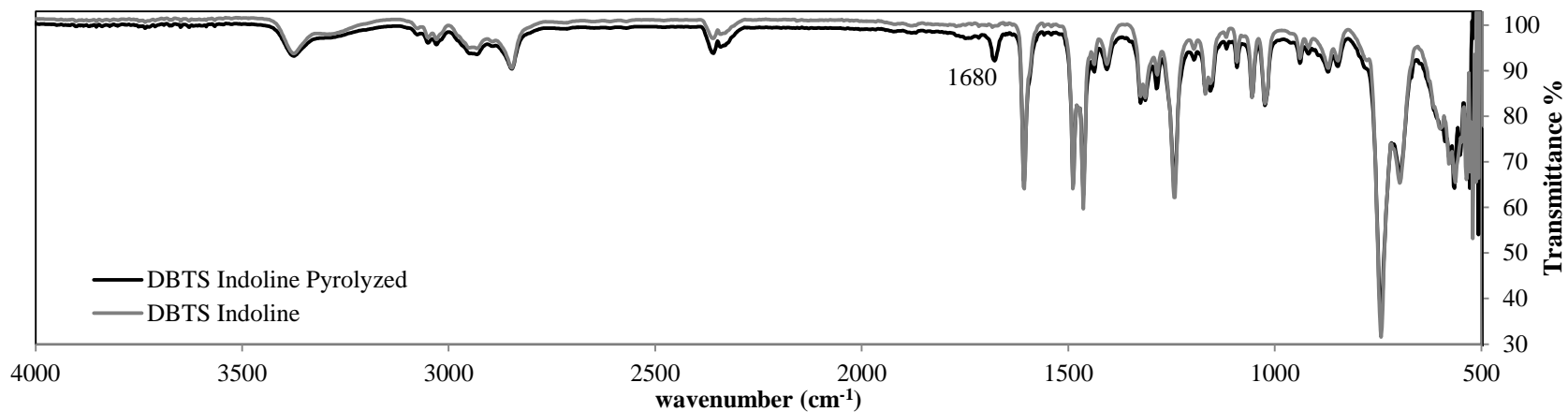
Figure 6-11. FTIR spectra of a DBTS-indoline solution and its pyrolyzed counterpart.
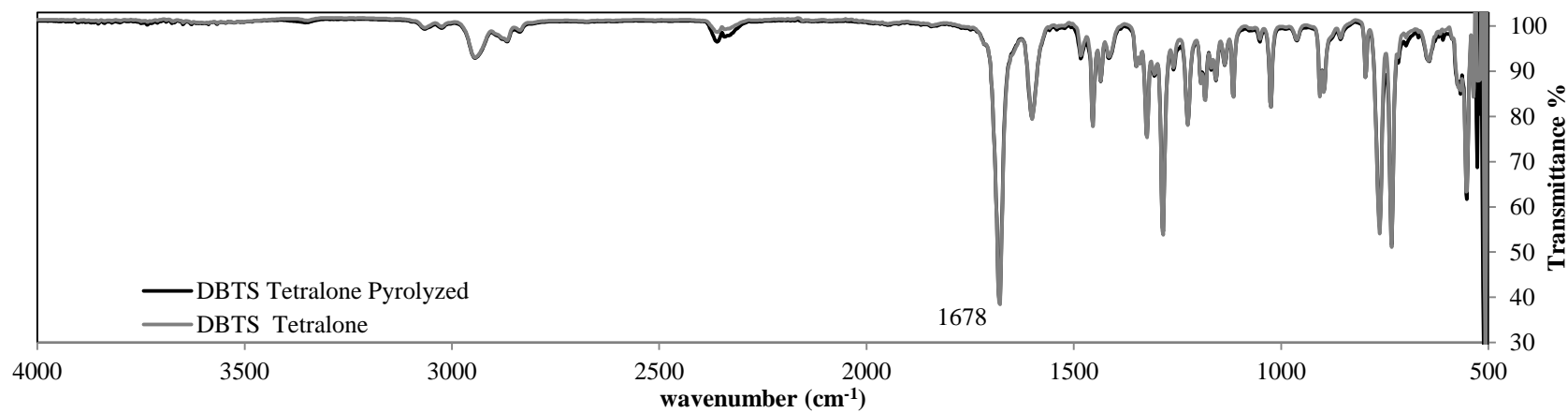
Figure 6-12. FTIR spectra of a DBTS- α-tetralone solution and its pyrolyzed counterpart.

In the case of the pyrolysis of dibenzothiophene sulfone (Figures 6-11 and 6-12), the case is very similar with very few differences appearing in the spectra among the pyrolyzed and original samples; the only noteworthy being the peak appearing at 1680cm^{-1} when DBTS is pyrolyzed in indoline. Once again there is no evidence that this difference is related to the presence of desulfurized product.

b) Mass Spectrometry

In an effort to determine by other analytical technique whether or not SO_2 is generated under the specified pyrolysis conditions, mass spectrometry of the produced pyrolysis gas was carried out in an analogous way to Section 6.3.1. As shown in Figures 6-13 to 6-16 there was no measurable presence of SO_2 in the produced gas. This result agrees with the observations made for FTIR scans. The outcome evidently is that under the reaction conditions employed no SO_2 evolves from the decomposition of DBTS or DPS.
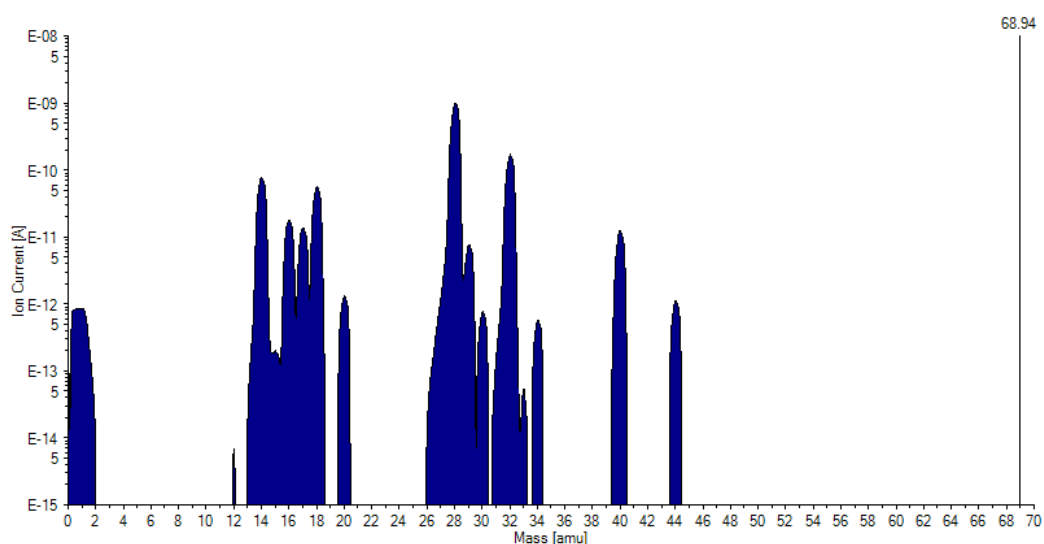
Figure 6-13. MS spectra of the pyrolysis gas from DPS diluted in indoline.
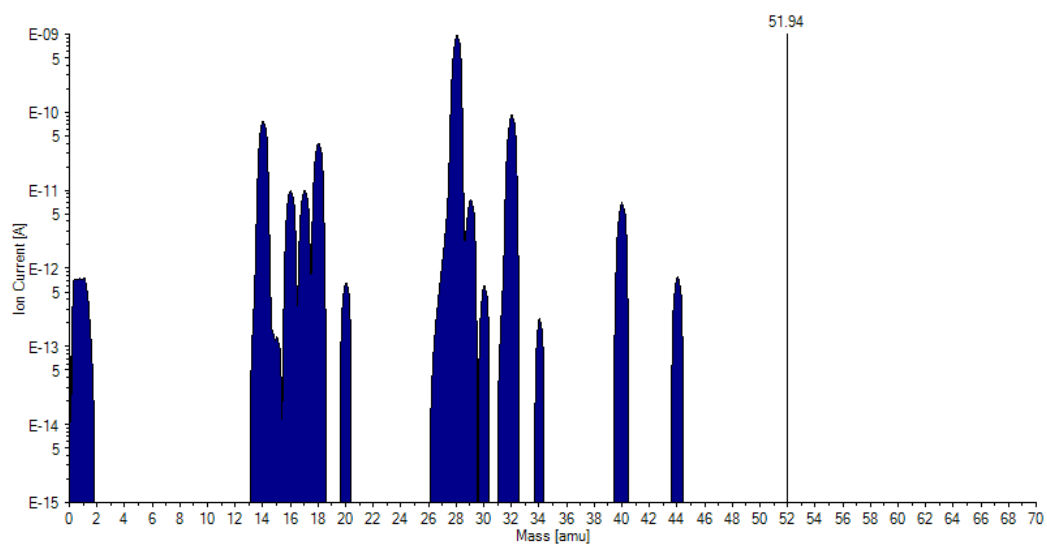
Figure 6-14. MS spectra of the pyrolysis gas from DPS diluted in tetralone.
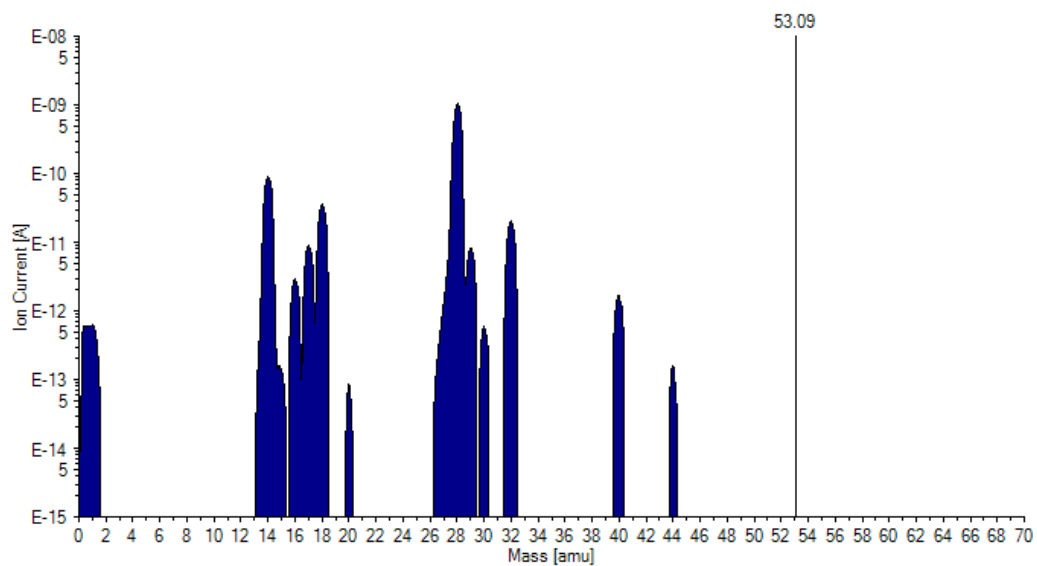
Figure 6-15. MS spectra of the pyrolysis gas from DBTS diluted in indoline.
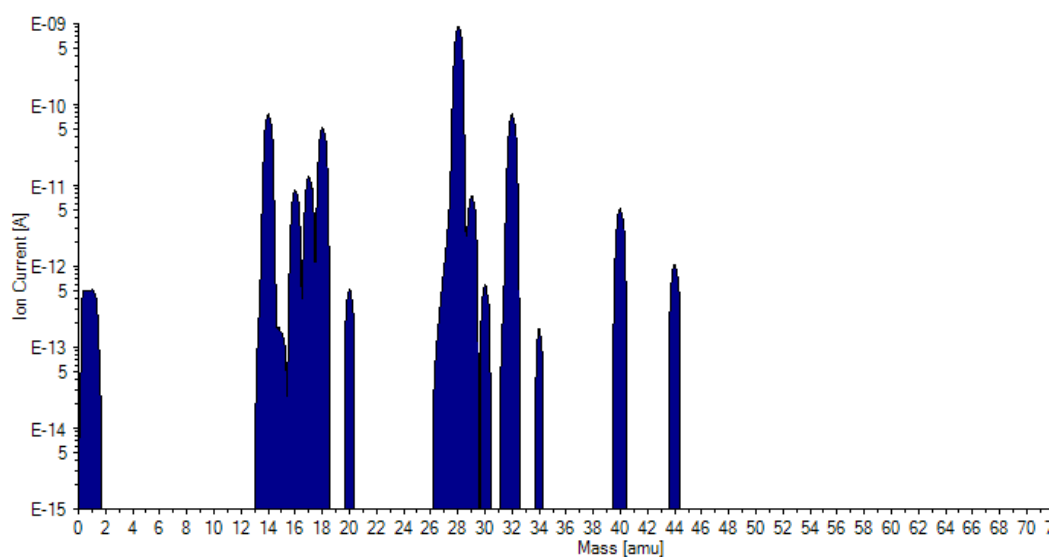
Figure 6-16. MS spectra of the pyrolysis gas from DBTS diluted in tetralone.

6.4   Conclusions

- Autoxidation of bitumen at the conditions employed through this work does not improve the degree of desulfurization achieved after pyrolysis.

- There is evidence that some oxidized compounds on bitumen can release SO_2 during pyrolysis. The results obtained with aromatic sulfones lead to suggest that the aliphatic sulfur is more thermally liable under pyrolysis than aromatic. This is still to be confirmed.

- Pyrolysis of dibenzothiophene sulfone and diphenyl sulfone at 290°C is unable to release sulfur as SO_2. Moreover, no major changes were detected after pyrolysis by FTIR analysis.

7. DEVELOPMENT OF A METHOD TO QUANTIFY COMPOUND CLASSES IN HYDROCARBONS BY HPLC

Abstract

High Performance Liquid Chromatography (HPLC) is in principle an analytical technique suitable for the analysis of heavy hydrocarbons due to the fact that vaporization of the sample is not required for the analysis. A normal phase HPLC method was developed in order to investigate the changes in composition of bitumen after oxidation; the method fails to generate useful data in the analysis of bitumen however good results are obtained for lighter products as Coal Liquids.

Keywords: HPLC, bitumen, coal liquids, normal phase HPLC.

7.1 Introduction

It is of interest to establish analytic methods to determine changes in the composition of bitumen after treatments as autoxidation are performed. As reviewed in Section 2.6 several methods of analysis have been developed for the separation of petroleum products into saturates, aromatics, resins (polars) and asphaltenes (SARA analysis) the analysis of heavy feedstock as bitumen by HPLC is limited to a couple of works [39, 40] . The analysis by HPLC of oxidized hydrocarbons has not been widely published except for model compound systems [46], however, the concept of establishing a SARA analysis method should in principle reveal the changes in composition, especially by showing the shift of non-polar hydrocarbons to polar hydrocarbons e.g. thiophenes to sulfones.

The development of this HPLC method was based in the literature review made earlier (Section 2.6). In this method which was normal phase chromatography, the analyte interacts with the stationary phase, typically trough hydrogen bonding or polar interactions [59]. The stationary phase is polar and the mobile phase in principle is non-polar. There are some compounds that due to their high polarity may adsorb strongly to the column and take very long time to be eluted; that is why it is necessary to have a backflush step in which the flow through the column is reversed and the mobile phase has higher elution strength. A conceptual diagram of the method is shown in Figure 7–1, a more detailed description will be presented later in this chapter.
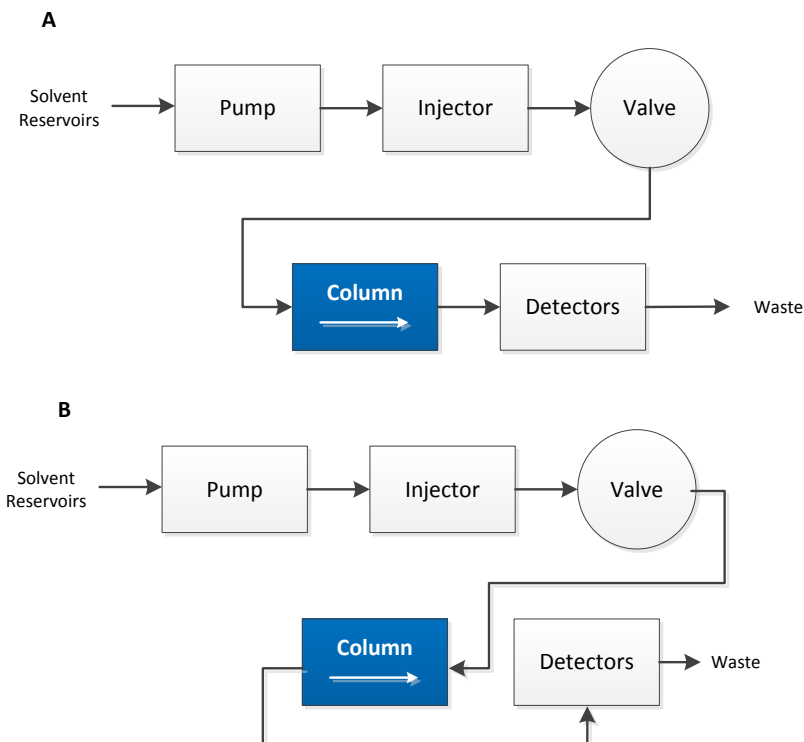
Figure 7–1. Conceptual HPLC diagram for the analysis of hydrocarbons A. normal flow mode and B. Backflush mode

7.2 Experimental

All experiments were carried out in an Alliance e2695 HPLC system (Waters) equipped with a 2998 Photo Diode Array (PDA) detector (Waters) and a 410 Refractive Index (RI) detector (Waters). The column system used consists of a 5mm precolumn and 3 columns in series μ-Bondapack NH$_2$ 3.9 $\times$ 300 mm 125Å (pore size) and 10μm (particle diameter) from Waters. A switching valve was also installed to allow the backflush of the strongly adsorbed compounds.

7.2.1 Materials

The solvent system consisted of HPLC grade hexanes 98.5% (Fisher) and HPLC grade chloroform 99.8% with 0.5-1% ethanol as stabilizer (Sigma Aldrich).

7.2.2 Experimental Conditions

Samples are prepared by dissolving the analyte in the solvent of preference at a concentration of 0.025g/ml. Hexane and chloroform are ideal since these are part of the mobile phase system and will be "invisible" in the chromatogram due to their low UV-cutoff (195 and 240 nm respectively). It should be noted that if hexane is used deasphalting will occur during sample preparation. All the samples were filtered through 0.22μm syringe filters before transferred to the chromatography vial in order to avoid presence of solids inside the instrument.

The amount of sample injected was in all cases 1µl and the solvent program employed is shown in Table 7–1.

Table 7–1. Summary of the HPLC method employed.

Time	Event	Description
0 – 20 min	100% hexane	Elution of non polars
20 min	Valve set to backflush mode	
20 – 25 min	Gradient from 100% hexane to 50% hexane – 50% chloroform	Transition to strong elution
25 – 40 min	50% Hexane 50% chloroform	Elution of polars
40 – 45 min	Gradient from 50% hexane – 50% chloroform to 100% hexane	Transition to hexane
45 min	Valve set to normal mode	
45 – 60	100% hexane	Equilibration to initial conditions.

The analysis of results was mainly made on the PDA chromatogram rather than on the RI. It is known that UV radiation is most suited to detect unsaturated fractions because of the high absorbance of aromatic in this wavelength range; hetero-compound groups also absorb strongly in the UV. On the contrary, saturates are not detected by the UV but are detected by the RI detector [60].

7.3   Results

Two sets of experimental results are presented. The first one is the analysis of a coal liquids sample in which it was possible to quantify the concentration of different aromatic groups in the sample. Also, the results of HPLC analysis of neat and oxidized bitumen are shown to illustrate the difficulties that arise when a heavy complex mixture is analyzed by this method.

7.3.1   Coal liquids results.

For the analysis of coal liquids it was of interest to focus on the distribution of aromatic rings. A model compound mixture of aromatic hydrocarbons ranging from toluene (1 aromatic ring) to coronene (7 aromatic rings) was prepared, the resulting chromatogram is shown in Figure 7–2 this example represents how the developed method performs the separation of aromatic compounds based on the number of aromatic rings. Once this information is defined, calibration curves can be made for each model compound in order to evaluate the concentration of different aromatic groups in a non-model mixture. As an example, a coal liquids cut (420°C) is considered. One can visually differentiate based on the retention

times the presence of different aromatic groups in the mixture, in this case 1 to 5 rings.

It is however unlikely that the peaks obtained from a complex hydrocarbon mixture resemble the peaks of the model mixture. In order to work around that, unknown peaks are quantified with the same parameters i.e. response factor as the closest known peak.

Finally, after all peaks are quantified, the resulting concentration is added for each compound group. This is called a timed group, a group of peaks whose concentration is added based on their retention time. The retention time is of course selected based on the results of the model compound mixture.

Table 7–2. Retention times, area, height and concentration of aromatic compounds in a model mixture

# of Aromatic Rings	Name	Retention Time [min]	Area	% Area	Height	Amount injected [ppm]
1	Mesitylene	9.877	56347	0.04	7365	1345.1
	Toluene+Xylene	10.063	156919	0.10	12644	1752.7
2	1-MethylNaphthalene	11.799	10059175	6.42	1424964	891.2
	Naphthalene	11.946	21533793	13.75	1839892	920.9
	Bi-Phenyl	12.230	3785229	2.42	347611	1069.5
3	Anthracene	15.009	38121033	24.34	2564926	1039.7
	Phenanthrene	15.385	22343726	14.27	1392293	1574.5
4	Pyrene	17.197	20684328	13.21	1147593	1604.2
	Fluoranthene	17.965	6189404	3.95	341838	831.8
	1,3,5-Triphenylbenzene	19.394	3153279	2.01	153260	475.3
	Chrysene	21.862	10016894	6.40	434868	505.0
5	Benzo[a]Pyrene	25.223	4436247	2.83	156785	623.8
	Perylene	27.524	2186501	1.40	66998	326.8
7	Coronene	32.807	13801039	8.81	219652	475.3
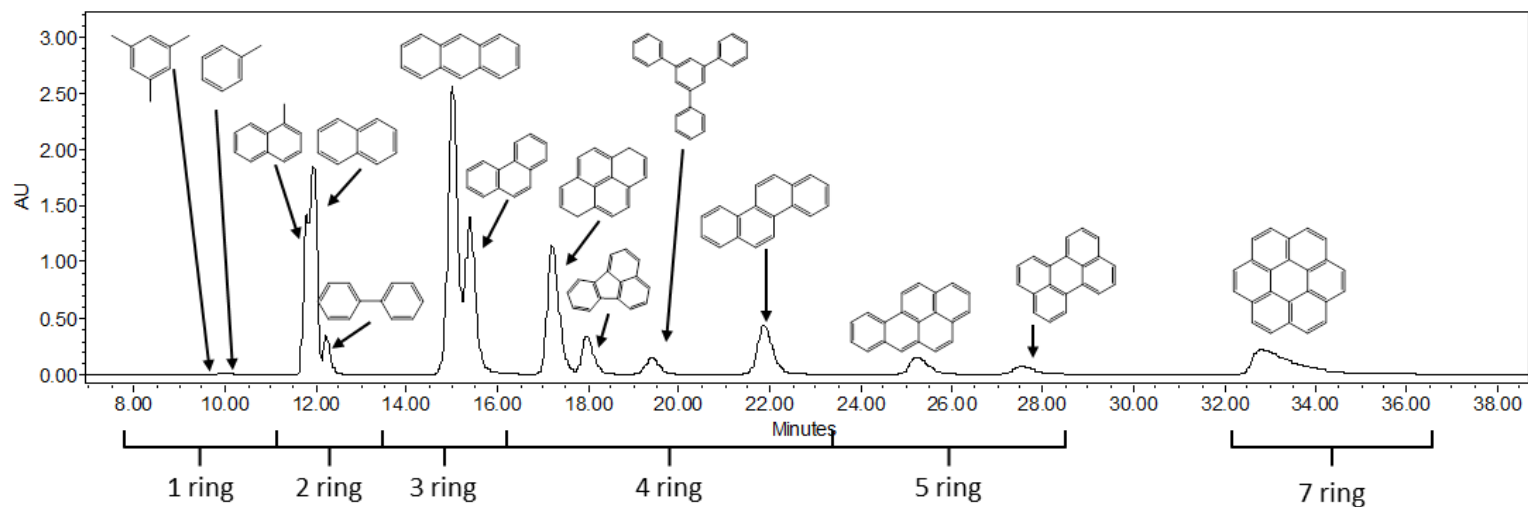
Figure 7–2. HPLC chromatogram of a model compound mixture of aromatic hydrocarbons
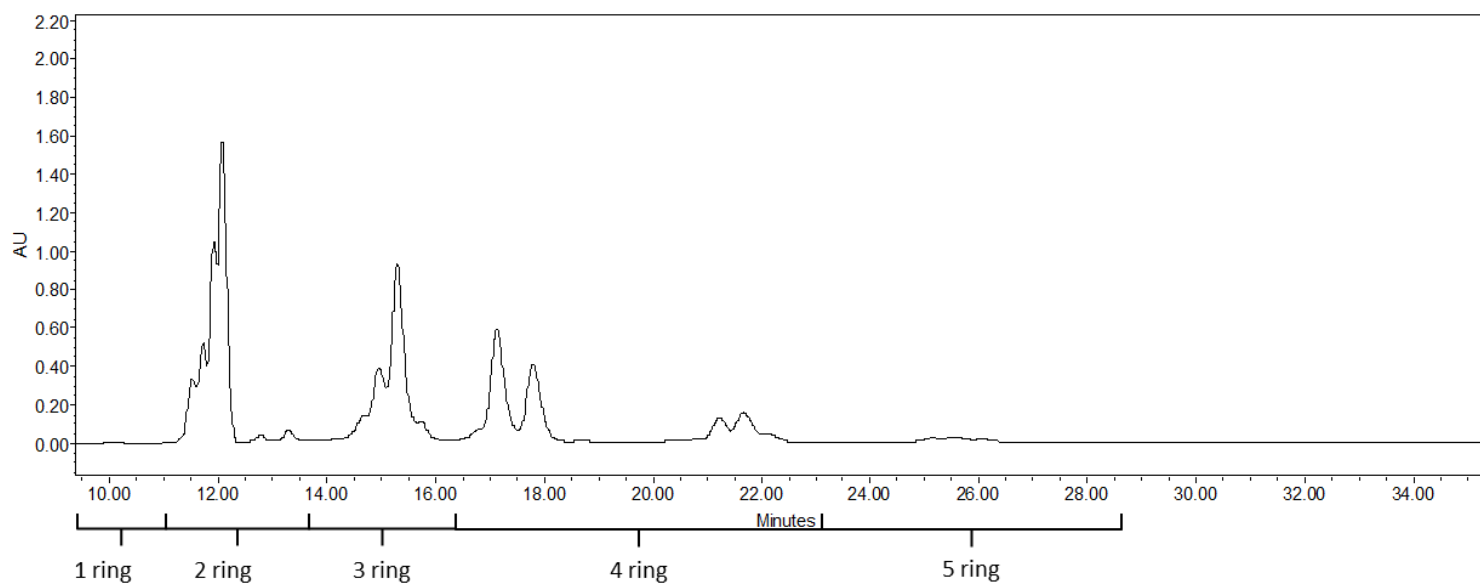
Figure 7–3. HPLC chromatogram of a coal liquids fraction Bp: 420°C

Another significant observation is that when good resolution, i.e. separation among peaks, is not obtained (see anthracene and phenantrene in Figure 7–2), it is recommended to perform the calibration based on peak height rather than peak area as the quantification value, since the integration of overlapped peaks may lead to increased error. Height is used for quantitation in this method.

The aromatic group distribution for the sample shown in Figure 7–3 is presented in Table 7–3 in order to illustrate the type of information that can be obtained from the method.

Table 7–3. Aromatic number of rings distribution on a coal liquid sample.

# of aromatic rings	Concentration [ppm]	Percentage in the sample [%]
1	865	10.7%
2	4082	50.3%
3	1307	16.1%
4	1607	19.8%
5+	260	3.2%
Total Aromatics	8121	100.0%

7.3.2   Bitumen Results.

As mentioned earlier the analysis of bitumen by this chromatographic method has presented several challenges. There is not a good separation in the aromatic fraction of bitumen. One example is presented in Figure 7–4 in this chromatogram, samples of neat and oxidized bitumen are shown. Evidently there is no presence of well-defined sharp peaks; moreover, the elution occurs in the form of a lump both for aromatic and polars. It is possible however to make some qualitative observations from these results. As can be seen in this chromatogram, when bitumen is oxidized there is a shift in the maximum from 3.5 min to 5 min. this may indicate the increased presence of heavier molecules in the oxidized sample. On the other hand, the polar "lump" is evidently larger for the oxidized sample. One can infer from that result that the amount of polars was increased by oxidation.

Table 7–4. Method conditions applied for the chromatogram presented in Figure 7–4.

Time	Event	Description
0 – 20 min	100% hexane	Elution of non polars
20 min	Valve set to backflush mode	
20 – 40 min	Gradient from 100% hexane to 50% hexane – 50% chloroform	Transition to strong elution
40 – 50 min	Gradient from 50% hexane – 50% chloroform to 100% hexane	Transition to hexane
50 min	Valve set to normal mode	
45 – 60	100% hexane	Equilibration to initial conditions.
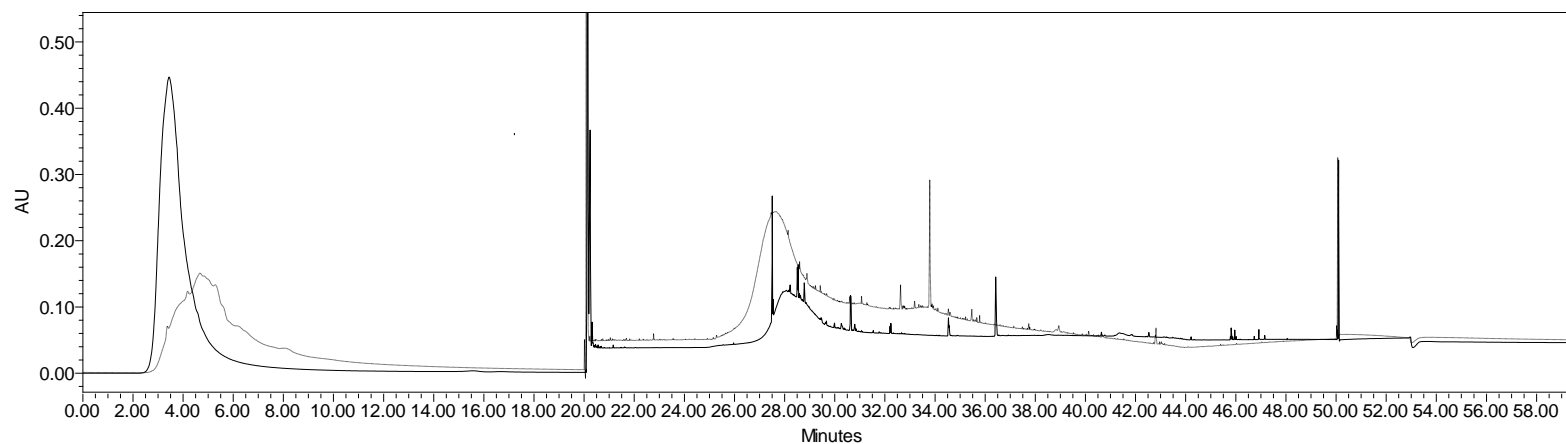
Figure 7–4. HPLC Chromatogram of neat bitumen (continuous) and oxidized bitumen.

8. CONCLUSIONS AND RECOMMENDATIONS

8.1   CONCLUSIONS

1. There is an inherent increase of the viscosity of bitumen when this is oxidized. The use of a solvent does not mitigate the viscosity increase of bitumen during autoxidation. However, the oxidation rate is increased measurably by the presence of a solvent.

2. Autoxidation of bitumen carried out at 140°C for 180 minutes causes a moderate increase in viscosity and a comparable oxidation degree compared to reaction temperatures of 160 and 180°C under same reaction times.

3. Autoxidation experiments performed on bitumen at 140°C for 720 minutes show that after an oxidation degree of about 3000 mg O_2/kg is reached, a sharp increase in viscosity occurs.

4. Pyrolysis of autoxidized bitumen generates SO_2. However sulfur removal by pyrolysis was not proven to be improved by oxidation, a possible explanation being low conversion of the autoxidation reaction.

5. Aromatic sulfones are stable, the release of SO_2 by thermal methods does not occur at temperatures below 290°C even in the presence of hydrogen donor solvents.

6. Bitumen autoxidation will always cause a viscosity increase and hence a reduction in the product quality. It is on the sulfur release step where the viscosity should also be reduced in order to guarantee an improvement in the product quality.

8.2 RECOMMENDATIONS

- A more detailed analysis of the oxidized products produced during autoxidation is required to discriminate the amount of oxygen that is bonded to sulfur from the whole oxygen incorporated to bitumen that would allow determining the selectivity of the process.

- Catalysis need to be considered, especially in the sulfone decomposition step since it was shown that sulfones are thermally stable.

- A reactor system in which mass transfer limitations between air (oxygen) and bitumen are reduced is required to optimize the oxidation process.

- Perform autoxidation experiments on distillable hydrocarbon products with moderate to high S content (%), e.g. vacuum gas oil or atmospheric gas oil. These products would be easier to handle and to perform analyses.

9. BIBLIOGRAPHY

1. Gary, J. H.; Handwerk, G. E.; Kaiser, M. J.Hydroprocessing and Resid Processing; *In Petroleum Refining Technology and Economics;* 5CRC Press: Boca Raton, FL, 2007; pp 181-193.

2. Ito, E.; van Veen, J. A. R. On novel processes for removing sulphur from refinery streams. *Catalysis Today* **2006***, 116*, 446-460.

3. Beatty, W. L.; Schroeder, K.; Kairies Beatty, C. L. Mineralogical Associations of Mercury in FGD Products. *Energy Fuels* **2012***, 26*, 3399-3406.

4. Schnelle, K. B.; Brown, C. A.Control of SO$_x$; *In Air Pollution Control Technology Handbook;* CRC Press: 2001; pp 1-21.

5. Nehb, W.; Vydra, K.Sulfur; *In Ullmann's Encyclopedia of Industrial Chemistry;* Wiley-VCH: Weinheim, 2000; Vol. 35, pp 6-68.

6. Javadli, R.; de Klerk, A. Desulfurization of Heavy Oils. Oxidative Desulfurization (ODS) As Potential Upgrading Pathway for Oil Sands Derived Bitumen. *Energy Fuels* **2012***, 26*, 594-602.

7. Javadli, R. Autoxidation for Pre-refining of Oil Sands, University of Alberta, Edmonton, Alberta, Canada, 2011.

8. Strausz, O. P.; Lown, E. M. *The Chemistry of Alberta Oil Sands, Bitumens and Heavy Oil;* Alberta Energy Research Institute: Calgary, Alberta, Canada, 2003; , pp 695.

9. Javadli, R.; de Klerk, A. Desulfurization of heavy oil. *Applied Petrochemical Research* **2012***, 1*, 3-19.

10. Hoyle, J.Oxidation of sulphoxides and sulphones; *In The Chemistry of Sulphones and Sulphoxides;* Patai, S., Rappopor, Z. and Stirling, C. J. M., Eds.; John Wiley & Sons Ltd.: Great Britain, 1988; pp 969--1000.

11. Seymour, D. T.; Verbeek, A. G.; Hrudey, S. E.; Fedorak, P. M. Acute toxicity and aqueous solubility of some condensed thiophenes and their microbial metabolites. *Environmental Toxicology and Chemistry* **1997***, 16*, 658-665.

12. You, N.; Kim, M. J.; Jeong, K.; Jeong, S.; Park, Y.; Jeon, J. Catalytic Removal of Sulfur Dioxide from Dibenzothiophene Sulfone Over Mg-Al Mixed Oxides Supported on Mesoporous Silica. *Journal of Nanoscience and Nanotechnology* **2010***, 5*, 3663-3666.

13. Herron, J. T.Thermochemistry of Sulfoxides and Sulfones; *In Sulphones and Sulphoxides (1988);* Patai, S., Rappoport, Z. and Stirling, C. J. M., Eds.; John Wiley & Sons, Ltd: Chichester, UK, 1988; pp 95-106.

14. Kocal, J. A.; Brandvold, T. A. US Patent 6,368,495, 2002.

15. Ma, X.; Sakanishi, K.; Mochida, I. Hydrodesulfurization Reactivities of Various Sulfur Compounds in Vacuum Gas Oil. *Ind Eng Chem Res* **1996***, 35*, 2487-2494.

16. Otsuki, S.; Nonaka, T.; Takashima, N.; Qian, W.; Ishihara, A.; Imai, T.; Kabe, T. Oxidative Desulfurization of Light Gas Oil and Vacuum Gas Oil by Oxidation and Solvent Extraction. *Energy Fuels* **2000***, 14*, 1232-1239.

17. Block, E.Oxidation and reduction of sulphides; *In Supplement E The Chemistry of Ethers, Crown Ether, Hydroxyl Groups and their Sulphur Analogues;* Patai, S., Ed.; John Wiley & Sons: St. Louis, 1980; Vol. 13, pp 539-608.

18. Plesnicar, B.Oxidation with Peroxy Acids and Other Peroxides; *In Oxidations In Organic Chemistry. Part C;* Trahanovsky, W. S., Ed.; Academic Press: New York, 1978; pp 211-294.

19. Ishihara, A.; Wang, D.; Dumeignil, F.; Amano, H.; Qian, E. W.; Kabe, T. Oxidative desulfurization and denitrogenation of a light gas oil using an oxidation/adsorption continuous flow process. *Applied Catalysis A: General* **2005***, 279*, 279-287.

20. Sheldon, R. A.Synthesis and uses of alkyl hydroperoxides and dialkyl peroxides; *In The Chemistry of Functional Groups, Peroxides;* Patai, S., Ed.; John Wiley & Sons Ltd: New York, 1983; pp 161-200.

21. Hiatt, R. R.; Irwin, K. C. Homolytic decompositions of hydroperoxides. V. Thermal decompositions. *J. Org. Chem.* **1968***, 33*, 1436-1441.

22. Jiang, Z.; Lu, H.; Zhang, Y.; Li, C. Oxidative Desulfurization of Fuel Oils. *Chinese Journal of Catalysis* **2011***, 32*, 707-715.

23. Sampanthar, J. T.; Xiao, H.; Dou, J.; Nah, T. Y.; Rong, X.; Kwan, W. P. A novel oxidative desulfurization process to remove refractory sulfur

compounds from diesel fuel. *Applied Catalysis B: Environmental* **2006***, 63*, 85-93.

24. Kim, M. J.; Kim, H.; Jeong, K.; Jeong, S.; Park, Y. K.; Jeon, J. Catalytic decomposition of dibenzothiophene sulfones over layered double hydroxide catalysts. *Journal of Industrial and Engineering Chemistry* **2010***, 16*, 539-545.

25. Park, Y.; Kim, S.; Kim, H.; Jung, K.; Jeong, K.; Jeong, S.; Jeon, J. Removal of sulfur dioxide from dibenzothiophene sulfone over Mg-based oxide catalysts prepared by spray pyrolysis. *Korean Journal of Chemical Engineering* **2010***, 27*, 459-464.

26. Webster, A. B.; Herbert, S. N. J.; Richard, R. US Patent 3,163,593, 1964.

27. Reichert, C.; Grant, L. In *In Liquid chromatographic chemical class analysis of bitumen and heavy petroleum crudes;* ACS, Division of fuel chemistry; ACS: 1978; Vol. 23, pp 72-75.

28. Grizzle, P. L.; Thomson, J. S. Liquid chromatographic separation of aromatic hydrocarbons with chemically bonded (2,4-dinitroanilinopropyl)silica. *Anal. Chem.* **1982***, 54*, 1071-1078.

29. Boduszynski, M. M.; Hurtubise, R. J.; Allen, T. W.; Silver, H. F. Determination of hydrocarbon composition in high-boiling and nondistillable coal liquids by liquid chromatography/field ionization mass spectrometry. *Anal. Chem.* **1983***, 55*, 232-241.

30. Pearson, D. C.; Gharfeh, S. G. Automated high-performance liquid chromatography determination of hydrocarbon types in crude oil residues using a flame ionization detector. *Anal. Chem.* **1986**, 307-311.

31. Leontaritis, K. J.; Mansoori, G. A. Fast crude-oil heavy-component characterization using combination of ASTM, HPLC, and GPC methods. *Journal of Petroleum Science and Engineering* **1989***, 2*, 1-12.

32. Lamey, S. C.; Hesbach, P. A.; White, K. D. Liquid fuel analyses using high-performance liquid chromatography and gas chromatography-mass spectroscopy. *Energy Fuels* **1991***, 5*, 222-226.

33. Hsu, C. S.; Qian, K. High-boiling aromatic hydrocarbons characterized by liquid chromatography-thermospray-mass spectrometry. *Energy Fuels* **1993***, 7*, 268-272.

34. Akhlaq, M. S. Rapid group-type analysis of crude oils using high-performance liquid chromatography and gas chromatography. *Journal of Chromatography A* **1993**, *644*, 253-258.

35. Akhlaq, M. S.; Götze, P. Detailed analysis of crude oil group types using reversed-phase high-performance liquid chromatography. *Journal of Chromatography A* **1994**, *677*, 265-272.

36. Sarowha, S. L. S.; Sharma, B. K.; Sharma, C. D.; Bhagat, S. D. Characterization of Petroleum Heavy Distillates Using HPLC and Spectroscopic Methods. *Energy Fuels* **1997**, *11*, 566-569.

37. Beens, J.; Tijssen, R. The characterization and quantitation of sulfur-containing compounds in (heavy) middle distillates by LC-GC-FID-SCD. *J. High Resol. Chromatogr.* **1997**, *20*, 1521-4168.

38. Ali, M. A. Resolution and Quantification of Ring Type Aromatics by HPLC Method Using n -Hexane Elution. *Petrol Sci Technol* **2003**, *21*, 963-970.

39. Woods, J. R.; Kung, J.; Pleizier, G.; Kotlyar, L. S.; Sparks, B. D.; Adjaye, J.; Chung, K. H. Characterization of a coker gas oil fraction from athabasca oilsands bitumen. *Fuel* **2004**, *83*, 1907-1914.

40. Woods, J.; Kung, J.; Kingston, D.; Kotlyar, L.; Sparks, B.; McCracken, T. **Canadian Crudes: A Comparative Study of SARA Fractions from a Modified HPLC Separation Technique**. *Oil & Gas Science and Technology* **2008**, *63*, 151-163.

41. Kopsch, H. *Thermal Methods in Petroleum Analysis;* VCH: Weinheim, Germany, 1995; .

42. Freitas, V. L. S.; Gomes, J. R. B.; Ribeiro da Silva, M. D. M. C. Molecular energetics of 4-methyldibenzothiophene: An experimental study. *The Journal of Chemical Thermodynamics* **2010**, *42*, 251-255.

43. Stephens, H. N. Studies in Auto-oxidation. V. The Induction Period in Auto-oxidation. *Journal of the American Chemical Society* **1936**, *58*, 219-224.

44. Silverstein, R. M.; Webster, F. X.Infrared Spectrometry; *In Spectrometric Identification od Organic Compounds;* 6John Wiley and Sons, Inc: New York, 1997; pp 106-107.

45. Schreiber, K. C. Infrared Spectra of Sulfones and Related Compounds. *Analytical Chemistry* **1949**, *21*, 1168-1172.

46. Castillo, K.; Parsons, J. G.; Chavez, D.; Chianelli, R. R. Oxidation of dibenzothiophene to dibenzothiophene-sulfone using silica gel. *Journal of Catalysis* **2009**, *268*, 329-334.

47. Forziati, A. F.; Norris, W. R.; Rossini, F. D. Vapor pressures and boiling points of sixty API-NBS hydrocarbons. *J. Res. Natl. Bur. Stand.* **1942**, *43*, 555.

48. Montgomery, D. C.; Runger, G. C.Chapter 9: Statistical Inference for Two Samples; *In Applied Statistics and Probability for Engineers;* John Wiley & Sons, Inc.: United States of America, 2011; pp 351.

49. Babu, D. R.; Cormack, D. E. Effect of oxidation on the viscosity of athabasca bitumen. *Can. J. Chem. Eng.* **1984**, *62*, 562-564.

50. Read, J.; Whiteoak, D.Durability of Bitumens; *In The Shell Bitumen Handbook;* 5ThomasTelford Publishing: Great Britain, 2003; pp 158-167.

51. Gipstein, E.; Wellisch, E.; Sweeting, O. J. The Effect of Î²-Hydrogen Atoms and Hydrocarbon Structure on the Thermal Stability of Sulfones1. *J. Org. Chem.* **1964**, *29*, 207-209.

52. Xu, X.; Li, X.; Wang, A.; Sun, Y.; Schweizer, W. B.; Prins, R. Synthesis of 4,6-Dimethyldibenzothiophene and 1,2,3,4-Tetrahydro-4,6-dimethyldibenzothiophene. *HCA* **2011**, *94*, 1754-1763.

53. Kuehm-Caubère, C.; Adach-Becker, S.; Fort, Y.; Caubère, P. Expeditious and efficient syntheses of pure 4-methyl and 4,6-disubstituted dibenzothiophenes. *Tetrahedron* **1996**, *52*, 9087-9092.

54. Ramírez-Verduzco, L. F.; Rojas-Aguilar, A.; De los Reyes, José A.; Muñoz-Arroyo, J. A.; Murrieta-Guevara, F. Solid-Liquid Equilibria of Dibenzothiophene and Dibenzothiophene Sulfone in Organic Solvents. *J. Chem. Eng. Data* **2007**, *52*, 2212-2219.

55. Haynes, W. M.Physical constants of organic compounds; *In Handbook of Chemistry and Physics;* 93rd Haynes, W. M., Ed.; CRC Press/Taylor and Francis: Boca Raton, FL, 2013; .

56. NIST Mass Spec Data Center Sulfur Dioxide. *http://webbook.nist.gov/cgi/cbook.cgi?ID=C7446095&Mask=200#Top* (accessed 09/06, 2013).

57. Hendessi, S. Pyrolysis of Sulfone compounds by High Pressure Differential Scanning Calorimetery. **2013**.

58. Dutta, R.; Martin, S.; Plummet, M.; Schobert, H. H. In *In Thermal Upgrading of Petroleum Resids Using Polar H-Donor Solvents;* ACS: Boston, 1998; Vol. 43, pp 538-542.

59. Meyer, V.Adsorption Chromatography; *In Practical high-performance liquid chromatography;* fifthJohn Wiley & Sons: Padstow, 2010; pp 159-172.

60. Woods, J. R.; Kung, J.; Adjaye, J.; Kotlyar, L. S.; Sparks, B. D.; Chung, K. H. **Characterization of a Gas Oil Fraction and Its Hydrotreated Products**. *Petroleum Science and Technology* **2004**, *22*, 347-365.

APPENDIX A

This appendix serves the purpose of determining the error that the mass balance presented in Section 5.3.2 have associated with the assumption on the equality of mass of gas in and out of the oxidation reactor. An example is presented in which the concentration of O_2 drops from 20.5% to 18.5% through the reactor, a change of 2%. The inlet flow of air is 100 ml/min and the calculated density of oxygen is 0.00133 g/ml.

First Scenario: The volumetric flow and the density of the gas are assumed equal.

$$\rho_{air,in} \approx \rho_{air,out} , \dot{V}_{air,in} \approx \dot{V}_{air,out} \rightarrow m_{in} = m_{out}$$

Second scenario. The assumption of equality of mass and volumetric flow rate in and out of the reactor is no longer made.

$$\dot{V}_{IN} \neq \dot{V}_{OUT}$$

The term $\dot{V}_{OUT}$ needs to be calculated in a different way. One can use the N_2 flow as nitrogen since it is assumed to be inert, so:

$$\dot{V}_{N_2 \ OUT} \left[\frac{ml}{min}\right] = \dot{V}_{N_2 \ IN} \left[\frac{ml}{min}\right] = \frac{(100 - \%O_{2IN})}{100} * \dot{V}_{IN} \left[\frac{ml_{air}}{min}\right]$$

But also

$$\dot{V}_{N_2 \ OUT} \left[\frac{ml}{min}\right] = \frac{\% N_2 \ (out)}{100} \left[\frac{ml_{N_2}(out)}{ml}\right] \times \dot{V}_{OUT} \left[\frac{ml}{min}\right]$$

$$\dot{V}_{N_2 \ IN} \left[\frac{ml}{min}\right] = \frac{(100 - \%O_{2IN})}{100} \times \dot{V}_{IN} \left[\frac{ml_{air}}{min}\right] = \frac{\% \boldsymbol{N_2} \ (\boldsymbol{out})}{\boldsymbol{100}} \left[\frac{ml_{N_2}(out)}{ml}\right] \times \dot{V}_{OUT} \left[\frac{ml}{min}\right]$$

$$\dot{V}_{OUT} \left[\frac{ml}{min}\right] = \frac{100 - \%O_{2IN}}{\% N_2 \ (out)} \times \dot{V}_{IN} \left[\frac{ml}{min}\right]$$

It is assumed however that the outlet gas is only composed by unreacted O_2 and N_2, note that the presence of water and CO_2 in the outlet is being neglected and these components if considered would increase the volumetric flow in the outlet.

$$\% \, N_2 \, (out) = 100 - \%O_{2\,OUT}$$

$$\dot{V}_{OUT} \left[\frac{ml}{min}\right] = \frac{100 - \%O_{2\,IN}}{100 - \%O_{2\,OUT}} \times \dot{V}_{IN} \left[\frac{ml}{min}\right]$$

Replacing in the mass balance:

$$\dot{V}_{OUT} \left[\frac{ml}{min}\right] = \frac{100 - 20.5}{100 - 18.5} \times \dot{V}_{IN} \left[\frac{ml}{min}\right]$$

$$\dot{V}_{OUT} \left[\frac{ml}{min}\right] = 0.975 \times \dot{V}_{IN} \left[\frac{ml}{min}\right]$$

$$\dot{V}_{IN} \left[\frac{ml}{min}\right] - \dot{V}_{OUT} \left[\frac{ml}{min}\right] = 0.025 \times \dot{V}_{IN} \left[\frac{ml}{min}\right]$$

As shown, the difference between considering a change in the volumetric flow rate and hence in the volumetric flow rate of gas in and out of the reactor is of 2.5% when the drop in oxygen concentration is of 2%. If CO_2 and H_2O were considered and quantified in the outlet stream the difference in flow rate in and out would be smaller.